

NGU Report 2010.037

Potential for rare earth element and Zr-, Be-, U-,
Th-, (W-)mineralisations in central and northern
Nordland

Report no.: 2010.037		ISSN 0800-3416	Grading: Confidential to 31.12.2012 Open	
Title: Potentials of rare earth element and Zr-, Be-, U-, Th-, (W-)mineralisations in central and northern Nordland				
Authors: Axel Müller		Client: Nordland Mineral		
County: Nordland		Commune:		
Map-sheet name (M=1:250.000) Mo i Rana, Saltdal, Bodø, Sulitjelma, Narvik		Map-sheet no. and -name (M=1:50.000)		
Deposit name and grid-reference:		Number of pages: 85	Price (NOK): 420,00 NOK	
Fieldwork carried out:		Date of report: 15.07.2010	Project no.: 305600	Person responsible: Rognvald Boydt <i>[Signature]</i>
Summary:				
<p>The Geological Survey of Norway (NGU) was contacted by Nordland Mineral (T. Vrålstad) in May 2010 to evaluate the potential of economic rare-earth-element (REE: Ce-Lu, Y) and Zr-mineralisations and related Be-, U-, Th-, (W-) mineralisations in Proterozoic basement windows and overlying Caledonian nappe complexes in central and northern Nordland between Mo i Rana in the south and Ofotfjorden in the north. The economic background for the study is the increasing demand for several of these elements. The general aim is to identify Zr-REE mineralisations with ≥ 2 wt.% REE(+Y) which are possibly enriched in Be, U and Th as well.</p> <p>Accessible literature and mineralogical, geochemical and geophysical data on REE-mineralisations and Zr-, Be-, U-, Th-, (W-) mineralisations, which might be associated with REE-mineralisations, were studied in order to indicate potential target areas for future exploration activity. The primary focus was to evaluate the potential of (1) the Høgtuva Be-REE-U-Sn mineralisation, (2) strongly fractionated granite intrusions, (3) REE-fluorite mineralisations, (4) regional REE anomalies in stream sediments and tills, (5) REE-silicates (allanite) in granites, (6) NYF pegmatites, (7) hydrothermal Fe-deposits with associated REE enrichments, (8) Th- and allanite-bearing rocks by checking regional radiometric measurements and (9) basement granites which possibly contain 2-3% REE-oxides by checking NGU databases. The results of the study indicate that mineralisations and mineralisation types named under points (1), (3), (6) and (7) are currently not of economic interest.</p> <p>The major outcome of the study is, that some of the more evolved Proterozoic TIB- type granites (TIB – Trans-Scandinavian Igneous Belt) of the Tysfjord basement window have a potential for sub-economic to economic Zr-REE-mineralisations. The possible carriers of the mineralisation are zircon and allanite. The identified Zr-REE-enriched TIB-2 granites are SiO₂-rich, subalkaline, metaluminous A-type (anorogenic) granites with low (Na₂O+K₂O)/CaO ratios (<6; Figs. 37-40). They represent a specific final fractionation trend of the TIB-2 granites. These mineralisation types are relatively unknown but have been described from Saudi Arabia. Possibly exploration target areas for Zr-REE-mineralised TIB-granites are suggested.</p>				
Keywords: Technical report		literature study		potential REE+Y deposits
rare metals Zr, Be, Th, U, W		Nordland		Høgtuva
Storjord				

Contents

1. Introduction	8
2. Geology of central and northern Nordland	10
3. Mineralisations of the Svecofennian basement windows	15
3.1 Tysfjord(-Hamarøy) window	15
3.1.1 Fluorite mineralisation at Mannfjellvatn	17
3.1.2 Y-Ce-La-rich magnetite mineralisation at Storjord	18
3.1.3 Tiltvik U-Th mineralisation	20
3.1.4 Kalvik Mo-U-(W) mineralisation	20
3.1.5 The REE-U-Th-Be enrichments in the younger Hellemobotn granites	22
3.1.6 Pegmatites associated with TIB-magmatism	23
3.1.7 Other deposits in the area	25
3.2 Rishaugfjell window	26
3.2.1 Harelifjell (Straumen) U-Mo mineralisation	26
3.3 Nasafjell window	28
3.4 Bjellåtinden window	28
3.4.1 Bjellåtinden W-Mo mineralisation	28
3.5 Glomfjord window	31
3.5.1 Rendalsvik U-Th mineralisation	31
3.6 Høgtuva window	33
3.6.1 Høgtuva Be-REE-U-Sn mineralisation	33
4. Mineralisations in the Caledonian nappe complexes	40
4.1 Skarn deposits of the Uppermost Allochthon	40
4.2 Deformed carbonatite dykes	40
5. NGU Uranal database of igneous rocks	40
6. NGU geochemical database of stream sediments	51
7. Summary, discussion and outlook	57
8. References	61

Figures

Figure 1. Geological map of central and northern Nordland according to Solli and Nordgulen (2006). The area considered in this study extends from Mo i Rana in the south to Ofotfjorden in the north (red dashed line)	10
Figure 2. Simplified geological map of central and northern Nordland showing the distribution of basement windows (red) within the Caledonian nappes (green). From Ramberg et al. (2006)	13
Figure 3. Geological map of Scandinavia showing the extension of the Trans-Scandinavian Igneous Belt (TIB). From Skår (2002)	14
Figure 4. Simplified geological map showing the major Caledonian nappe complexes in central and northern Nordland. From Ramberg et al. (2006)	14
Figure 5. Airborne Th-radiation map of the Hellemobotn-Linnajavrre-Gjerdal area (eastern Tysfjord window) obtained by NGU in 1991. For explanations see text.	16
Figure 6. Airborne Th-radiation map of the Ulsvåg (Hamarøy, Tysfjord window) area obtained by NGU in 1976. For explanations see text.	17
Figure 7. Geological map of the Tysnes peninsula, Hamarøy, by Karlsen (2000) showing the locations of U-Th, Fe, and Cu-mineralisations. 1 – Storjord, 2 – Tiltvika north, 3 –	

Tiltvika south, 4 – Skarvik, 5 – Hundemullen, 6 – Lillebotn, 7 – Lillebotn south, 8 – Skogvoll, 9 – Lødhaugen (Karlstrøm 1990, NGU database).	19
Figure 8. Concentrations of Zr versus Y+La+Ce of different rocks associated with the magnetite mineralisation at Storjord (data from Rønning 1986 and unpublished data by A. Korneliussen). The Y-Ce-La mineralisation is related to amphibolite enclaves in meta-volcanites with an average of 0.5 % REE.	20
Figure 9. Location of the Kalvik basement window. From Hansen (1983).	21
Figure 10. U-Mo mineralisations of the Kalvik window according to Hansen (1983). U – uranium mineralisation, Mo – molybdenite, Mt – magnetite.	22
Figure 11. Concentrations of Zr versus Y+La+Ce+Sm for some Tysfjord TIB-type granites (data from Romer et al. 1992). Some of the younger Hellemobotn granites show relatively high concentrations of all these elements. It is assumed that these younger granites are responsible for the heavy element enrichment in stream sediments detected by Kjeldsen (1987) and Korneliussen et al. (1989).	23
Figure 12. Pegmatite localities and types in the Tysfjord area. With permission from P. Ihlen (unpublished).	24
Figure 13. The Hundholmen pegmatite according to Foslie (1941). The pegmatite, which is famous for its yttrifluorite and REE minerals, is hosted by allanite-rich TIB-granites (UTM 33W 552625E/7559832N).	25
Figure 14. Location of the Harelifjell U-mineralisation occurrence within the Rishaugfjell basement window according to Lindahl (1983).	26
Figure 15. Schematic profile of the Harelifjell uranium occurrence according to Lindahl (1983). The host rock is fine-grained gneiss within coarse-grained granite with a weak foliation.	27
Figure 16. Concentrations of Zr versus Y+La+Ce+Sm of rocks of the Rishaugfjell window including the Harelifjell mineralisation (REE-rich aplites). One TIB-granite sample plots outside the diagram area with 11700 ppm Zr and 884 ppm Y+La+Ce (sample "Memaurvatnet", UTM 33W 529233E/7472096N; see also Figs. 23-25). Data are from the NGU Uranal database.	27
Figure 17. Geological map and cross sections of the Bjellåtinden basement window (quartz monzonitic gneiss) and of W-Mo mineralisation situated in Precambrian-Palaeozoic schists, meta-pelites and marbles immediately above the tectonic boundary to the basement rocks. From Larsen (1991). The number within the tungsten-molybdenum-zone (WMZ) correspond to different mineralisations found in the area.	30
Figure 18. a - Topographic map with the location of Rendalsvik Gruber (old graphite mine) on the southern side of Holandsfjord, Meløy. b – Detailed topographic map showing the approximate distribution of U-rich graphite schist (red area) according to Gust and Thoresen (1981).	32
Figure 19. Concentrations of Zr versus Y+La+Ce+Sm in U-rich graphite schist from Rendalsvik (data from Gust and Thoresen 1981).	33
Figure 20. Geological map of the southeastern part of the Høgtuva basement window according to Wilberg (1987a) showing the distribution of the Be mineralisations.	35
Figure 21. Radiometric map and cross sections of the Bordvedåga Be mineralisation according to Lindahl and Grauch (1988).	36

Figure 22. Concentrations of Zr versus Y+La+Ce+Sm of the Høgtuva mineralisation. Note that only data >1000 ppm Zr and >1000 ppm Y+La+Ce are plotted. Source: NGU Ural database.	36
Figure 23. Simplified geological map of central and northern Nordland with Y concentrations of rock samples registered at the NGU Ural database. The pink areas are the basement windows comprising predominantly deformed and undeformed TIB-granites.	42
Figure 24. Simplified geological map of central and northern Nordland with La concentrations of rock samples registered at the NGU Ural database. The pink areas are the basement windows comprising predominantly deformed and undeformed TIB-granites.	43
Figure 25. Simplified geological map of central and northern Nordland with Ce concentrations of rock samples registered at the NGU Ural database. The pink areas are the basement windows comprising predominantly deformed and undeformed TIB-granites.	44
Figure 26. Simplified geological map of northern Nordland with Y concentrations of rock samples registered at the NGU Ural database. The pink areas are the basement windows comprising predominantly deformed and undeformed TIB-granites.	45
Figure 27. Simplified geological map of northern Nordland with La concentrations of rock samples registered at the NGU Ural database. The pink areas are the basement windows comprising predominantly deformed and undeformed TIB-granites.	46
Figure 28. Simplified geological map of northern Nordland with Ce concentrations of rock samples registered at the NGU Ural database. The pink areas are the basement windows comprising predominantly deformed and undeformed TIB-granites.	47
Figure 29. Simplified geological map of central Nordland with Y concentrations of rock samples registered at the NGU Ural database. The pink areas are the basement windows comprising predominantly deformed and undeformed TIB-granites.	48
Figure 30. Simplified geological map of central Nordland with La concentrations of rock samples registered at the NGU Ural database. The pink areas are the basement windows comprising predominantly deformed and undeformed TIB-granites.	49
Figure 31. Simplified geological map of central Nordland with Ce concentrations of rock samples registered at the NGU Ural database. The pink areas are the basement windows comprising predominantly deformed and undeformed TIB-granites.	50
Figure 32. Simplified geological map of central and northern Nordland with Y concentrations of stream sediments registered at the NGU geochemical database. The distinct cluster of elevated Y concentrations in the Tysfjord basement window supports the conclusion that the most fractionated TIB-granites occur in this area. Another Y-rich sample originates from inner Værangsfjord, Glomfjord window.	52
Figure 33. Simplified geological map of central and northern Nordland with La concentrations of stream sediments registered at the NGU geochemical database. The distinct cluster of elevated La concentrations in the Tysfjord basement window supports the conclusion that the most fractionated TIB-granites occur in this area. Other La-rich samples originate from the Glomfjord window, the eastern margin of the Høgtuva window, the Valnesfjord W-skarn and inner Misværffjord.	53
Figure 34. Simplified geological map of central and northern Nordland with Ce concentrations of stream sediments registered at the NGU geochemical database. The distinct cluster of elevated Ce concentrations in the Tysfjord basement window supports the conclusion that the most fractionated TIB-granites occur in this area. Other Ce-rich	

samples originate from the inner Værangsfjord (Glomfjord window), the eastern margin of the Høgtuva window and the inner Misvær fjord.	54
Figure 35. Simplified geological map of central and northern Nordland with La concentrations of stream sediments in areas covered by Caledonian nappes. Source NGU geochemical database. The concentration distribution illustrates that there are no particular REE-anomalies in these areas.	55
Figure 36. Simplified geological map of central and northern Nordland with Ce concentrations of stream sediments in areas covered by Caledonian nappes. Source NGU geochemical database. The concentration distribution illustrates that there are no particular REE-anomalies in these areas.	56
Figure 37. Subalkaline-alkaline classification diagram showing that the older TIB-1 granites have alkaline character which develop to subalkaline TIB-2 granites (orange arrow). The REE-enriched TIB-2 granites from Hellemobotn (red ellipse) show a specific fractionation with decreasing SiO ₂ during further evolution. Data from Romer et al. (1992).	58
Figure 38. Peraluminous-metaluminous classification diagram showing that the TIB-1 and TIB-2 granites plot in the peraluminous as well in the metaluminous field. The mineralised TIB-2 granites plot in the metaluminous field (red ellipse). A/CNK – Al ₂ O ₃ /(CaO+Na ₂ O+K ₂ O) in molecular weight. Data from Romer et al. (1992).	58
Figure 39. Metaluminous-peralkaline classification diagram showing that none of the TIB-1 and TIB-2 granites plot in the peralkaline field. The mineralised TIB-2 granites are indicated by the red ellipse. A/NK – Al ₂ O ₃ /(Na ₂ O+K ₂ O) in molecular weight. Data from Romer et al. (1992).	59
Figure 40. A-type granite classification diagram showing that most of the TIB-granites have A-type affinity in particular the REE-enriched granites from Hellemobotn (red ellipse). Data from Romer et al. (1992).	59
Figure 41. Simplified geological map of northern Nordland with suggested target areas for sampling of REE-Zr-enriched TIB-2 granites.	60

Tables

Table 1. Atomic numbers and upper crust abundance of REEs. The upper crust abundances (in ppm) are according Taylor and McClennan (1985). Promethium has not been proven on Earth.	9
Table 2. Be-mineralisations in the eastern part of the Høgtuva window. Concentrations of Be, Zr, Y, Nb and U are average values of mineralized rocks according to Wilberg and Lindahl (1991) and Wilberg (1987b, 1989a, 1989c).	38

Appendix

Appendix 1.....67
Appendix 2.....68
Appendix 3.....70
Appendix 4.....72
Appendix 5.....78
Appendix 6.....81

1. Introduction

The Geological Survey of Norway (NGU) was contacted by Nordland Mineral (T. Vrålstad) in May 2010 to evaluate the potential of economic rare-earth-element (REE: Ce-Lu, Y) and Zr-mineralisations and related Be-, U-, Th-, (W-) mineralisations in Proterozoic basement windows and overlying Caledonian nappe complexes in central and northern Nordland between Mo i Rana in the south and Ofotfjorden in the north (Fig. 1).

The economic background of the study is the increasing demand for several of these elements, in most cases related to their use in high-technology applications. The REE are a group of 17 elements including the 15 lanthanides (Ce to Lu), scandium (Sc) and yttrium (Y) (Table 1). Two groups of REE are distinguished based on their atomic weight: light REE (LREE: Sc, Y, La-Sm) and heavy REE (HREE: Eu-Lu). Light REE, for which demand is, in general, greatest, are easier to extract from mineral concentrates and are generally of lower value than the heavy REE. REE have very specific uses in a multitude of markets. For example, Nd is critical to the properties of NdBFe high-strength, high-temperature magnets used in electric car batteries, wind turbines and hard disk drives: no substitutes are known for this and many other applications for Nd. La is a critical component in rechargeable Ni-metal hydride batteries (such as used in the Toyota Prius): current consumption is 10-15 kg/vehicle. La is also strategically important in its use as a catalyst breaking down crude oil to produce gasoline, diesel and jet fuel. Ce is used in glass for CRT, LCD, and TFT televisions. REE in general are critical components in a wide range of military equipment such as missiles and guidance systems and, thus, they have strategic importance. World resources of REE are contained primarily in bastnaesite and monazite. Bastnaesite deposits in China and the United States constitute the largest percentage of the world's rare-earth economic resources, while monazite deposits in Australia, Brazil, China, India, Malaysia, South Africa, Sri Lanka, Thailand, and the United States constitute the second largest segment. Apatite, cheralite, eudialyte, loparite, phosphorites, REE-bearing (ion adsorption) clays, spent uranium solutions, and xenotime make up most of the remaining resources (Formula of the named minerals are listed in Appendix 1). Allanite, LREE-bearing titanite and fluorite are less used REE-minerals. Undiscovered resources are thought to be very large relative to expected demand. However, China began to control the REE market in the late 1980s and accounts at present for over 95% of the world production. The Chinese government has now implemented export restrictions for REE. Western dependence on REE from China and China's export restrictions have led to a wave of global exploration activity (Industrial Minerals, 25th May 2010).

The general aim is to identify Zr-REE mineralisations with ≥ 2 wt.% REE(including Y) which are possibly enriched in Be, U and Th as well. Zr is usually bound in zircon, which is a valuable industrial mineral if its U- and Th-contents are low. Zr-REE mineralisations and related deposits are usually connected with alkali magmatic rocks, especially syenites, alkali granites and their pegmatites, as well as carbonatites. High concentrations of high-field-strength elements (HFSE: Zr, Hf, Nb, Ta, Ti), REE and some low-field-strength elements (Th, U) are related to the elevated solubility of these elements in alkaline and fluorine- and/or CO₂-rich alkaline magmas and post-magmatic fluids (e.g. Möller 1989a, b, Linnen and Cuney 2005). REE and Zr are relatively mobile in hydrothermal or hydrothermal-metamorphic and metasomatic systems where they locally form large mineral deposits (Möller 1989b, Samson and Wood 2005).

Table 1. Atomic numbers and upper crust abundance of REEs. The upper crust abundances (in ppm) are according Taylor and McLennan (1985). Promethium has not been proven on Earth.

Element	Symbol	Atomic number	Upper crust abundance
Scandium	Sc	21	30
Yttrium	Y	39	22
Lanthanum	La	57	30
Cerium	Ce	58	64
Praseodymium	Pr	59	7.1
Neodymium	Nd	60	26
Promethium	Pm	61	-
Samarium	Sm	62	4.5
Europium	Eu	63	0.88
Gadolinium	Gd	64	3.8
Terbium	Tb	65	0.64
Dysprosium	Dy	66	3.5
Holmium	Ho	67	0.8
Erbium	Er	68	2.3
Thulium	Tm	69	0.33
Ytterbium	Yb	70	2.2
Lutetium	Lu	71	0.32

The report is based on an unpublished memorandum by Peter Ihlen from NGU written in 2003. This report is a continuation and development of Peter Ihlen's report, with special emphasis on the assessment of potential target areas. It is a theoretical study based on the NGU mineral resources database, the Ural granite geochemistry data base, NGU reports and published scientific literature. According to the suggestions by Nordland Mineral the report focuses on the following potential indications and mineralisation types:

- 1) The Høgtuva Be-REE-U-Sn mineralisation and other mineralisations of the same type
- 2) Strongly fractionated granite intrusions
- 3) REE-fluorite mineralisations
- 4) Regional REE anomalies in stream sediments and tills
- 5) REE-silicates (allanite) in granites
- 6) NYF pegmatites
- 7) Hydrothermal Fe-deposits with associated REE enrichments
- 8) Th and allanite-bearing rocks indicated by the regional radioactivity
- 9) Basement granites, one containing 2-3% REE-oxides, by checking existing analyses

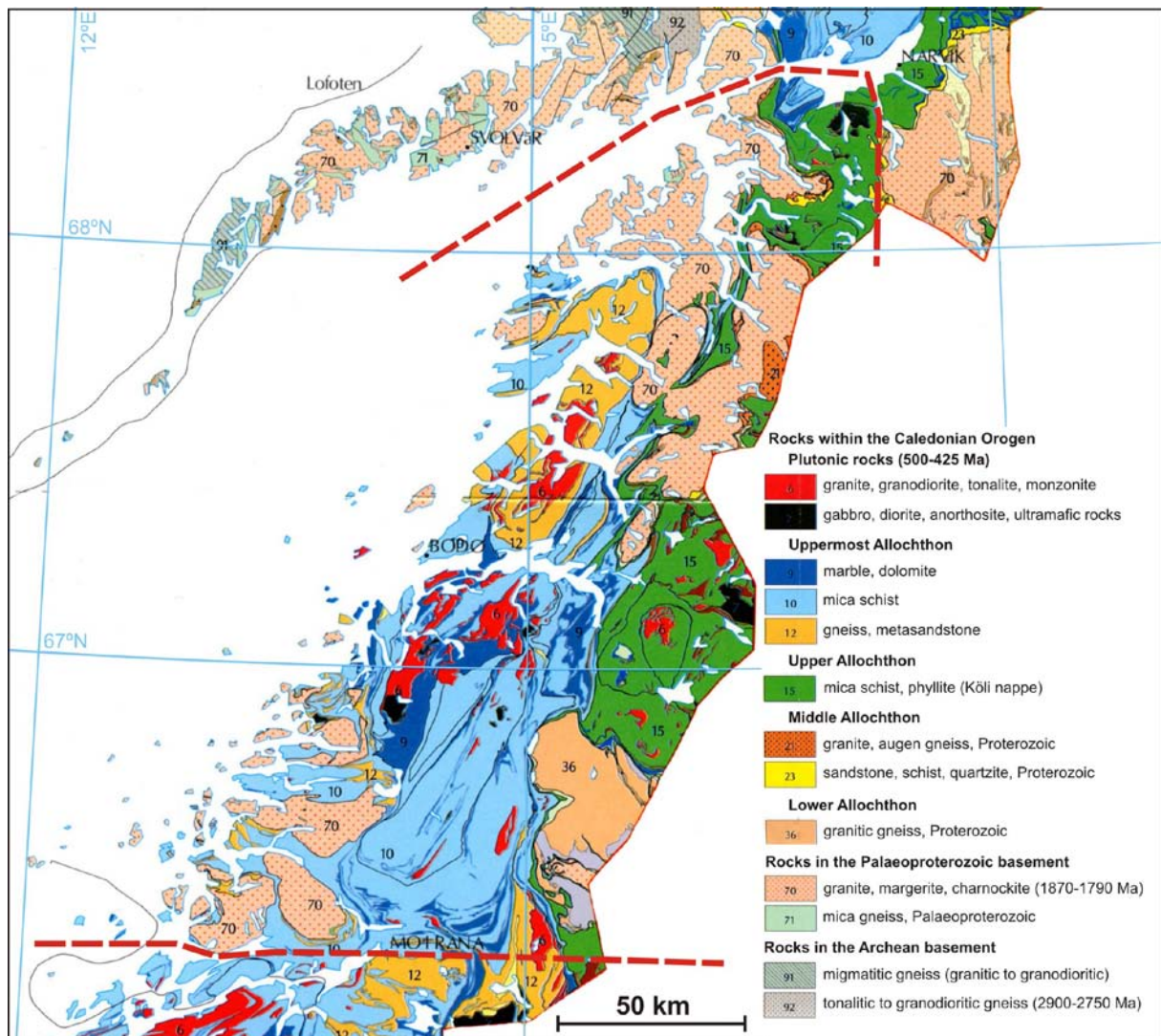


Figure 1. Geological map of central and northern Nordland according to Solli and Nordgulen (2006). The area considered in this study extends from Mo i Rana in the south to Ofotfjorden in the north (red dashed line).

2. Geology of central and northern Nordland

The geology of central and northern Nordland is dominated by Caledonian nappe complexes overlying the Svecofennian basement of the ancient continent Baltica. The basement is exposed in the tectonic windows (from south to north) of Sjona, Høgtuva, Svartisen, Nasafjell, Glomfjord, Bjellåtinden (Laksådal), Rishaugfjell, and Tysfjord (Fig. 2). The Rombak window, southeast of Narvik is not considered in the study.

The *Svecofennian rocks* exposed in the tectonic windows comprise predominantly undeformed and deformed, early Proterozoic granites, which are the oldest rocks in the study area. These igneous rocks document a more or less continuous and voluminous magmatic activity between 1850 to 1630 Ma, which developed between the Svecofennian (1920-1790 Ma) and Gothian orogeneses (1640-1520 Ma) (Lahtinen et al. 2008 and Bingen et al. 2008 respectively). They belong regionally to the Trans-Scandinavian Igneous Belt (TIB), which comprises a giant elongated array of batholiths extending c. 1400 km along the Scandinavian Peninsula from south-easternmost Sweden to Troms in north-western Norway (Gorbatshev

1985; Fig. 3). The regional TIB complexes comprise a number of individual batholiths, partially associated with continental volcanic rocks, pegmatites and migmatites.

At a mega-scale the TIB complexes are discordant to the Svecofennian units (NNE-SSW), but at a local scale the individual batholiths are concordant to the Svecofennian structures (NNW-SSE and NW-SE). The TIB has a complex structure and is related to a number of orogenic belts developed in the period between 1850 and 1660 Ma as a result of microcontinent-microcontinent and island-arc-microcontinent collisions at margin of the Baltic continent. That means that the TIB plutons, which are predominantly post-orogenic granites, occur together with syn-orogenic granites and have ages which correspond to the orogenic activity at other places of the craton. The TIB comprises the granite massifs of Småland, Värmland, Rätan, Dala, Sorsele and Revsund, south and east of the Caledonian front. The granite massifs exposed as windows within the Caledonides are not well differentiated except for the Tysfjord granites. A number of the granite complexes within the Caledonides and at the eastern margin of the Sveconorwegian orogeny in Värmland underwent amphibolite-facies metamorphism.

The TIB magmatism in southern Sweden has been tentatively separated into two different episodes: TIB-1 group of 1810–1770 Ma and TIB-2 group of 1710–1660 (Lathinen et al. 2008). The southern part of the belt from the Grong-Olden window to the south is dominated by TIB-2 plutons and associated volcanic rocks, whereas the northern part of the belt – the study area – consists mainly of both TIB-1 and TIB-2 plutons. For examples, the meta-monzonites and -syenites of the Sjøna and Høgtuva windows show ages of 1797 ± 3 Ma and 1800 ± 2 Ma, respectively (Skår 2002).

The granites are characterised by the occurrence of biotite and/or hornblende and allanite-epidote. Because of accessory magnetite, the plutons cause regional magnetic anomalies, which can be easily identified on magnetic maps. These magnetite granites are typical for I-type (igneous source) rocks and A-type (anorogenic source) rocks (e.g. Whalen et al. 1987, Chappell and White 2001, Bonin 2007). Associated volcanic magmatism has commonly a bimodal character (basalt/rhyolite) with predominance of felsic continental volcanic rocks (within-plate volcanites). This is typical for A-type magmatism, which develops in connection with extensional tectonics (rifting) in the continental crust away from subduction zones. I-type magmatism is generally found close to subduction zones and develops in island arcs with calc-alkaline granitoids comprising diorites, granodiorites, tonalites and granites (pre- to syn-orogenic granitoids). Both types of magmatism occur in the TIB, which can be considered as a mature continental island-arc complex above an east-trending subduction zone (Högdahl et al. 2004).

Geochemical investigations of TIB plutons east and south of the Caledonides reveal a sub-alkaline character in the magma with an alkali-calcic differentiation trend (e.g. Högdahl et al. 2004). The older TIB magmatism shows locally calc-alkaline and calcic differentiation trends. The granites and rhyolites typically have a high K/Na ratio and a meta-aluminous to weak per-aluminous (<1% normative corundum) composition locally also with per-alkaline phases. The granite complexes comprise monzonitic, syenitic and peralkaline granitic differentiates, whereas trachytes (volcanic equivalent of syenite) and rhyolites occur in the volcanic complexes. A number of the TIB plutons are considered as high heat-production (HHP) granites because of their relative high U (~4 ppm) and Th (~10 ppm) contents (Wilson and Åkerblom 1980). Bjørlykke et al (1991) reported 10 ppm U and 35 ppm Th in the Revsund granites, which is ten times higher than the average U and Th contents of the continental crust.

TIB plutons outside the Caledonides and some of the felsic volcanic sequences are associated with U, Mo, W and Li-Sn-Ta mineralisations (Öhlander 1986, Gower 1992). In the Torsbyo area north of Vänern there are REE-mineralisations in veins of per-alkaline granite (1690 Ma; TIB-2) and in Sveconorwegian pegmatites (942 MA, Romer and Smeds 1996).

The latter represent presumably re-melted TIB plutons enriched in Nb, Ta, Li, Y, REE and Be. Granitic pegmatites enriched in U, Sn, and Li-Sn-Ta occur in meta-greywacke at the contact of the Råtan and Revsund TIB-1 granites in the Skelleftefelt in central north Sweden. TIB-2 granites southeast of the Skelleftefelt are associated with and greisen mineralisations containing wolframite and scheelite. Molybdenite mineralisations with fluorite, pyrite, chalcopyrite and scheelite occur in aplitic intrusives and pegmatite veins at the contacts of large TIB-1 granite massifs north of the Skelleftefelt. The indicated resources in this area are 1 to 1.5 Mt with 0.1-0.2 Mo. Uraninite and uranotitanate occur in veins and are disseminated in TIB granites, intermediate volcanic rocks and dolerites in the Arvidsjaur and Arjeplog districts (Skelleftefelt; Öhlander 1986). The Pleutajokk deposit, which has U resources of 6000 t, is situated in the Arjeplog district. U-mineralisations are common in Vendian and Cambrian sediments along the eastern Caledonian margin in Sweden. stratabound, disseminated uraninite and uranotitanate mineralisations occur in a rhyolite-arenite sequence (ca. 1750 Ma) west of the Skelleftefelt (Dobblon area) with up to 0.3 % U and 0.2 % Mo (Öhlander 1986). The U mineralisation is assumed to be associated with the devitrification of ignimbrites, which contain titanite, apatite, and U-rich zircon. However, economic mineralisation are - so far - not known in the TIB plutons and associated bimodal volcanites occurring in the Norwegian Caledonides of the study area, except the Høgtuva Be-REE-U-Sn-mineralisation. The Høgtuva mineralisation is located in TIB-type granitic gneisses and comprises 350 000 t ore with 0.18 % Be (Lindahl and Grauch 1988; see also chapter 3.6.1).

The *Caledonian nappe complexes* were emplaced on the Baltic continent (today Scandinavia and Baltic region) during the Silurian–Devonian (430-390 Ma) closure of the Iapetus ocean and the subsequent collision of the continents Laurentia and Baltica. The nappe complexes consist of four allochthons (rock units which have been moved from their original site of formation): the Lower, Middle, Upper, and Uppermost Allochthons (Gee and Sturt 1985, Roberts and Gee 1985, Gee et al. 2008). The nappe complexes exposed in the study area comprise parts of the Upper Allochthon (Köli nappe) and the Uppermost Allochthon (Helgeland and Röddingsfjell nappe complexes; Fig. 4). Thin units belonging to the Middle and Lower Allochthons occur at the periphery of the Nasafjell basement window.

The *Köli nappe* (upper part of the Upper Allochthon) is dominated by metamorphosed sedimentary and igneous rocks – mica schist, phyllite, greenstone - derived from the ancient Iapetus Ocean, including ophiolites and island arc complexes (Stephens 1988, Andréasson 1994, Grenne et al. 1999, Roberts 2003).

The Uppermost Allochthon (*Helgeland and Röddingsfjell nappe complexes*) is generally interpreted to have formed in a continental margin setting with affinities to the Laurentian margin and comprises calc-silicate units, calcareous, pelitic, psammitic, and clastic metasedimentary rocks (see review in Roberts et al., 2007). The rocks underwent different grades of metamorphism from greenschist to high-grade amphibolite facies.

The evolution of the Caledonian orogen was accompanied with different types and stages of mafic, intermediate and felsic magmatism (e.g. Stephens et al. 1985). There is a cluster of Caledonian granitic and granodioritic plutons in the Uppermost Allochthon south and northeast of Bodø which has not been studied in detail so far. The minor W-(Mo) skarn mineralisations at Bjellåtind (Laksådal) and Målvika (Bindal; not in the study area) were previously interpreted as regional (not intrusion-related) skarn mineralisations. However, recent studies revealed that they are related to the Caledonian intermediate to felsic magmatism (Müller 2008, Drivenes 2010). The infiltration of the Caledonian nappe complexes by granitic magmas bear the potential that skarn and hydrothermal vein deposits were formed due to the release of mineralising magmatic fluids. Another interesting mineralisation type is metamorphic U-Mo-(W) mineralisations at the basement window/Caledonian nappe boundaries, such as the Harelifjell mineralisation at the western

contact of the Rishaugfjell window (Lindahl 1983; see chapter 3.2.1). These are discussed in the chapters on the particular basement window, where they occur.

In summary, possible REE- and rare metal mineralisations are related to three major metallogenic time periods and settings: 1) Proterozoic metal enrichments in granites and pegmatites, 2) Early Palaeozoic stream/clastic sediments and 3) Caledonian pegmatites and hydrothermal veins situated immediately above the tectonic cover/basement boundary. The latter represent precipitated fluids/melts which leached the metals from the basement rocks.

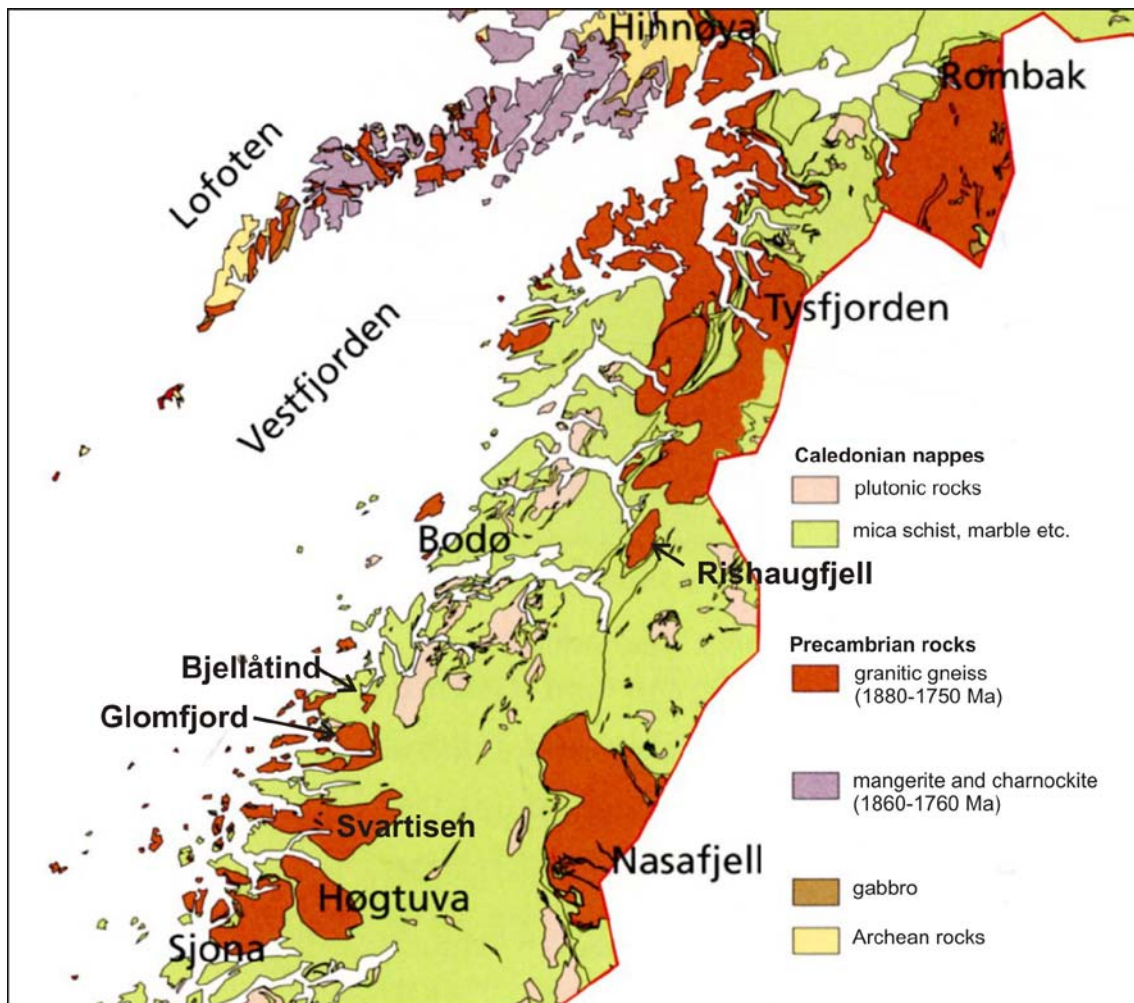


Figure 2. Simplified geological map of central and northern Nordland showing the distribution of basement windows (red) within the Caledonian nappes (green). From Ramberg et al. (2006).

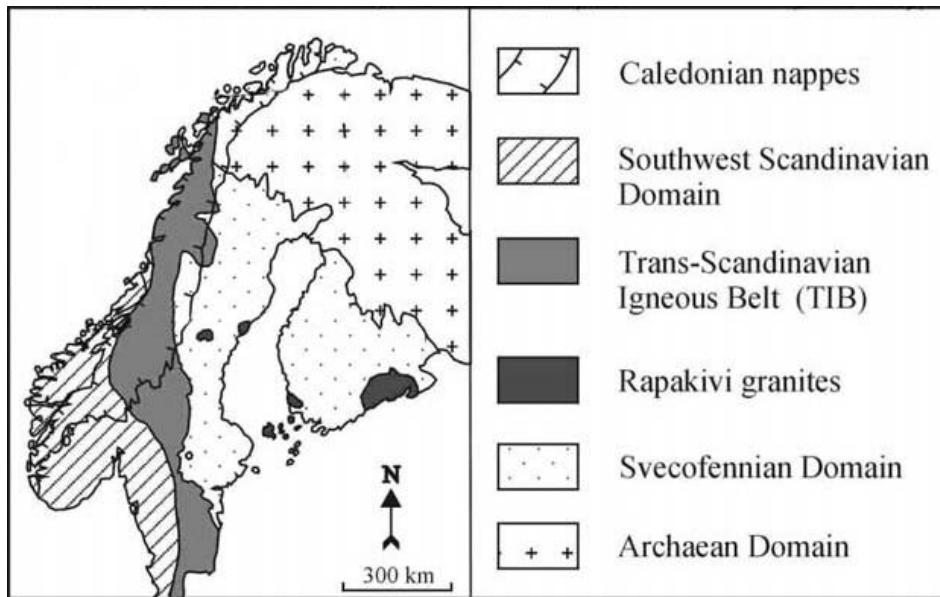


Figure 3. Geological map of Scandinavia showing the extension of the Trans-Scandinavian Igneous Belt (TIB). From Skår (2002).

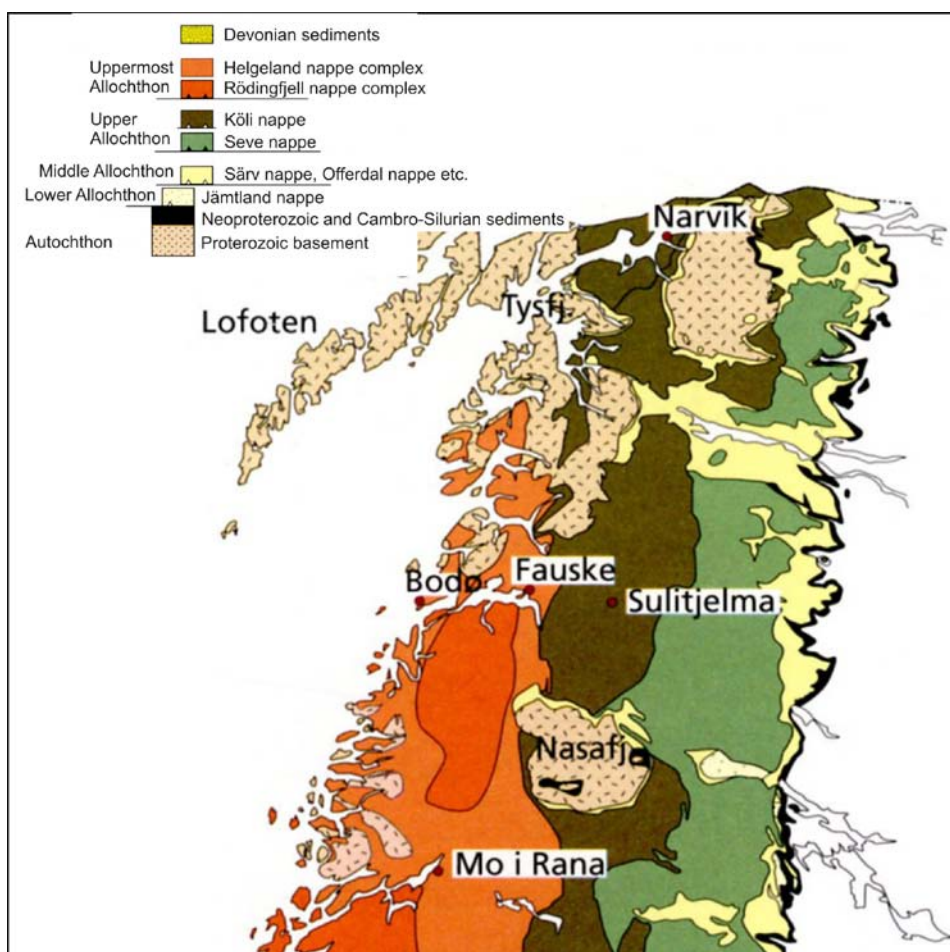


Figure 4. Simplified geological map showing the major Caledonian nappe complexes in central and northern Nordland. From Ramberg et al. (2006).

3. Mineralisations of the Svecofennian basement windows

TIB plutons and associated bimodal volcanic sequences which are exposed in basement windows within the Caledonides of Nordland represent predominantly deformed and gneissic equivalents of TIB intrusions exposed east and south of the Caledonian front. In the following, the basement windows and their REE, Zr, Be, U, Th, (W) mineralisations in central and northern Nordland are discussed from north to south.

3.1 Tysfjord(-Hamarøy) window

In the Tysfjord basement window there are a number of ortho-magmatic enrichments of Be, Mo, U, Th, Y, REE and Sn in pegmatites, in different types of meta-aluminous to per-alkaline granites (TIB types) and in enclaves of volcano-sedimentary sequences within the TIB granites (Wildberg 1987). The U-Pb ages of the granites in the area fall into two groups 1796-1770 Ma (TIB-1) and 1719-1703 Ma (TIB-2; Romer et al. 1992).

The TIB granites of the entire Tysfjord area contain accessory fluorite (Foslie 1941). Granites in the southernmost part of the Tysfjord window contain elevated concentrations of U, Th, Be, Li, Y, REE, Zr, Sn and Nb (Stendal 1990). The most anomalous granites, which are radioactive due to U-bearing micas, are strongly leucocratic and occur preferentially along the contact to Vendian-Cambrian meta-sediments. These granites have low K/Rb, Sr/Rb, Ba/Rb and Mg/Li ratios, which reflect their high degree of differentiation. Stendal (1990) reported strong enrichments of REE in the Sommerseth granite (a small basement window at the southern end of the Tysfjord window) with up to 1.3 % Zr, 0.9% Ce, 0.45 % La, 0.35 % Nd, 0.2 % Y, 0.16 % Th and 0.1 % Nb. He stated that the TIB granites in the southern part of the Tysfjord window have a good potential for REE mineralisations, in particular highly fractionated granites with low K/Rb, Ba/Rb and Mg/Li and high Rb/Sr. Granites in the area also have elevated Be, Li, Nb, Sn, U, and Y concentrations.

Figures 5 and 6 show maps of airborne surveys of Th radiation in the Hellemobotn-Linnajavrre-Gjerdal and Ulsvåg (Hamarøy) areas. The measurements were carried out by NGU in 1991 and 1976, respectively. Both areas are dominated by TIB-granites. The map of the Hellemobotn-Linnajavrre-Gjerdal area shows strong signals at Gallotjåhkjavrre, Tjårok, Rumbogierjavrre, Reinoksfjellet and Gasskatjåhkkå (Fig. 5). The Ulsvåg map has high Th-radiation signals at Tilthornet and Kjerrfjellet-Kjerrvatnet (Fig. 6) indicating the Th-enrichment of particular TIB-granites. These granites, being highly evolved, have the potential to be enriched in REE. These granites should be sampled in order to check their contents of REE and other elements. The REE concentrations of these granites might not reach 2 %, but possibly 0.5 %. However, the intrusions are rather large, making them economically interesting.

The granites contain numerous pegmatite lenses which were mined for feldspar. Today some of the pegmatites are the source of high-purity quartz (Norwegian Crystallites AS, Drag; see chapter 3.1.6)

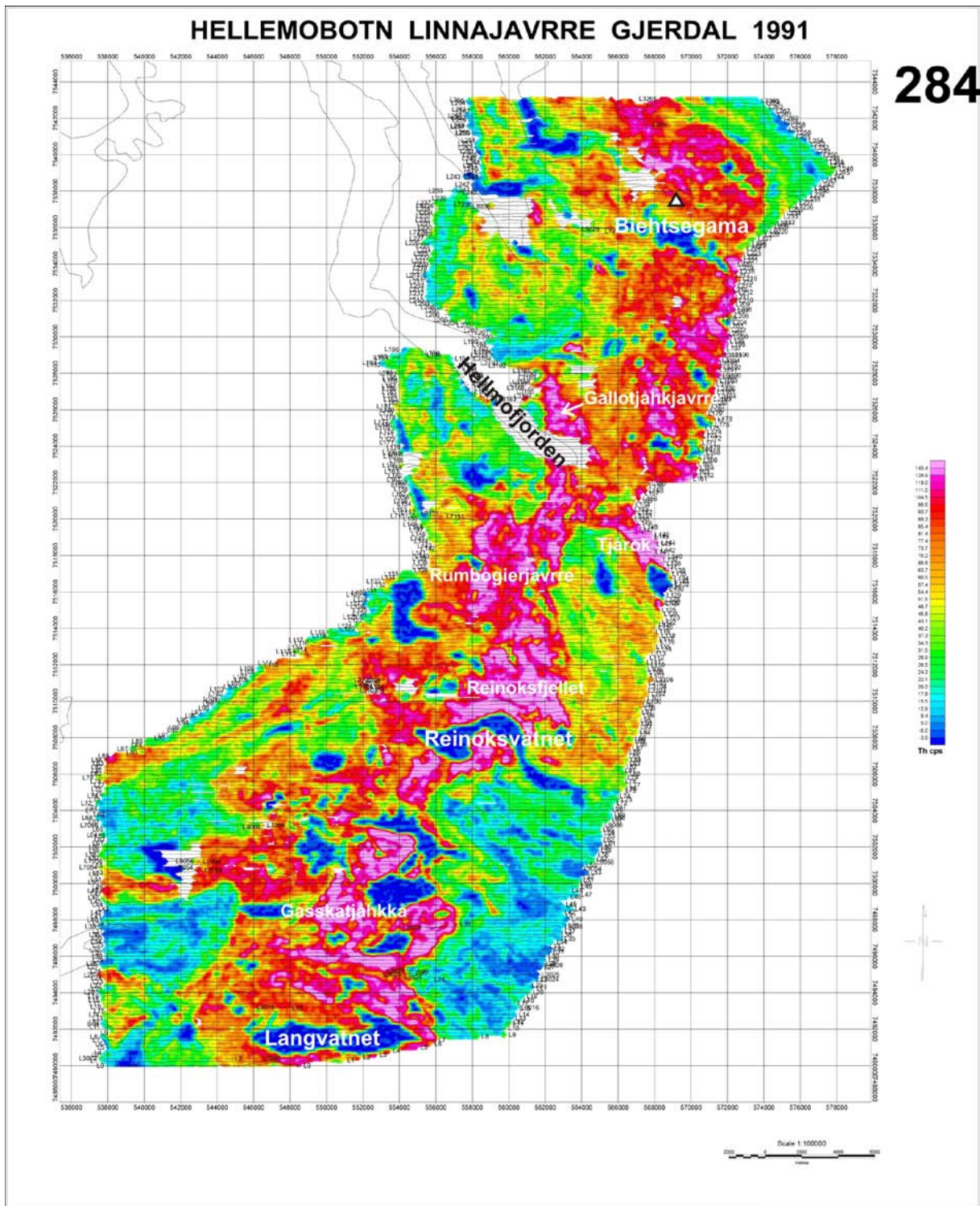


Figure 5. Airborne Th-radiation map of the Hellemobotn-Linnajavrre-Gjerdal area (eastern Tysfjord window) obtained by NGU in 1991. For explanations see text.

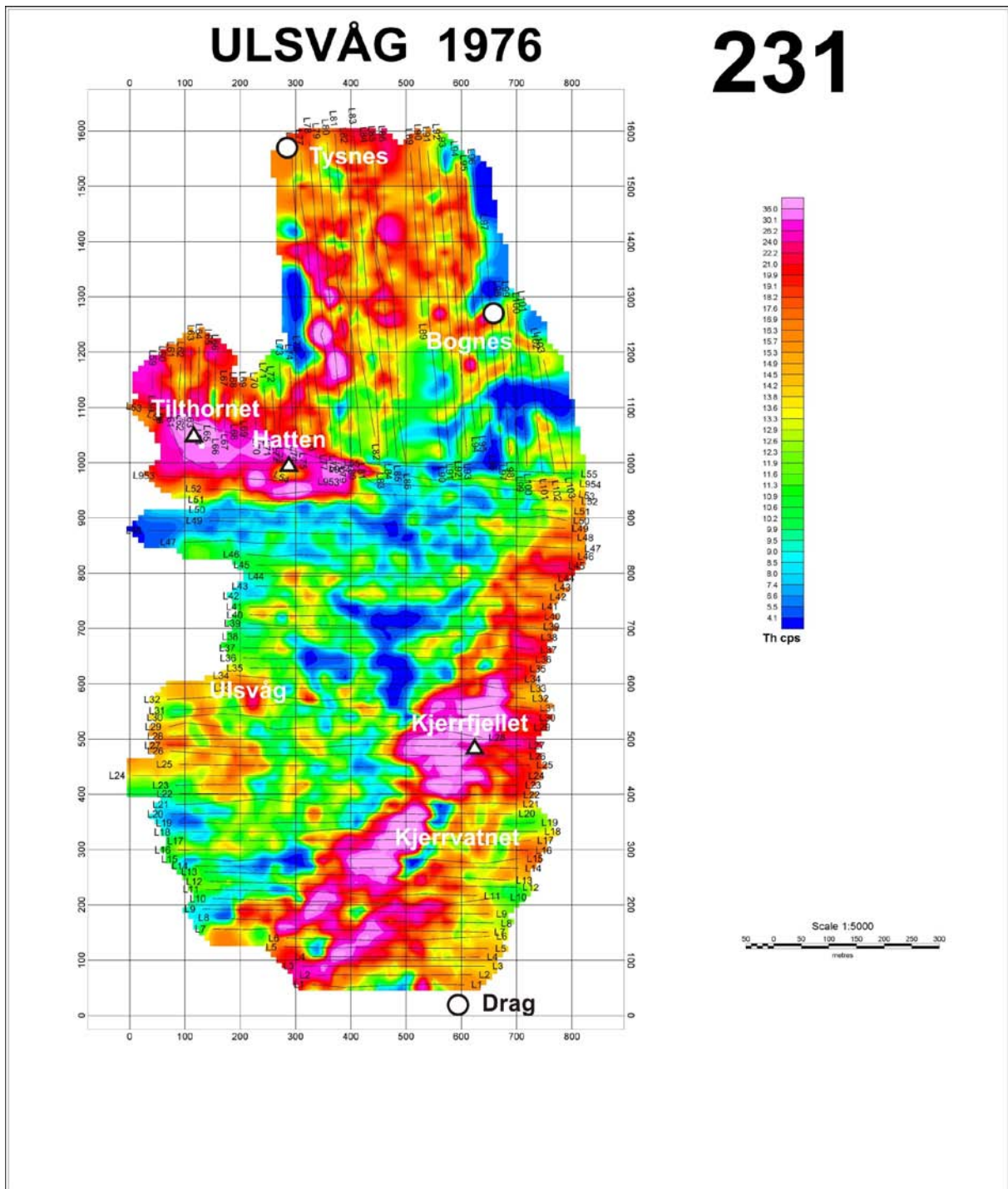


Figure 6. Airborne Th-radiation map of the Ulsvåg (Hamarøy, Tysfjord window) area obtained by NGU in 1976. For explanations see text.

3.1.1 Fluorite mineralisation at Mannfjellvatn

At the northern border of the Tysfjord basement window between the Store and Lille Mannfjellvatn there are fluorite mineralisations, which were first described by Foslie (1921). Foslie (1921) described fluorite concentrations of up to 30% in quartzite immediately above the tectonic contact to the Tysfjord granites and overlying allochthonous meta-sediments. Neither P. Ihlen nor L.-P. Nilsson could verify Foslie's fluorite-rich quartzite occurrence (personal comm.). Part of the reason for not being able to confirm Foslie's fluorite occurrence

may be that the topographic maps in his day were of very poor quality. However, Nilssen (2004) identified a fluorite-bearing quartz-calcite vein in the Tysfjord granite, ca. 20 m below the contact to the overlying quartzites in the area, which was described by Foslie (1921; UTM 33 W 567610E/7544170N). The vein is about 50 m long, 1.3 m wide at the ENE end and 0.2 m at the WSW end. The vein is situated in a shear zone and contains irregular impregnations of fine-grained, violet fluorite. A fluorite-rich sample which was analysed by Norsk Hydro, contained 7 % F. Thus, the high fluorite concentration described by Foslie (1921) may be misleading. The vein is interpreted as a hydrothermal mobilization which leached fluorite from the Tysfjord granite in connection with the Caledonian thrusting (Nilsson 2004). The fluorite mineralisation is too small to be of economic interest.

Similar carbonate-fluorite mineralisations occur at Langvann in Linnajarvi. The steep-dipping, meter-wide carbonate layers occur within coarse-grained TIB-granites. Foslie (1942) interpreted the layers as meta-sedimentary enclaves. However, they presumably represent calcite-fluorite(colourless)-veins of a type found also at Mannfjellvatn, Roktdal (Grong-Olden window), Høgtuva and Nasafjell (P. Ihlen; personal comm.).

3.1.2 Y-Ce-La-rich magnetite mineralisation at Storjord

At Storjord and Jernlia there are supracrustal enclaves within the TIB granites which contain small magnetite mineralisations with common fluorite, REE- and U-minerals, for example uraninite, thorite, allanite, and xenotime (Lindahl 1984, Appendix 1, Fig. 7).

The Storjord mineralisation is situated in amphibolitic gneisses at the top of the 120-m high Storhaugen, 300 m east of the E6 and 2.5 km south of the Bognes holiday camp. The ore is banded and rich in 0.2 to 8 mm large magnetite grains. The mineralisation occurs in two amphibolite lenses (interpreted as enclaves) embedded in K-rich meta-volcanites which were subsequently intruded by TIB-type granites (A. Korneliussen; personal comm.). The tonnage of the northern lens is 20 500 t (6.25 x 40 x 20 m) and of the southern lens 246 000 t (17.14 x 70 x 50 m) with a total 266 500 t magnetite ore. The average concentrations of 6 ore samples determined by Norsk Jernverk are 52.1 % Fe_{tot.}, 50.9 % Fe_{magn.}, 0.4 % MnO, 0.9 % TiO₂, 0.08 % P, and 0.005 % S.

The deposit was sampled and studied by Are Korneliussen from NGU between 1983 and 1985. The analytical results, including magnetic measurements, were published by Rønning (1986). Korneliussen sampled the mineralisation and detected high concentrations of Y, Ce, La, U and Th in the ore. Analyses of 18 mineralized amphibolite samples revealed average concentrations of 1157 ppm Y, 2391 ppm Ce, 888 ppm La, 93 ppm U and 221 ppm Th. Thus, the average REE concentration of the magnetite ore is approx. 0.5 % (Fig. 8; Appendix 2). For comparison the host rocks (18 analyses) contain 140 ppm Y, 283 ppm Ce, 109 ppm La, 2 ppm U and 30 ppm Th.

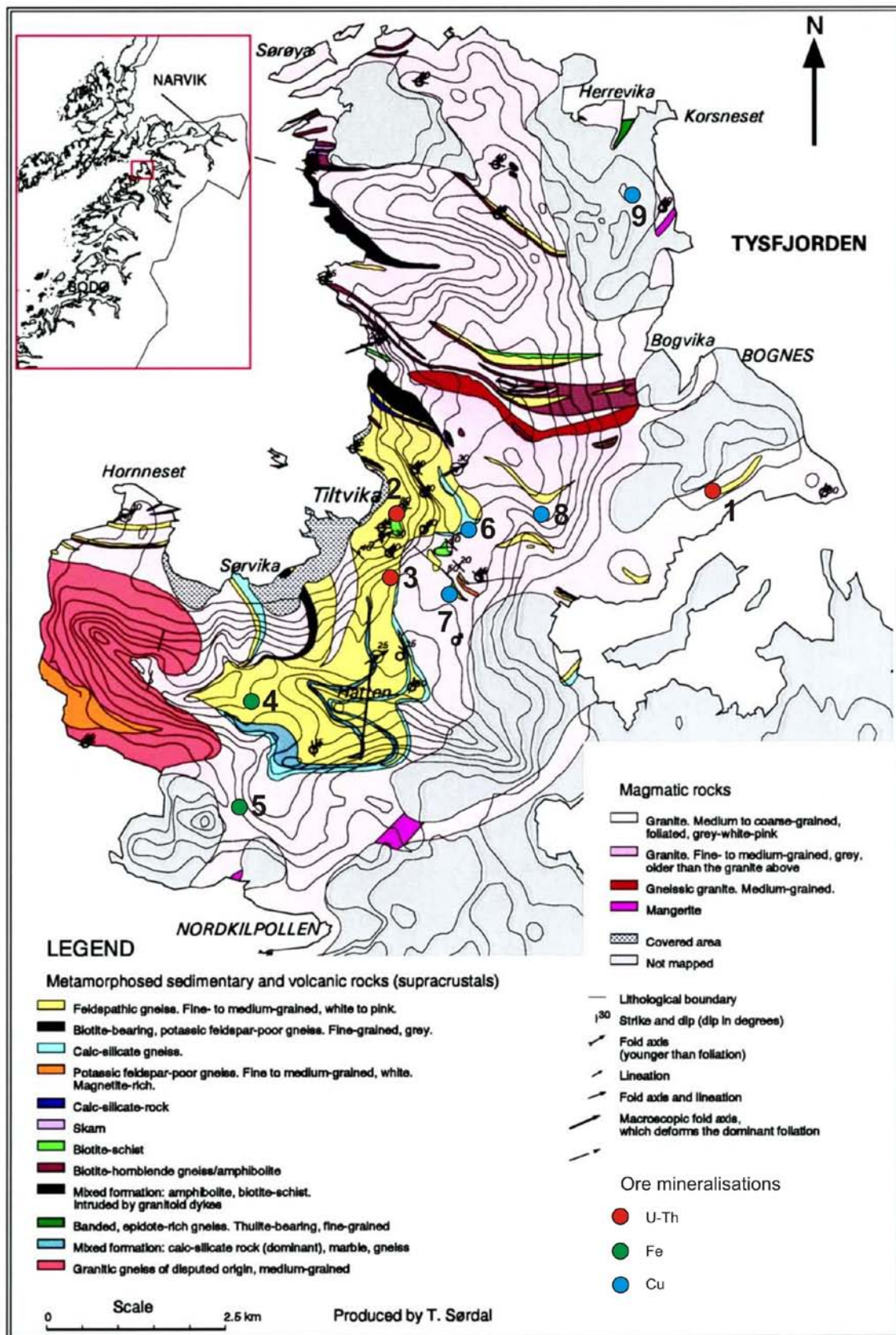


Figure 7. Geological map of the Tynes peninsula, Hamarøy, by Karlsen (2000) showing the locations of U-Th, Fe, and Cu-mineralisations. 1 – Storjord, 2 – Tiltvika north, 3 – Tiltvika south, 4 – Skarvik, 5 – Hundemullen, 6 – Lillebotn, 7 – Lillebotn south, 8 - Skogvoll, 9 – Lødhaugen (Karlstrøm 1990, NGU database).

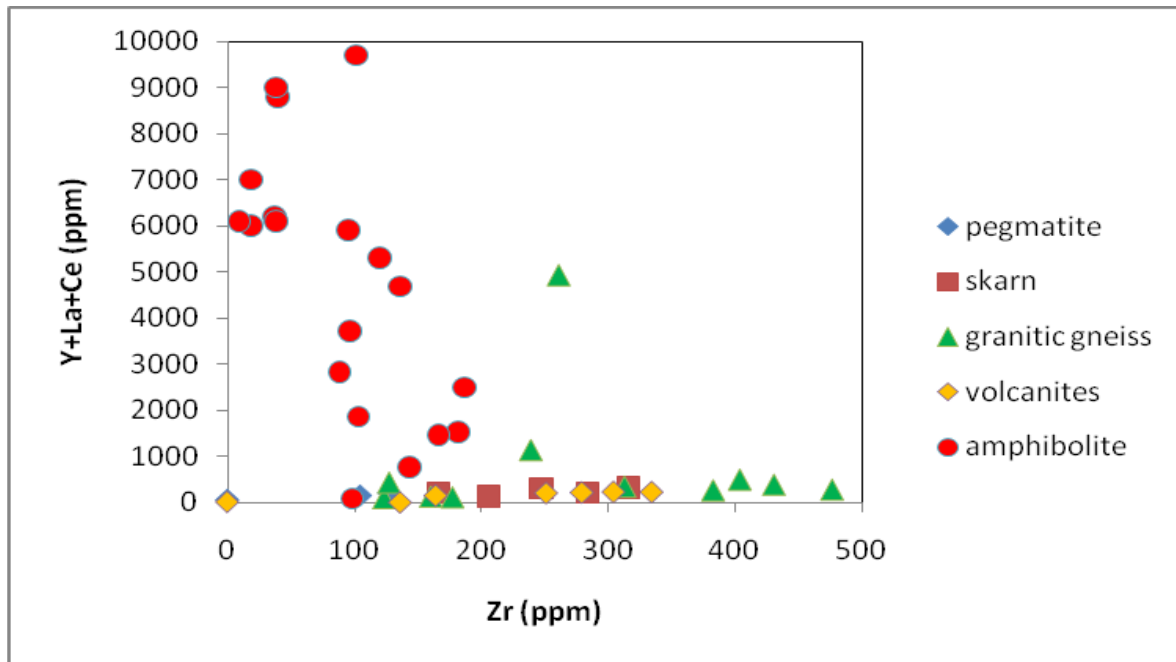


Figure 8. Concentrations of Zr versus Y+La+Ce of different rocks associated with the magnetite mineralisation at Storjord (data from Rønning 1986 and unpublished data by A. Korneliussen). The Y-Ce-La mineralisation is related to amphibolite enclaves in meta-volcanites with an average of 0.5 % REE.

3.1.3 Tiltvik U-Th mineralisation

Two U-Th sulfide mineralisations occur east of Tiltvik in K-rich meta-rhyolites within a large enclave of volcanites and meta-sediments on Tysnes peninsula (UTM 33 540133E/7565346; 540333E/7565896N; Fig. 7). The mineralisations have not been described but they are very small (P. Ihlen, personal comm.). Beside these two U-Th mineralisations several small Cu-(Zn) and magnetite mineralisations were identified in epidote- and/or garnet-rich zones (Karlstrøm 1990). The Storjord magnetite mineralisation occurs in the same area and units. Airborne radiometric survey data (Håbrekke, 1979) indicate that the magnetite mineralisations are very small.

3.1.4 Kalvik Mo-U-(W) mineralisation

Hansen (1983) describes Mo-U-(W) mineralisations at the contact of granitic gneiss (TIB-type) and a Caledonian meta-sedimentary sequence in the Kalvik window on the southern shore of Leirfjord, Sørfold (Fig. 9). The Kalvik window is a very small basement window immediately SW of the Tysfjord window, exposing granitic gneisses in an area of approx. 3 km². Because of the close proximity to the Tysfjord window, the Kalvik window is here considered as part of the Tysfjord window. The granitic gneisses revealed a Rb-Sr whole rock age of 1730-1780 Ma (Wilson and Nicholson 1973). The granitic gneiss contains 10 ppm U, 35 ppm Th, 5 ppm Mo, 288 ppm Zr, 21 ppm Nb, and 51 ppm Y (average of 7 analyses). The mineralisation was discovered in 1918. In 1979 NGU drilled two holes through the basement/cover sequence without finding any mineralisation. In 1981/82 H. Stendal and A.K. Hansen from København University studied the mineralisation in detail (Hansen 1983).

U-Mo mineralisations occur in a 5 m wide, mica-rich layer of granitic gneiss and in the contact zone in a 1 m wide belt. Mo-W mineralisations occur in the overlying sediments. All the mineralisations seem to be related to granitic pegmatites and segregations. A 50 to 100 m² large pegmatite (quartz, feldspar and mica) occurs at UTM 33 526200E/7489600N in pelitic schists. The pegmatite is rich in large molybdenite crystals (up to 10%). Often (1979) reported up to 582 ppm Mo and 1.13 % W from here. Ca. 30-40 m below the tectonic contact in the granitic gneiss, a 5 m thick, garnet- and mica-rich layer is exposed (UTM 33 528600E/7491150N). The layer can be followed ca. 1 km parallel to the contact (Fig. 10). The layer is locally enriched in Mo and U, in particular in an area with small folds. Molybdenite grains are up to 2 cm and form up to 5 % in the mineralized zones. There are also Mo-U-mineralisations at the contact (UTM 33 527750E/7491550N and 528450E/7491450N). The mineralized areas are small, from several cm up to 1 m. The U seems to be associated with coarse-grained biotite. Fluorite and scheelite were observed in some of the sedimentary rocks where Mo and U occur together. Average bulk analyses show concentrations of 0.07 % and 0.12 % MoS₂ (Flood 1944). Stendal (1990) provided average bulk rock concentrations of the ore with 1.3 % Zr, 0.9 % Ce, 0.45 % La, 0.35 % Nd, 0.20 % Y, 0.16 % Th, and 0.10 % Nb. He stated that the TIB granites in the southern part of the Tysfjord window have a potential for REE and rare metal mineralisations because of their low K/Rb, Mg/Li, Ba/Rb and high Rb/Sr ratios. The granites in the area are characterised by elevated Be, Li, Nb, Sn, U and Y. However, the Mo-U mineralisations in the Kalvik window are very small but locally rich in U, Mo, W, Y and REE. They are non-economic.

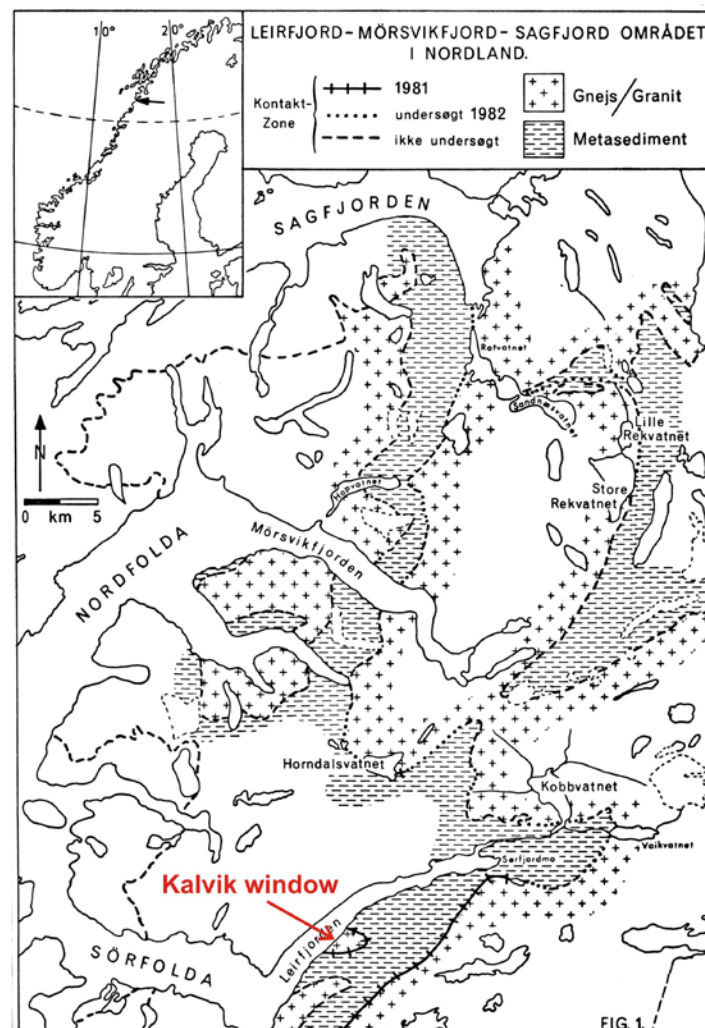


Figure 9. Location of the Kalvik basement window. From Hansen (1983).

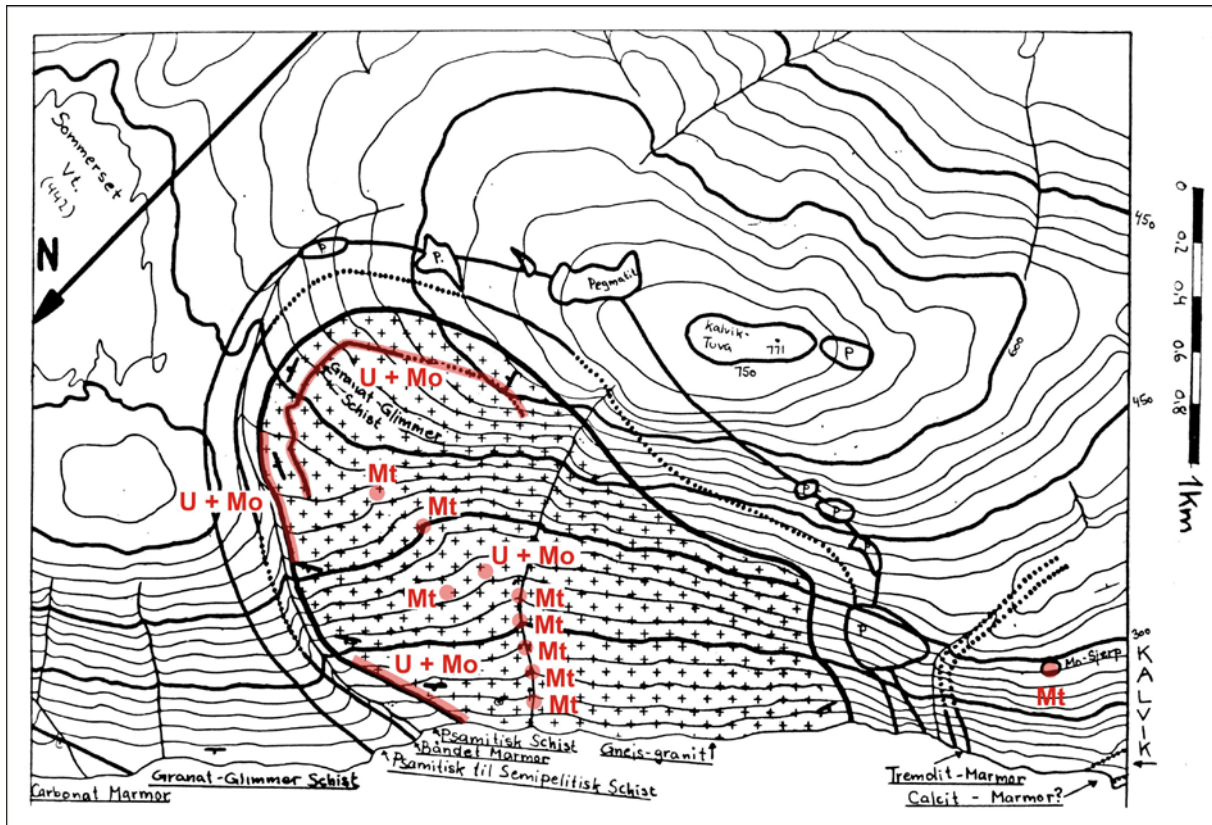


Figure 10. U-Mo mineralisations of the Kalkvik window according to Hansen (1983). U – uranium mineralisation, Mo – molybdenite, Mt – magnetite.

3.1.5 The REE-U-Th-Be enrichments in the younger Hellemobotn granites

Sampling of stream sediments at Hellemobotn was carried out in connection with regional investigations in Nordland and Troms (Kjeldsen 1987, Korneliussen et al. 1989), which indicated enrichment of La, Ce and Be in the Hellemobotn-Linnajavri area. Other indications came from airborne radiometric measurements in the area *Veikvatn – Gjerdal – Linnajavri* (Furuhaug 1990).

In 1988 rock samples were collected from this area (one sample per km², altogether 246 samples; Furuhaug 1990). The average concentrations for the granite samples are 0.9 ppm Be, 84 ppm La and 152 ppm Ce (Korneliussen et al. 1989). The maximum values are 336 ppm La, 512 ppm Ce and 358 ppm Be. Within the granites there are radioactive aplite dykes with up to 722 ppm La, 1150 ppm Ce, 232 ppm Y, 999 ppm Zr, 249 ppm Th and 52 ppm U (Korneliussen et al. 1989). However, according to A. Korneliussen (personal comm.), the Be-REE enrichments are far from being of economic interest.

Romer et al. (1992) provided a geochemical data set from the Hellemobotn granites. They distinguish older granites ca. 1.79 Ma (TIB-1) and younger granites ca. 1.71 Ma (TIB-2). The older, less evolved granites (5 analyses) contain 184 ppm Zr, 29 ppm Y, 79 ppm La, 146 ppm Ce, 26 ppm Th, and 4 ppm U. The younger, more evolved granites contain (22 analyses) 390 ppm Zr, 82 ppm Y, 178 ppm La, 305 ppm Ce, 81 ppm Th and 19 ppm U. The highest concentrations are 1200 ppm Zr, 232 ppm Y, 722 ppm La, 1150 ppm Ce, 249 ppm Th and 53 ppm U (samples GH5-39, GH6-40, GH6B-41, KH63-18, Fig. 11; Appendix 3).

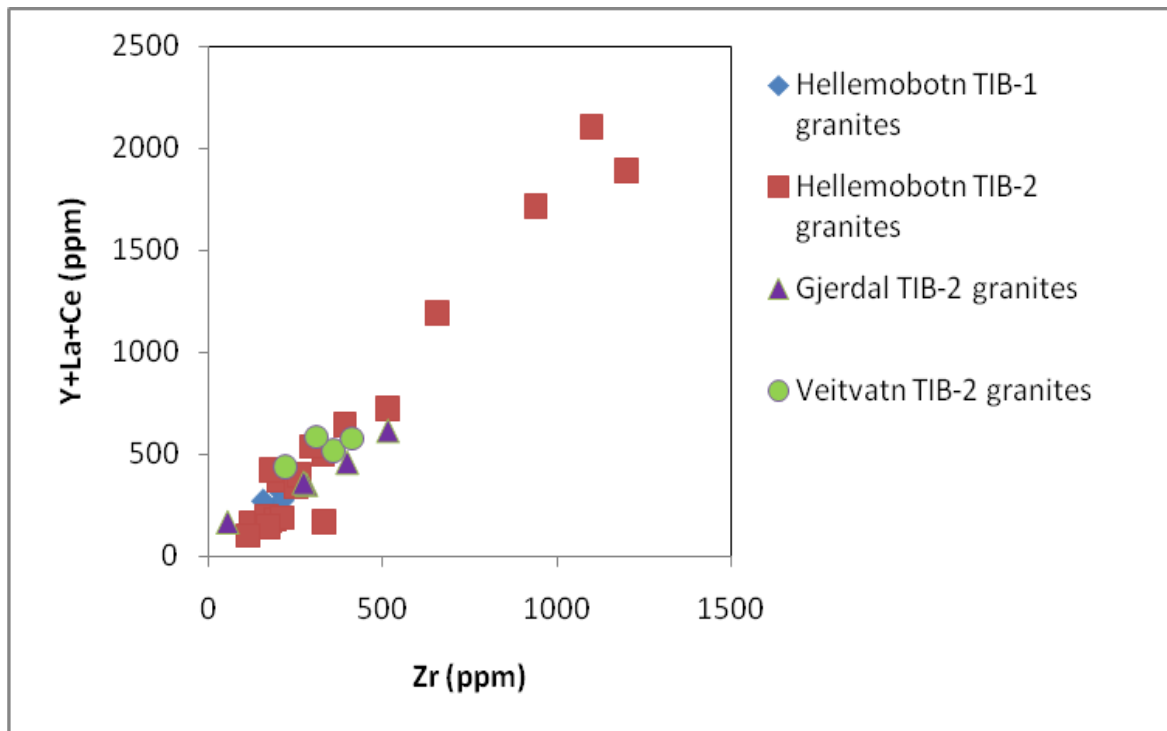


Figure 11. Concentrations of Zr versus Y+La+Ce+Sm for some Tysfjord TIB-type granites (data from Romer et al. 1992). Some of the younger Hellemobotn granites show relatively high concentrations of all these elements. It is assumed that these younger granites are responsible for the heavy element enrichment in stream sediments detected by Kjeldsen (1987) and Korneliussen et al. (1989).

3.1.6 Pegmatites associated with TIB-magmatism

Many TIB-granite-related pegmatites in the Tysfjord area commonly contain fluorite which is partially enriched in Y and Ce in the form of yttrifluorite, cerfluorite and fluocerite, for example in the Drag and Hundholmen pegmatites (Fig. 12). According to Husdal (2008) two types of pegmatites occur in the Tysfjord area:

- 1) Large lenticular bodies of mainly microcline, quartz, biotite with sub-ordinate muscovite, plagioclase and fluorite. Diffuse borders against the granite and abundant interior strain indicators suggest a pre-Caledonian age; these pegmatites most probably represent the latest crystallisation stages of the Tysfjord TIB-granites. Accessory minerals are rich in REE, F, Nb, Ti, Ta, As, Th, U and Be (Vogt 1923, Neumann 1985, Lindahl 1990, Wilberg and Lindahl 1991). Apart from Tennvatn and Hellemobotn, all the pegmatites are of this type.
- 2) Small, undeformed, highly evolved pegmatites rich in amazonite, quartz, platy albite (cleavelandite), with smaller amounts of schorl. The bodies have sharp boundaries and cut the foliation of the granitic gneisses. A xenotime-(Y) from Tennvatn was dated to 370 Ma (Emma Rehnström; personal comm. in Husdal 2008) thus confirming the post-tectonic appearance. Replacement units of cleavelandite make significant volumes, and late fluids have deposited a number of rare minerals rich in Pb, Bi, REE, As, F, Nb, Be, U, Th and Sb.

Mining started in Hundholmen (1906; Fig. 13) and in different pegmatites in the Drag area (1907) and continued in these and additional occurrences in Tysfjord and Hamarøy continually or in intervals up to around 1970. Most pegmatites were mined for feldspar and some quartz. Two of these pegmatites were mined for minor high-quality fluorite: The

Hundholmen pegmatite (Foslie 1941) and the Jennyhaugen pegmatite at Drag, Tysfjord (Rekstad 1919, Vogt 1923). The Tennvatn pegmatite was exploited for amazonite during a short period in the 1960s. Recent activity includes mining for quartz in Nedre Eivollen (underground) and Håkonhals, and occasional blasting in Jennyhaugen for gravel production.

With respect to REE, Y, Th and U mineralisations the partly exploited pegmatites have no economic potential because of the small size (1000 – 50 000 m³). However, the host granite of the Hundholmen pegmatite is described as a grey medium-to coarse-grained biotite-amphibole alkali granite with very common allanite and titanite (Vogt 1922). The amphibole is hastingsite – a Na-Ca amphibole. Whole-rock analyses of this granite are not reported. Due to its mineralogical description, the host granite of the Hundholmen granite may have REE concentrations >0.5%.

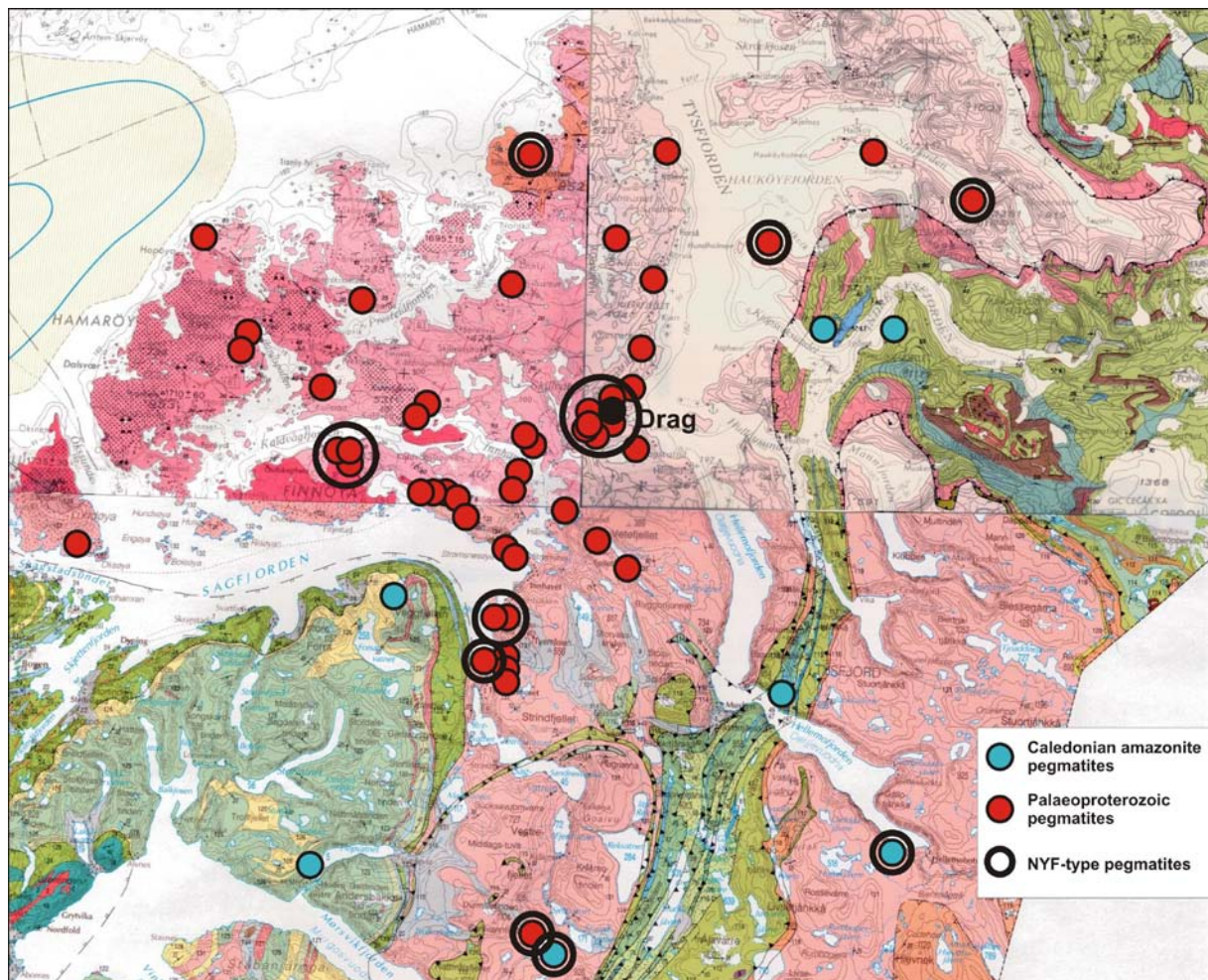


Figure 12. Pegmatite localities and types in the Tysfjord area. With permission from P. Ihlen (unpublished).

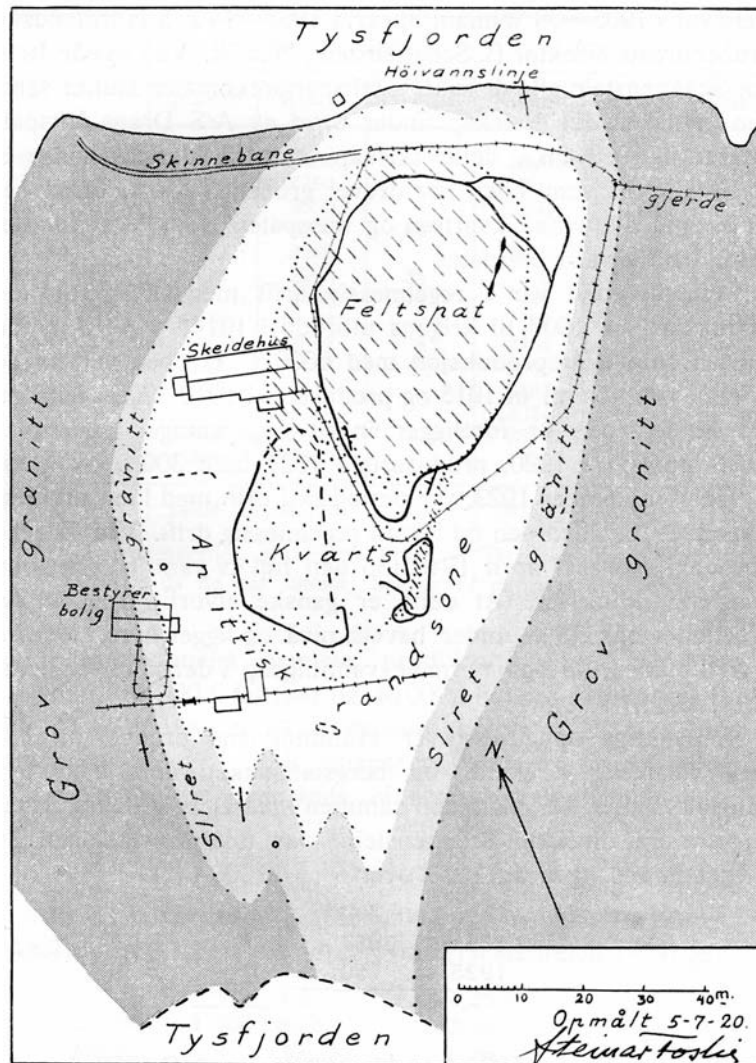


Figure 13. The Hundholmen pegmatite according to Foslie (1941). The pegmatite, which is famous for its yttrifluorite and REE minerals, is hosted by allanite-rich TIB-granites (UTM 33W 552625E/7559832N).

3.1.7 Other deposits in the area

A Mo-U mineralisation was identified at *Forsa* at the northern shore of the Forsahavet, Ballangen, by Lindahl (personal comm.). The mineralisation represents the metamorphic U-Mo-(W) mineralisation type, which is related to basement window/Caledonian nappe boundaries. The deposit has not been described.

Concentrations of colourless fluorite within deformed calcite lenses were identified at Mannfjordfjellet by Foslie (1941) within a sequence of Precambrian quartzites and schists and in underlying granites. The sequence is situated immediately below and above the tectonic contact between supracrustal rocks and the Tysfjord granites (L.P. Nilsson; personal comm.).

3.2 Rishaugfjell window

3.2.1 Harelifjell (Straumen) U-Mo mineralisation

The Harelifjell occurrence SE of Straumen in Sørfolda is a typical, promising U-Mo mineralisation (Lindahl 1983, 1984; Fig. 14). The rocks belong to the Rishaugfjell basement window. The locality is near the basement/cover border zone, and is influenced by the Caledonian thrusting. The basal sedimentary sequence occurs as remnants below the thrust plane on Harelifjell mountain, with meta-arkoses and, in one locality, a thin conglomerate. The Harelifjell occurrence has not yet been mapped in detail. The mineralisation is located in a vein or series of veins steeply dipping to the east. A schematic section is shown in Fig. 15. The mineralisation outcrops continuously over a length of 300 m, and the radiometric anomaly, as determined by the helicopter-borne surveys, extends about 5 km further to the south. The mineralisation lies in a finely grained, aplitic gneissic rock of granitic composition. In the mineralized zone 1-3% sulfides are present, and the main uranium mineral is uraninite. The isotope composition has been determined, indicating the deposition age to be late Caledonian (~400 Ma). No intrusion of that age is known in this region; thus the mineralisation is thought to have been developed by metamorphic fluids, with sulphides acting as a chemical trap (Lindahl 1983). Thus, it represents a vein type deposit, presumably associated with aplites within TIB-type granites. According to the NGU Uranal database the average concentrations (104 analyses) of the mineralized aplite are 185 ppm Zr, 129 ppm Y, 119 ppm Ce, 58 ppm La, 3763 ppm U and 52 ppm Th (Fig. 16; Appendix 4). With respect to REE-Zr the deposit is not economic.

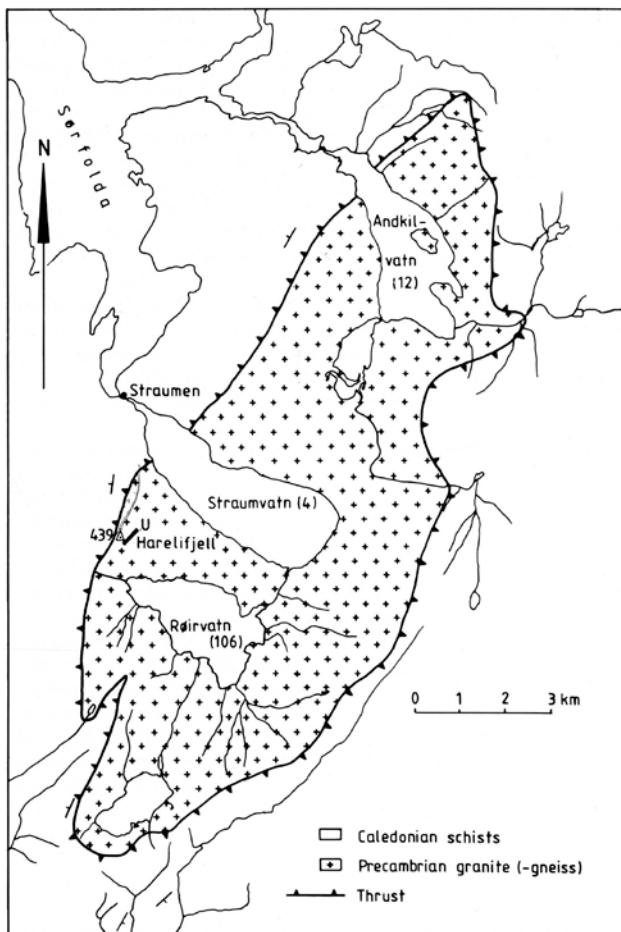


Figure 14. Location of the Harelifjell U-mineralisation occurrence within the Rishaugfjell basement window according to Lindahl (1983).

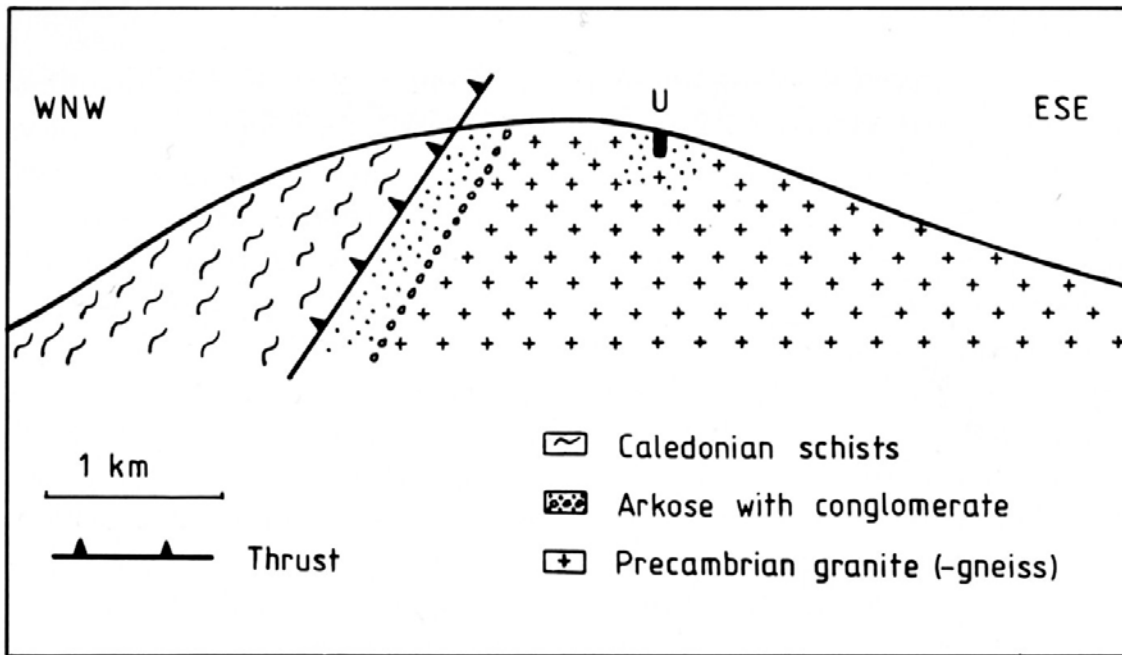


Figure 15. Schematic profile of the Harelifjell uranium occurrence according to Lindahl (1983). The host rock is fine-grained gneiss within coarse-grained granite with a weak foliation.

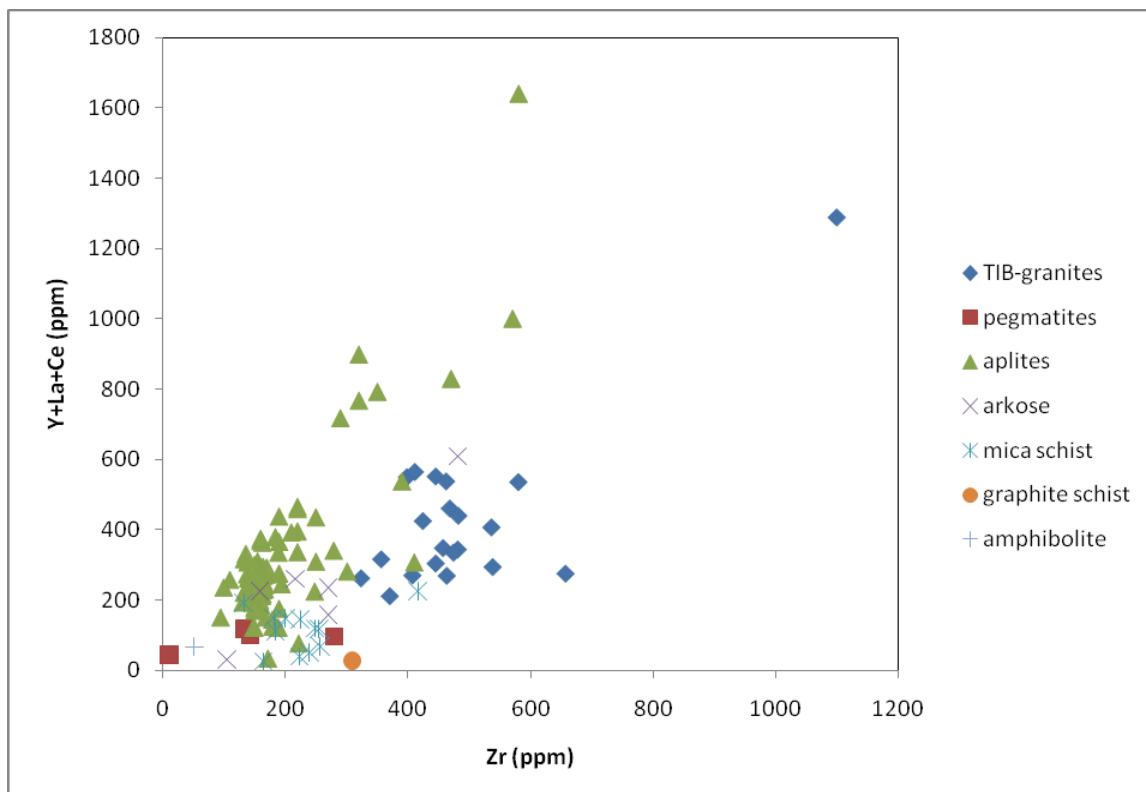


Figure 16. Concentrations of Zr versus Y+La+Ce+Sm of rocks of the Rishaugfjell window including the Harelifjell mineralisation (REE-rich aplites). One TIB-granite sample plots outside the diagram area with 11700 ppm Zr and 884 ppm Y+La+Ce (sample "Memaurvatnet", UTM 33W 529233E/7472096N; see also Figs. 23-25). Data are from the NGU Uranal database.

3.3 Nasafjell window

The Nasafjell window comprises various types of coarse- to medium-grained granitic gneisses and augen gneisses which represent deformed TIB-1 intrusions (ca. 1800 Ma; Essex and Gromet 1996). These gneisses intersect a sequence of acidic volcanic rocks with zones of sericite schist. The latter covers large areas south of the boundary of the natural park at Bolna. The gneisses which form the Lower Allochthon lie structurally above less deformed granites. The granites are exposed in a little window between Bolna and Stødi. Both the granites and gneisses are overlain by a basal sequence of Vendian-Cambrian schist and quartzites. The basal sequence is transected by enormous sub-concordant veins of hydrothermal quartz with carbonate and sulfide veins. The sulfide veins were mined for silver occurring in galena at the Swedish-Norwegian border.

The occurrence of small and deformed lenses (1 x 2 m) of fluorite and calcite with grains of galena, chalcopyrite and pyrite have been reported in the northern and southern part of the window ca. 50 m below the tectonic boundary to the Middle and Upper Allochthon (P. Ihlen; personal comm.). The lenses, which can be traced over a distance of 100 m, occur in shear-deformed granitic gneisses.

In the northwestern part of the window there are many small mineralisations of molybdenite associated with quartz veins, pegmatites and veins in granitic gneisses along a regional shear zone (Lønnsdalen). Molybdenite also occurs as dissemination in the overlying, strongly deformed schists along the shear zone on the western side of the Bjellåvann. At Leirjordfall on the eastern side of Saltdal there are Mo-bearing pegmatites higher in the nappe sequence.

The Vendian-Cambrian sequence, which lies on the top of the basement gneisses and granites and crops out at several places at the periphery of the Nasafjell window, contains sporadic molybdenite and in one location, uraninite (Lindqvist 1988). The uraninite mineralisation occurs on the Swedish side of the window (southern margin), where a basal arkose contains a 10-cm thick layer enriched in uraninite (Lindqvist 1983). The layer lies ca. 1 m above the contact to porphyritic volcanic rocks. The layer is about 100 m long. The mineralisation is interpreted to be an enrichment of heavy minerals originating from the underlying volcanic rocks and granites or Proterozoic mineralisations within them. This is consistent with the observations that stream sediments derived from granitic gneisses east of Bjellåvatn (Bjellåvann) contain unusually high U (>10 ppm) in a large area (Lindahl 1984).

3.4 Bjellåtinden window

The dominant rocks in the small (~12 km²) Bjellåtind basement window are quartz-monzonite gneisses (Ruthland and Sutherland 1967), which were dated by Cribb (1981) at 1749±53 Ma. At its periphery the basement window is overlain by a supracrustal Precambrian-Palaeozoic meta-sedimentary sequence belonging to the Röddingsfjell Nappe Complex and comprising augen gneiss, meta-pellites and -psammites, schist and marble.

3.4.1 Bjellåtinden W-Mo mineralisation

Several Mo-W mineralisations of different types and probably different ages occur along the periphery of the Bjellåtind basement window ca. 100 m above the tectonic boundary between basement and cover (Fig. 17). The following mineralisations, some of which were mined, are known (Lindahl and Furuhaug 1987a, Often 1980, Busch 1989, Larsen 1991; compare localities shown in with Fig. 17):

Locality 1: Scheelite in scapolite skarn, diopside skarn, quartz veins in hornblende gneiss and plagioclase skarn occurring in scapolite skarn and hornblende gneiss.

Locality 2: Fine-grained scheelite in plagioclase skarn and quartz veins

Localities 3 and 4: molybdenite and scheelite (fluorite, magnetite, chalcopyrite) in calcite lenses and veins healing brecciated pegmatites, in thin, boudinaged diopside skarn zones, thin quartz veins and as impregnation in the pegmatite host rocks. Locality 4 corresponds to the former Laksådal mines and locality 3 to the Oterstrand mine. The vertical pegmatite lens at Oterstrand is 400 x 100 x 50 m in size.

Localities 5 and 6: Scheelite-bearing diopside skarn. Locality 6 (Bjellåtind) is under exploration by Nordic Mining, who documented a layered scheelite-bearing diopside skarn over a length of 600 meters with a thickness of 0.3 – 1.0 meter. Nordic Mining has 10 mineral claims for W and Mo in the Laksådalen/Bjellåtind area.

Re-Os molybdenite ages are 430 ± 5 Ma for the scapolite skarn mineralisation and 398-407 Ma for the mineralisation occurring in the quartz veins (Larsen 2007). Granitic magmatism that is normally associated with W-Mo mineralisation is not observed in the Bjellåtinden area. However, previous U-Pb dating in the Uppermost Allochthon documents batholith-scale magmatism at 435-430 Ma (Barnes et al. 2007) and the 406-400 Ma ages coincide with the emplacement of granitic pegmatite swarms in the western part of the Röddingsfjell Nappe Complex. Our study underlines the importance of long-lived shear zones as conduits for ore-forming fluids and documents that ore-forming events indeed may occur during high-grade metamorphism. REE concentrations in the scheelite-mineralised skarn at Bjellåtind (locality 6) have been recently determined by Drivenes (2010). Only one of 50 samples contains about 0.1 % REE while the others contain < 0.01 % REE. Thus, the Bjellåtinden W-Mo mineralisations seem to be poor in REE.

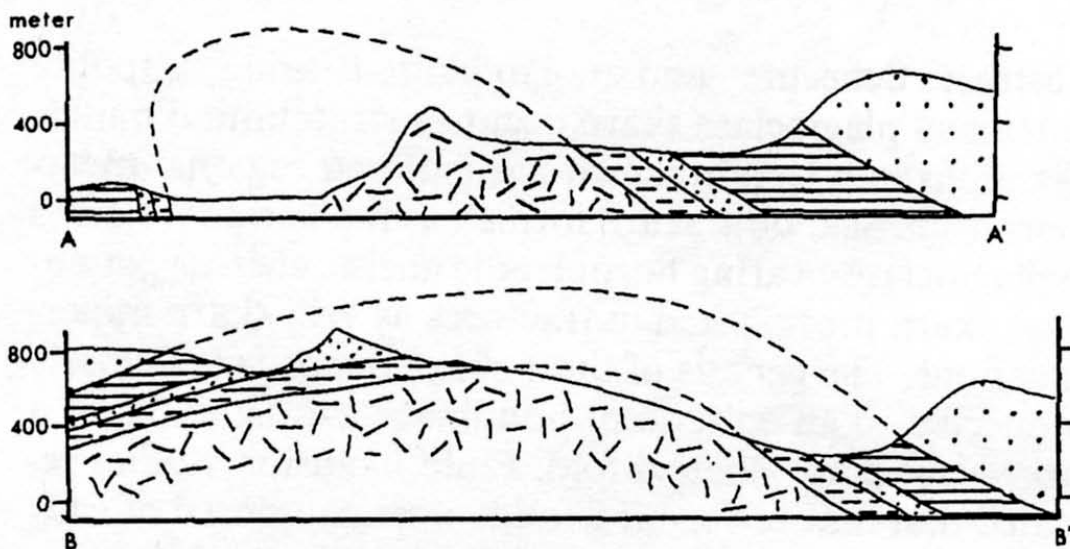
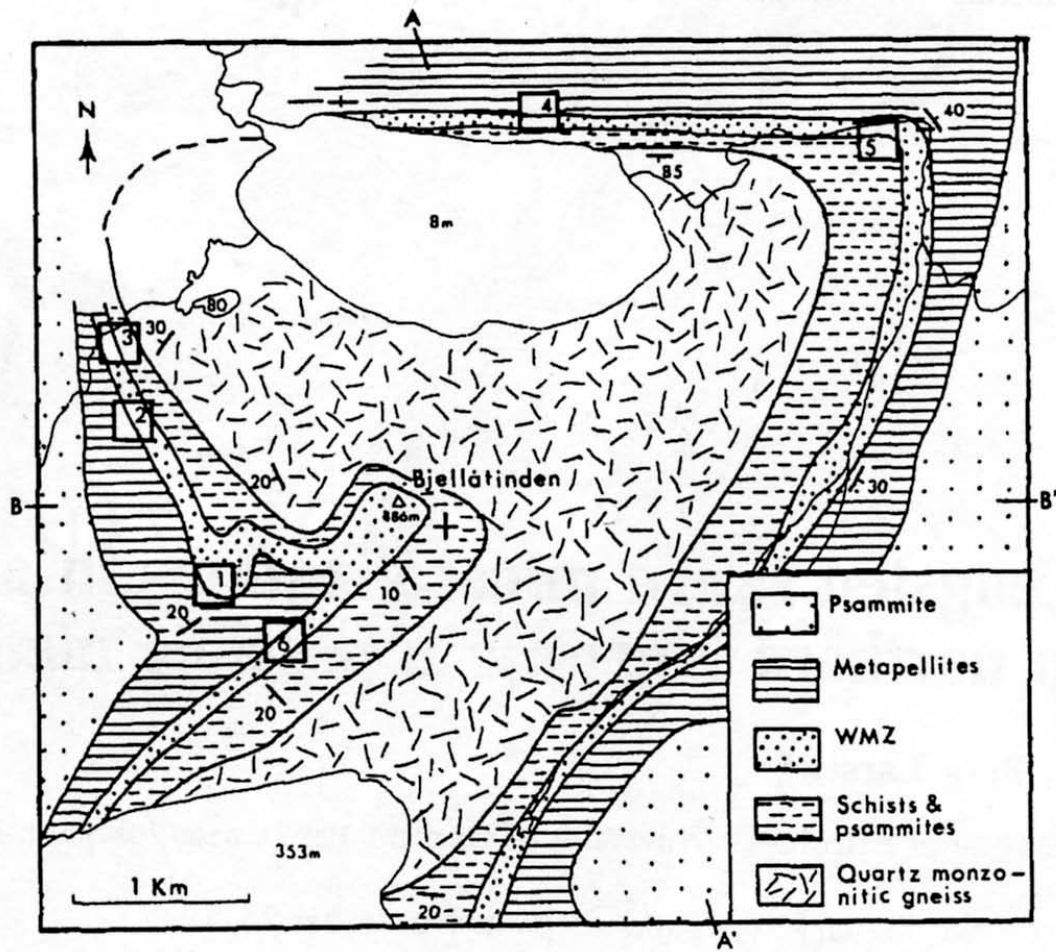


Figure 17. Geological map and cross sections of the Bjellåtinden basement window (quartz monzonitic gneiss) and of W-Mo mineralisation situated in Precambrian-Palaeozoic schists, meta-pelites and marbles immediately above the tectonic boundary to the basement rocks. From Larsen (1991). The number within the tungsten-molybdenum-zone (WMZ) correspond to different mineralisations found in the area.

3.5 Glomfjord window

The southern part of the Glomfjord window is composed of granite-monzonite gneisses, whereas the central part of the window consists mainly of grey granodioritic gneisses (Rutland et al. 1960). Whole-rock Rb-Sr dating of several rock types in the Glomfjord area yielded ages of 1694 ± 73 (Wilson and Nicholson 1973) and 1747 ± 86 Ma (Cribb 1981).

Mo mineralisations are found in the basement and overlying Caledonian schists north of Glomfjord (Bugge 1963). Beryl or aquamarine occur in pegmatites at the contact zone of the basement windows at Fykanvannet and Storglomvann. The most interesting pegmatites occur at Ågskardet at the southern side of Holandsfjord, where a small basement window with granitic gneisses crops out. This is the only known spodumene-bearing pegmatite in Norway. Spodumene occur together with columbite, microlite, helvite, beryl, cassiterite, monazite, alkali-rich tourmaline and apatite in an cleavandite-rich zone of K-feldspar-quartz-dominant pegmatite rich in coarse-grained muscovite (Ofteidal 1950, Neumann 1985; For mineral formula see Appendix 1).

3.5.1 Rendalsvik U-Th mineralisation

Rendalsvik in Meløy municipality is a high-grade, radioactive graphite schist occurrence on the south side of Holandsfjord, ca. 400 - 500 m a.s.l. (Fig. 18) The radioactivity was first described by Neumann (1952). The regional geology was mapped by Skjeseth and Sørensen (1953). The graphite-mica schist is part of a strongly folded mica schist and quartzite sequence close to the tectonic boundary to basement granitic gneisses. Graphite was mined between 1934 and 1945. Lindahl (1977) provided a complete report of the mining activity and advice for future investigations. The mineralisation was then studied by Gust and Thoresen (1981). The graphite schist is thought to be of Cambro-Silurian age and contains up to 10% graphite and 8% ore minerals (Sverdrup et al. 1967). Uraninite could not be proven by Gust and Thoresen (1981). Systematic sampling of the graphite schist gave an average of 45 ppm U (range 8 – 183 ppm). Concentrations of other elements are 85 ppm Cu, 105 ppm Zn, 40 ppm Pb, 85 ppm Mo and 450 ppm V (Lindahl 1983). The mineralisation is classified as sedimentary with a high-grade metamorphic overprint (Lindahl 1983). On the basis of drilling, geophysics and geological interpretation the resource of crystalline graphite ore was estimated to be 3 Mt. Assuming the tonnage to average 45 ppm U, this amounts to a total of about 100 t U (Lindahl 1983). Gust and Thoresen (1981) analysed 75 graphite schist samples giving an average of 185 ppm Zr, 40 ppm Y, 31 ppm La, 68 ppm Ce, 11 ppm Th and 42 ppm Th (Fig. 19; Appendix 5). With respect to REE the deposit is not of economic interest.

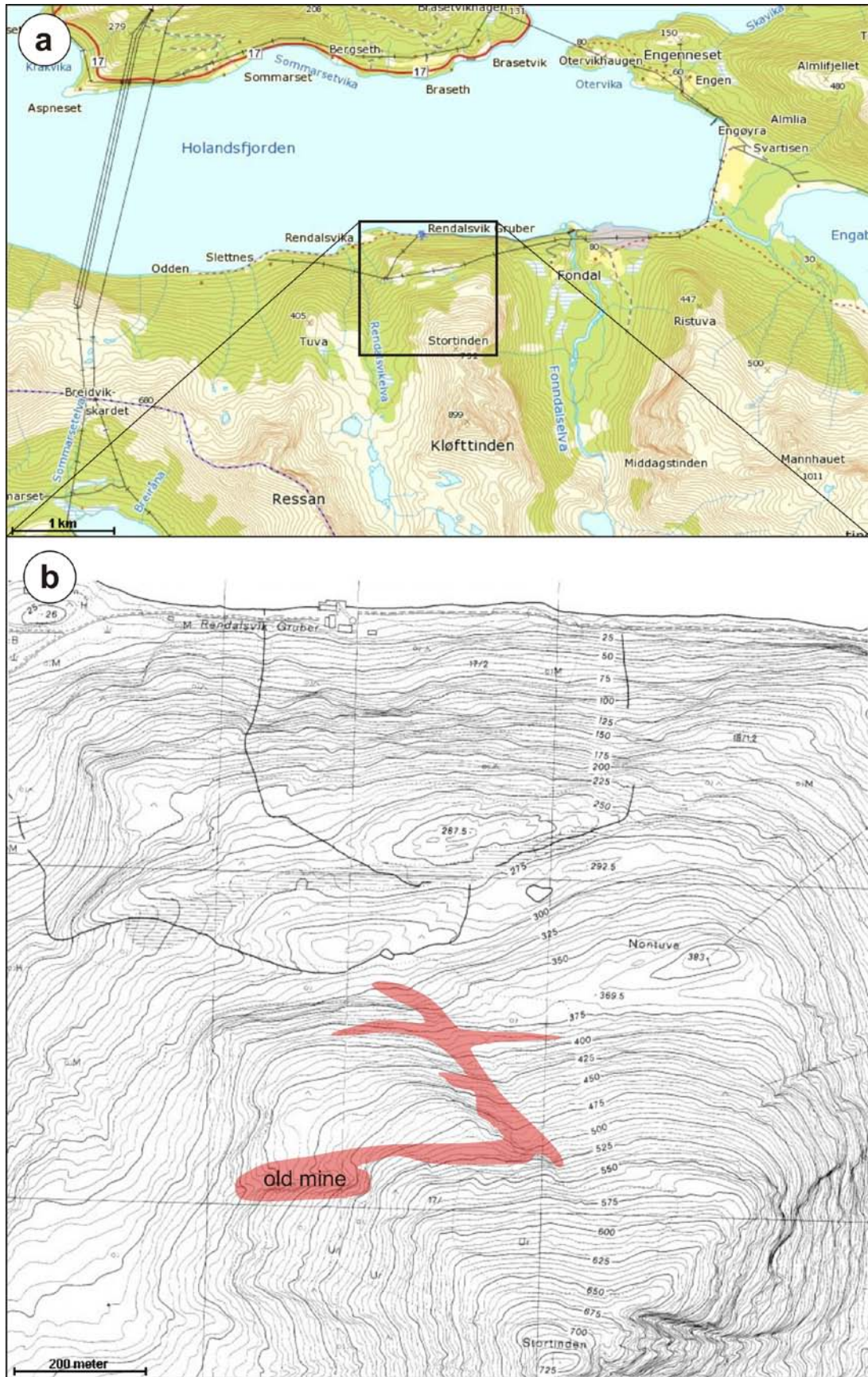


Figure 18. a - Topographic map with the location of Rendalsvik Gruber (old graphite mine) on the southern side of Holandsfjord, Meløy. b – Detailed topographic map showing the approximate distribution of U-rich graphite schist (red area) according to Gust and Thoresen (1981).

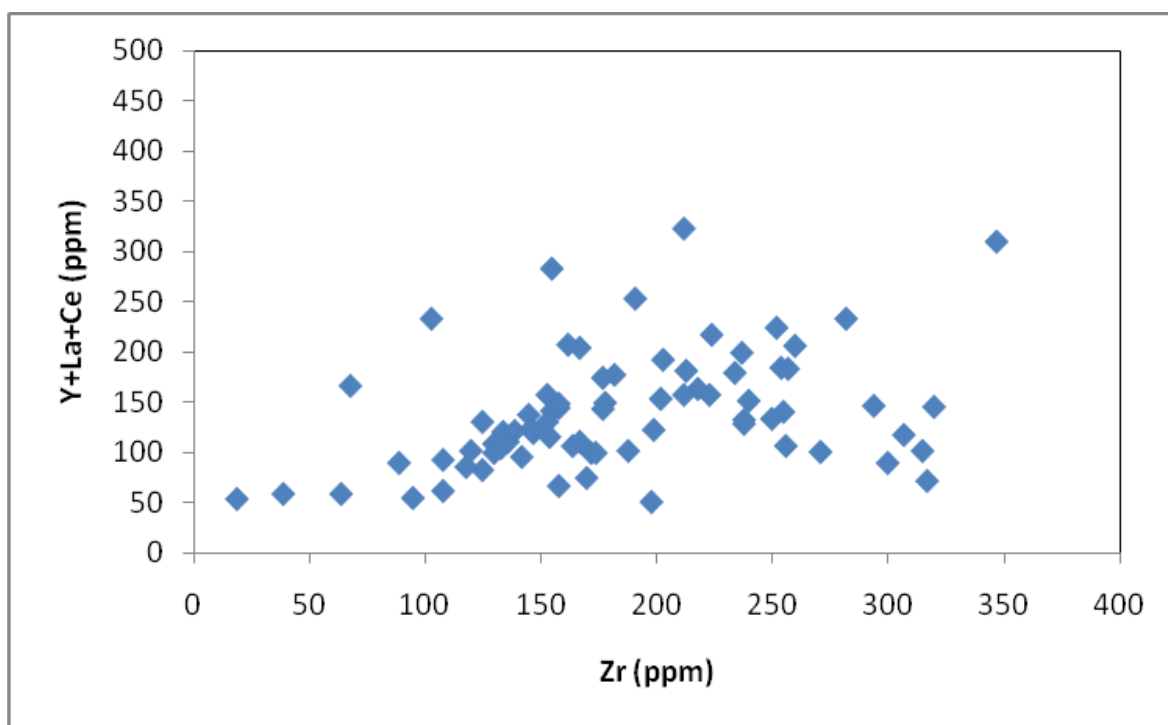


Figure 19. Concentrations of Zr versus Y+La+Ce+Sm in U-rich graphite schist from Rendalsvik (data from Gust and Thoresen 1981).

3.6 Høgtuva window

The Høgtuva window is predominantly composed of foliated equigranular, medium-grained granitic biotite gneiss with concordant layers of biotite schist interpreted to represent altered basic dykes (Gustavson and Gjelle 1991). The rocks are strongly foliated. The protolith age of the granitic to syenitic gneisses is 1800 ± 2 Ma (TIB-1 stage; Skår 2002). The amphibolite-facies overprint was at 414 ± 10 Ma.

3.6.1 Høgtuva Be-REE-U-Sn mineralisation

One of the most famous mineralisations in Nordland is the *Høgtuva* Be-REE-U-Sn-mineralisation also known as Bordvedåga (Lindahl and Furuhaug 1987b, Lindahl and Grauch 1988). The mineralisation is embedded in biotite-rich, fine-grained, strong foliated granitic gneiss in the southeastern part of the Høgtuva basement window (Figs. 20 and 21). The mineralized gneiss has lower concentrations of SiO_2 , K_2O og Al_2O_3 and higher concentrations of Fe_2O_3 and Na_2O compared to the surrounding gneiss units. The mineralized gneiss is approximately 150 m wide and 2.5 km long, strikes NW-SE and plunges $20\text{-}30^\circ$ NE. It is visually hardly distinguishable from the surrounding gneiss units apart from the presence of amazonite-bearing semi-concordant pegmatite veins within the mineralized gneiss.

The mineralized gneiss is enriched in Be (0.12 %; average of 35 analyses), U (149 ppm), LREE (La+Ce+Sm = 687 ppm), HREE (Eu+Tb+Yb+Lu = 237 ppm), Th (278 ppm), F, Li, Nb (293 ppm), Y (644 ppm), Zr (7733 ppm) and Sn (94 ppm; Wilberg and Lindahl 1991, Wilberg 1989d; Fig. 22; Appendix 6). This rare mineralisation type is caused by an uncommon assemblage of accessory minerals including magnetite with inclusions of

cassiterite and uraninite, zircon, allanite, fluorite, phenacite, gadolinite, genthelvite, høgtuvaite, Nb-U oxide, Y-Th silicates and REE carbonates. The Be content is predominantly bound in phenacite, and to a lesser extent in gadolinite, genthelvite and høgtuvaite. Høgtuvaite was first described from Høgtuva (Grauch et al. 1994; for mineral formula see Appendix 1) and is a metamorphic mineral that crystallized under amphibolite facies conditions in quartzofeldspathic orthogneiss enriched in Be and other rare metals prior to metamorphism. However, høgtuvaite contains only about 1% Be and is, therefore, not an important Be-ore. For comparison, element concentrations of non-mineralized gneiss (footwall and hanging-wall gneiss) are listed in Table 2.

Phenacite – the major Be-ore mineral – is enriched in thin, irregular fluorite-rich lenses and layers within the mineralized gneiss and is disseminated in the surrounding gneiss. Elements which are enriched in the Be ore include U, Th, Zr, Nb, Sn, W, Mo, Cu og Ba. The ore lenses are surrounded by gneiss which contains at least 200 ppm Be. Immediately below and above the Be-rich lenses occurs the so-called Y-zone (>1000 ppm Y; average 1557 ppm) which is enriched in Y, Ce, La, Rb, Li, Zn, Pb og Co (Table 2). Concentrations of LREE in the Y-zone are 873 ppm (La+Ce+Sm) and of HREE 246 ppm (Eu+Tb+Yb+Lu; Wilberg 1989d). For comparison the Be-rich zone contains 557 ppm LREE and 280 ppm (HREE). For the economic evaluation of the deposit it is, therefore, important to consider not only the Be-rich mineralisations but also the possible Y- and other REE-resources. In the event of mining the Be ore it would be natural to utilize several of the enriched incompatible elements as by-product. The assumed Be resources are calculated to 350,000 t with an average of 0.18% Be applying a cut-off grade 0.1 % Be and a volume of 400 x 20 x 1.5 m (Wilberg and Lindahl 1991, Table 2). A processing test (flotation) on phenacite-rich rocks gave a concentrate with 23 % BeO with a recovery of 80%. The study showed also that Be can easily be leached from the phenacite concentrate with acid.

The exploration of the Bordvedåga mineralisation started in 1974 with sampling in the framework of a granite project at NGU. Because of anomalously high U and Th values of some of the rock samples found at Høgtuva, ground surveys of the radioactivity at Bordvedåga were carried out in 1981. In the following years the work in the area were extended by helicopter-borne radiometric, magnetic and VLF surveys, car-borne radiometric surveys, panning of stream sediments, detailed geological mapping, major and trace-element whole-rock chemistry, and core drilling (Furuhaug 1984, Wilberg 1987a, 1987b, 1987c, 1987d, 1988, 1989a, 1989b, 1989c, 1989d, Wilberg and Furuhaug 1989, Wilberg and Lindahl 1991). In 1983 the Be-mineral phenacite was identified and herewith the strong Be-enrichment of the U-Th-mineralized gneiss. In 1987 Follidal Verk A/S (later Norsulfid A/S), Nordland county, Rana Utviklingsselskap and NTNf contributed to an exploration project. Core drilling was carried out between 1986 and 1988. Altogether 45 holes were drilled with a total length of 2215 m. In 1988/89 a study of the economic potential of the Bordvedåga mineralisation was carried out by SINTEF and NGU but the project was terminated before completion.

The Høgtuva mineralisation is unique in its trace element signature. Two deposits of a somewhat similar type are known. The Thor Lake deposit near Yellowknife, NWT, Canada (Černý and Trueman 1985) is located within albitized and greisenized peralkaline granite and syenite, 1270±10 Ma. The Spor Mountain Be deposit in Utah is hosted by a water-lain tuff in Tertiary acidic volcanic rocks (Lindsay 1982).

The formation of the Høgtuva Be-mineralisation is still under debate. The primary enrichment of the incompatible elements is presumably a result of differentiation of the protolith magma of the granitic gneisses (Wilberg and Lindahl 1991). Further Be enrichment occurred via hydrothermal fluorine-rich fluids. The rocks were then overprinted by amphibolite-facies metamorphism which resulted in the partial redistribution of the incompatible elements.

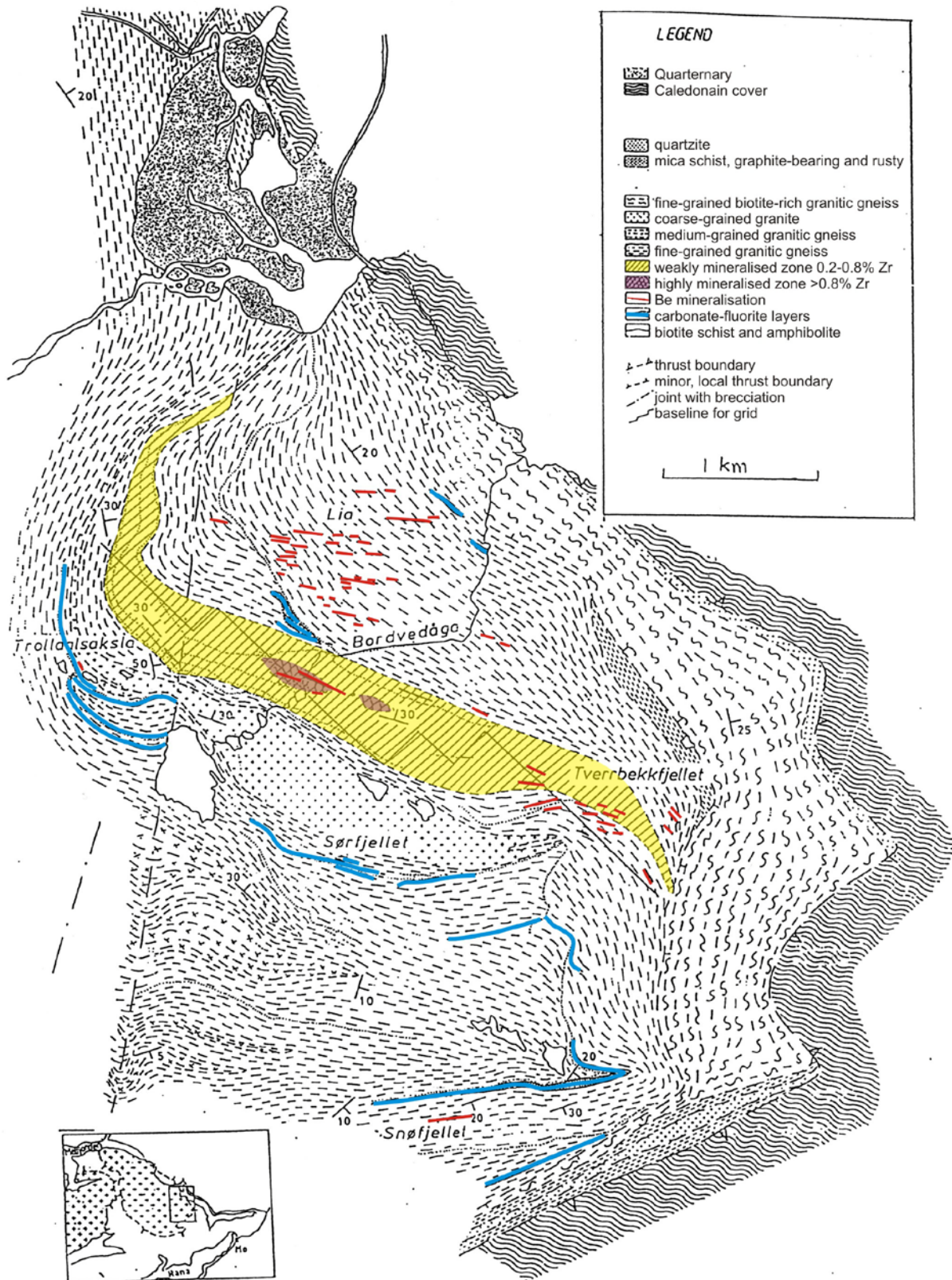


Figure 20. Geological map of the southeastern part of the Høgtuva basement window according to Wilberg (1987a) showing the distribution of the Be mineralisations.

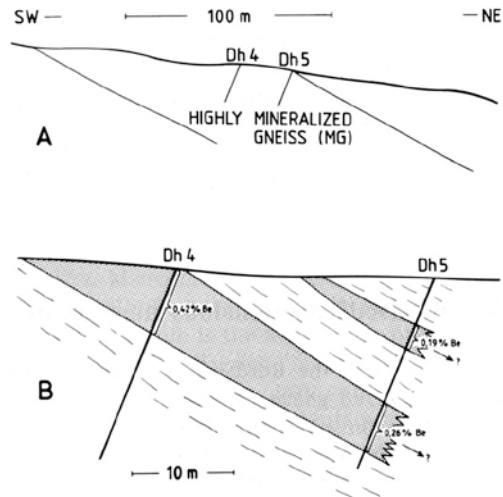
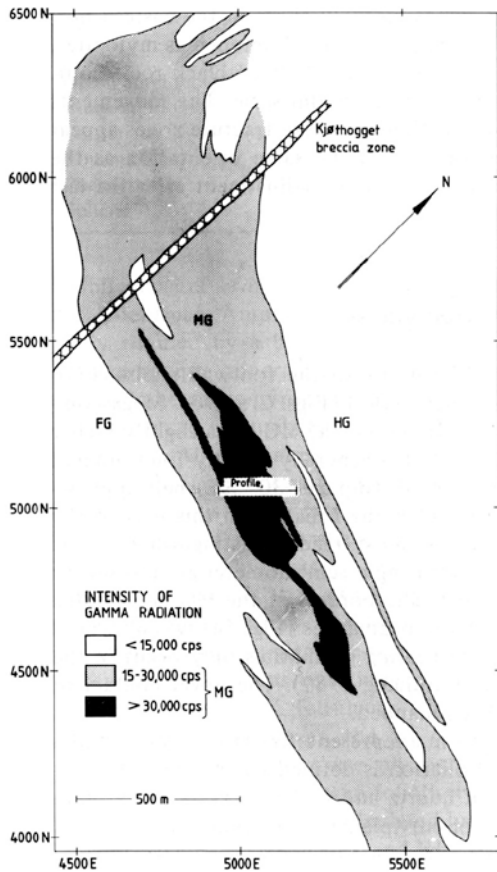


Fig. 4. A: Cross section of the Bordvedåga anomalous gneiss (MG). B: Location of the Be mineralization within the highly mineralized gneiss.

Fig. 3. Radiometric map delineating the Bordvedåga anomalous gneiss (MG), with the hanging-wall gneiss (HG) and the footwall gneiss (FG). Interpretation of ground surveys with 50 or 100 m line spacing and 12.5 or 25 m between measured points.

Figure 21. Radiometric map and cross sections of the Bordvedåga Be mineralisation according to Lindahl and Grauch (1988).

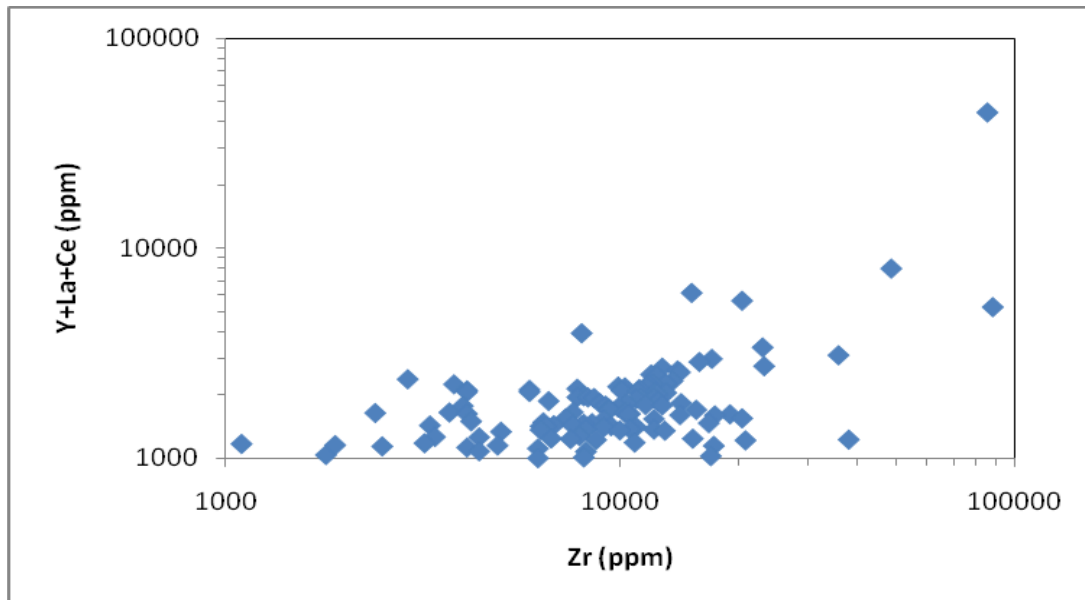


Figure 22. Concentrations of Zr versus Y+La+Ce+Sm of the Høgtuva mineralisation. Note that only data >1000 ppm Zr and >1000 ppm Y+La+Ce are plotted. Source: NGU Uranal database.

The Bordvedvåga mineralisation is the major mineralisation within a cluster of Be-mineralisations occurring in an area of about 8 km² in the eastern part of the Høgtuva window (Table 2). These mineralisations are of different types with varying geochemistry and mineralogy. The following mineralisation types were identified: 1) granitic gneiss, 2) fluorite-rich layers in gneiss, 3) fluorite-rich skarn, 4) aplite, 5) pegmatite and 6) undeformed quartz veins. The Be-minerals phenacite, høgtuvaite, beryl, gadolinite, danalite, genthelvite and helvite occur in different parageneses in different mineralisation types (see Appendix 1 for mineral formula). The Bordvedvåga mineralisation represents mineralisation type (1), which is economically the most interesting. However, the zircons, which would be the most valuable by-product of the Høgtuva ore, are rich in U and Th, and, thus, the economic potential of the deposit is low (T. Vrålstad; personal comm.). The time available for this report had not allowed to carry out a really systematic analysis of all the data available for Bordvedvåga. An appropriate and conclusive chemical characterization and systematic overview of the different mineralisations at Høgtuva are lacking.

Table 2. Be-mineralisations in the eastern part of the Høgtuva window. Concentrations of Be, Zr, Y, Nb and U are average values of mineralized rocks according to Wilberg and Lindahl (1991) and Wilberg (1987b, 1989a, 1989c).

mineral		UTM84			Be	Zr	Y	Nb	La	Ce	U	Th	Be resources	mineralisation type
		zone	easting	northing	(%)	(%)	(ppm)	(ppm)	(ppm)	(ppm)	(ppm)	(ppm)		
Bordvedåga Høgtuva 1	mineralised gneiss including Be- and Y-zones	33	449680	7365550	0.18	0.8	644	293	107	346	149	278	350,000 t (0.18% Be)	granitic gneiss, pegmatite
	Be-zone				0.37	1.2	789	620	92	433	297	747		granitic gneiss, pegmatite
	Y-zone				0.10	1.0	1557	525	174	603	244	516		granitic gneiss, pegmatite
	weakly mineralised gneiss				0.02	0.28	263	118	110	356	60	101		granitic gneiss
	footwall gneiss				<0.001	0.04	64	36	54	142	18	37		granitic gneiss
	hanging-wall gneiss				<0.001	0.06	97	34	109	228	15	31		granitic gneiss
Lia Høgtuva 2		33	449720	7366200	0.22	0.22	300	91	117	349	34	63	Ca. 500 t (0.1% Be)	granitic gneiss
Tverrbekkfjell Høgtuva 3+4		33	451000	7365000	0.02	0.21	466	n.d.	152	378	44	98	-	granitic gneiss, fluorite-rich layers, pegmatite, quartz veins
Snøfjellet Høgtuva 5		33	450432	7362797	0.03	0.16	418	n.d.	166	353	76	119	6000-7000 t (0.03% Be)	granitic gneiss, aplite, pegmatite, quartz veins
Sørfjellet Høgtuva 6		33	448332	7365647	n.d.	n.d.	n.d.	n.d.	n.d.	n.d.	n.d.	n.d.		skarn, granitic gneiss

n.d. – not determined

The Be mineralisation at *Lia* (Høgtuva 2) is north of the Bordvedåga mineralisation. The *Lia* area comprises 18 small Be-mineralisations exposed in an area of 2 km². Exploration and sampling were carried out by NGU between 1986 and 1988. The Be ore - a phenacite-høgtuvaite-gadolinite assemblage - is disseminated in medium- to fine-grained granitic gneiss. The mineralisation is both concordant and discordant in respect to the foliation. The mineralisations are up to 600 m long and a few decimeters wide. 54 samples were analysed. 23 of them had >0.1% Be with a maximum of 0.94% Be (Wilberg 1989c, Wilberg and Furuhaug 1989). The identified Be minerals are phenacite and Be-rhönite. Concentrations of other incompatible elements are much lower than at Bordvedåga. 11 short holes and one 300-m hole were drilled in the area given similar results as the surface samples.

During the field season in 1988 several Be-mineralisations were identified at *Tverrbekkfjell* (Høgtuva 3 and 4; Wilberg and Furuhaug 1989). The mineralisations occur as fluorite-rich concordant veins, disseminated ore, small discordant veinlets and pegmatite lenses within the granitic gneiss. The fluorite-rich layers contain up to 6% Be and are several decimeter wide. The mineralisations can be followed for up to 600 m (UTM 450830E/7365490N, 450640E/7365560N, 450340E/7365620N). 100 to 200 ppm Be were recorded in a 200 m long and 8-10 m wide gneiss band. Average concentrations of the mineralisations are listed in Table 2. The dominant Be-mineral assemblage at *Tverrbekkfjell* is beryl, phenacite and gadolinite. In the eastern part of the *Tverrbekkfjell* area høgtuvaite occurs instead of beryl. At UTM 451100E/7364880N green to yellowish-green beryl occurs disseminated in the gneiss and concentrated in short, cm-wide, discordant veins. Euhedral beryl has been found in small quartz veins. Concentrations of 3.2% Be have been reported from these mineralisations but the high concentrations are limited to very small mineralisations (Wilberg and Furuhaug 1989). However, drilling carried out in 1988 gave another picture (Wilberg 1989c). The mineral assemblage observed in the core samples of 5 drill holes comprises Be-rhönite, phenacite, gadolinite and beryl. Be concentrations in the phenacite-Be-rhönite ore are in the range of 100 to 300 ppm Be with a maximum of 500 ppm Be over 0.75 m. Be concentrations in the fluorite-rich beryl-phenacite ore are up to 6% but the mineralisations are very small. The identified Be resources at *Tverrbekkfjell* are too small to be of economic interest.

In 1987 beryl and phenacite were found in radioactive aplites at *Snøfjellet* (Høgtuva 5; Wilberg 1989a). In 1988 the area was mapped, scintillometer and beryllometer measurements and core drilling were carried out. In addition to Be the aplite is enriched in Zr, Y, Nb, U, Th, Co, Ce og La. Average concentrations of the mineralisations are listed in Table 2. The mineralisation type and chemistry are similar to Bordvedåga with the difference that phenacite shows a corona of beryl. The Be-mineralized area is 330 m long and up to 15 m wide and comprises granitic gneiss, aplite, pegmatite segregations and late, un-deformed beryl-bearing quartz veins. Core drilling (10 hole) proved 6000-7000 t ore with 300-400 ppm Be to a depth of 10 to 12 m. However, the tonnage and Be concentrations are too low to be of economic interest.

Several Be-skarn-mineralisations (garnet-diopside-magnetite skarn) were identified between *Sørfjellet* in SE and *Trolldalsaksla* in NW (Høgtuva 6; Wilberg 1989a). The mineralisation is associated with fluorite- and carbonate-rich gneiss layers which are up to 0.5 m wide and several meters long. The Be minerals include danalite, helvite, høgtuvaite and gadolinite. The garnet-diopside skarn is enriched in a number of trace elements. The mineralisations at *Trolldalsaksla* comprise zircon-biotite-segregations which occur in and next to the mineralized gneiss. Some of these segregations are enriched in Be. At *Sørfjellet* (UTM 450050E/7364500N) beryl occurs in several thin fluorite-rich layers within the granitic gneiss. In addition discordant fluorite-beryl mineralisations with up to 0.36% Be occur an area of 50 x 50 m. The mineralisations at *Sørfjellet* are too small to be of economic interest.

4. Mineralisations in the Caledonian nappe complexes

4.1 Skarn deposits of the Uppermost Allochthon

Skarn deposits can be enriched in REE and U (Lentz 1991, 1998), e.g. the Mary Kathleen skarn deposit in Queensland, Australia (Kwak and Abeysinghe 1987). Vesuvianite and epidote with as much as 20 wt.% REE (Ce>La>Pr>Nd) have been found in some Au and Zn skarns (Gemmel et al. 1992).

The western parts of the Mid-Norwegian Caledonides, i.e. the Helgeland and Röddingsfjell nappe complexes are recognized as a regional W-Mo province comprising several scheelite-molybdenite mineralisations. The largest showings comprise the Målvika mineralisation situated in the Helgeland nappe complex of the Bindal area (south of the study area) and the Bjellåtinden mineralisation in the Röddingsfjell nappe complex in the Laksådal area. These two mineralisations are under exploration by Nordic Mining for their economic potential. Because of the strong relationship of the Bjellåtinden skarn to the rocks of the Bjellåtind basement window it is discussed in chapter 3.4.1.

Another skarn deposit of the same type is the *Valnesfjord* mineralisation in the Uppermost Allochthon near Fauske. A tungsten exploration program in the Valnesfjord region (Petersen and Stendal 1987) resulted in the recognition of three types of W-mineralisation: (a) tourmalinites with large scheelite crystals in vugs; (b) small crystals of scheelite in quartz pegmatites; and (c) disseminated scheelite in calcareous biotite schists. The latter is the most interesting from an economical point of view. However, the mineralisations are very small and no chemical analyses are reported. It is assumed that the skarn mineralisation is poor in REE+Zr similar to the Bjellåtinden and Målvika occurrences. However, stream sediment samples taken in the area show elevated La-Ce concentrations (see chapter 6).

4.2 Deformed carbonatite dykes

Deformed carbonatite veins have been identified in the Caledonian nappe units of the Beiarn area south of Bodø (P. Ihlen; personal comm.). The veins are up to 10 m long and 0.3 m and have a miascitic composition (Na+K<Al). The veins were found during exploration for apatite. The identified veins are too small to be of economic interest. In addition, carbonatites of miascitic composition have little potential for REE mineralisation (H. Gautneb; personal comm.).

5. NGU Uranal database of igneous rocks

The Uranal database comprises 2509 whole-rock analyses predominantly of deformed and undeformed TIB-type granitoids (~90%) and partially of schists, quartzites, and gneisses (~10%). The database was created at the end of the 1980s and has not been updated since then. The figures 23 to 32 show the regional distribution of Y, La, Ce concentrations of all samples registered in the database. The density of sampling locations is very heterogeneous. Some of the basement windows, in particular the Sjona and Høgtuva window, have a high sampling density. Other basement windows, such as the central and southern Tysfjord, Nasafjell and Svartisen windows, are poorly investigated, partly due to difficult access (most of the Svartisen window is covered by glaciers).

Most of the Y, La and Ce anomalies shown in Figures 23 to 32 are associated with mineralisations discussed above (Høgtuva, Storjord, Kalvik, Harelifjell). Some of the

anomalies represent pegmatite samples in the Tysfjord area (Figs. 26-28). There are a few TIB-granite samples in the Mannfjord area east of Drag and the outer Efjord, which show elevated Y, La and Ce concentrations. The Tysfjord granite sample at Gjerdalsvatn (UTM 33W 548233E/7509196N) is rich in La (541 ppm) and Ce (1200 ppm). The sample was collected by J. Hysingjord in the 1970s. Another REE-rich TIB-granite sample originates from Memaurvatn in the Rishaugfjell window (UTM 33W 529233E/7472096N). It contains 11700 ppm Zr and 884 ppm Y+La+Ce. The TIB-granites of the basement windows in central Nordland (Høgtuva, Sjøna, Svartisen, Glomfjord, Bjellåtind) are not enriched in REE except for the Be-REE-U-Sn mineralisation at Høgtuva (Figs. 29-31).

In summary, the data of the Ural database support the statement that highly evolved TIB-granites and, thus, the highest REE-mineralisation potential is found in the Tysfjord basement window. The particular areas comprises Mannfjord and outer Efjord. Stendal (1990) stated that the most evolved TIB-granites occur in the southernmost Tysfjord window. However, there appear to be no analyses (except the Kalvik window) which can confirm this statement.

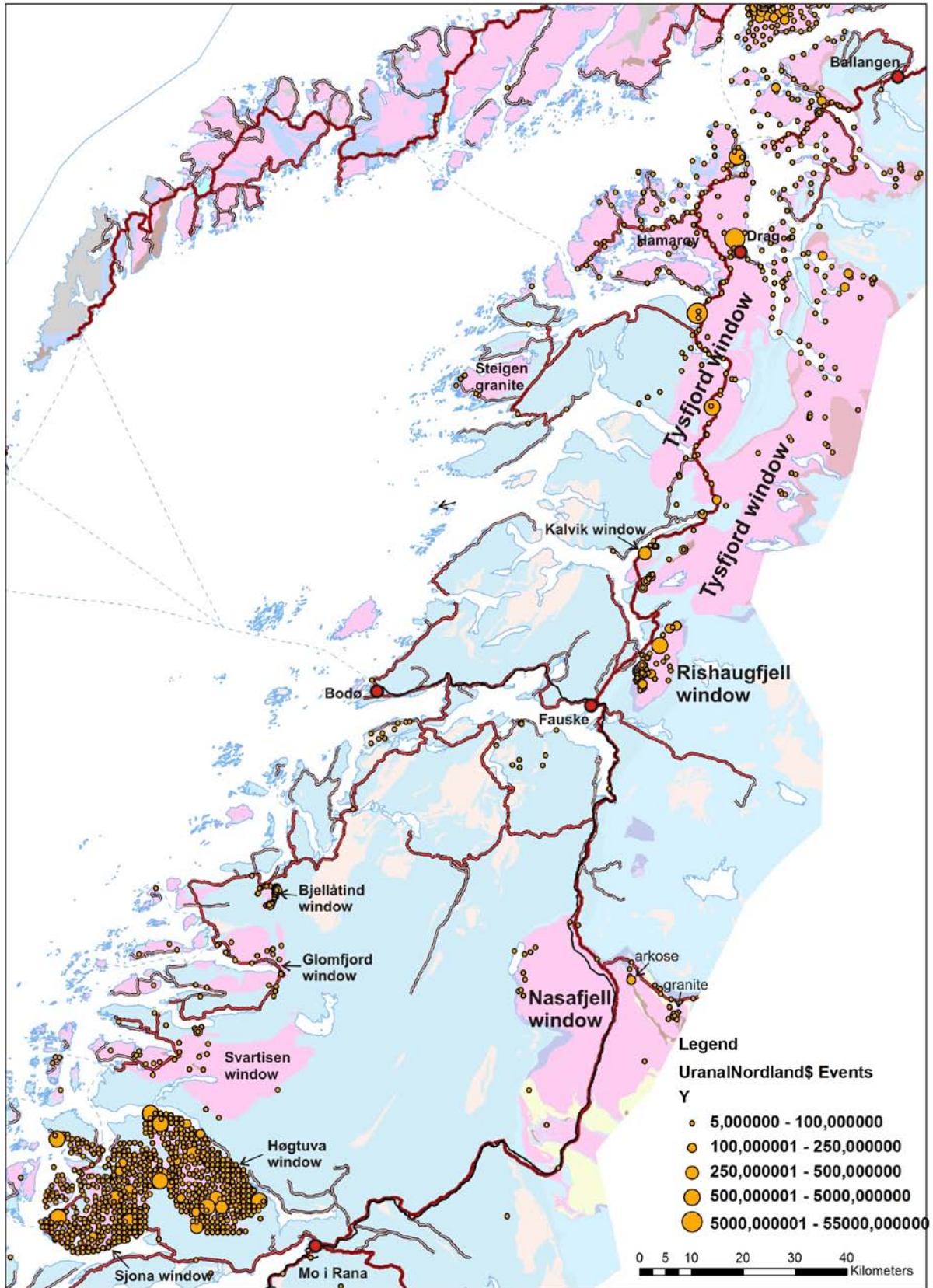


Figure 23. Simplified geological map of central and northern Nordland with Y concentrations of rock samples registered at the NGU Uranal database. The pink areas are the basement windows comprising predominantly deformed and undeformed TIB-granites.

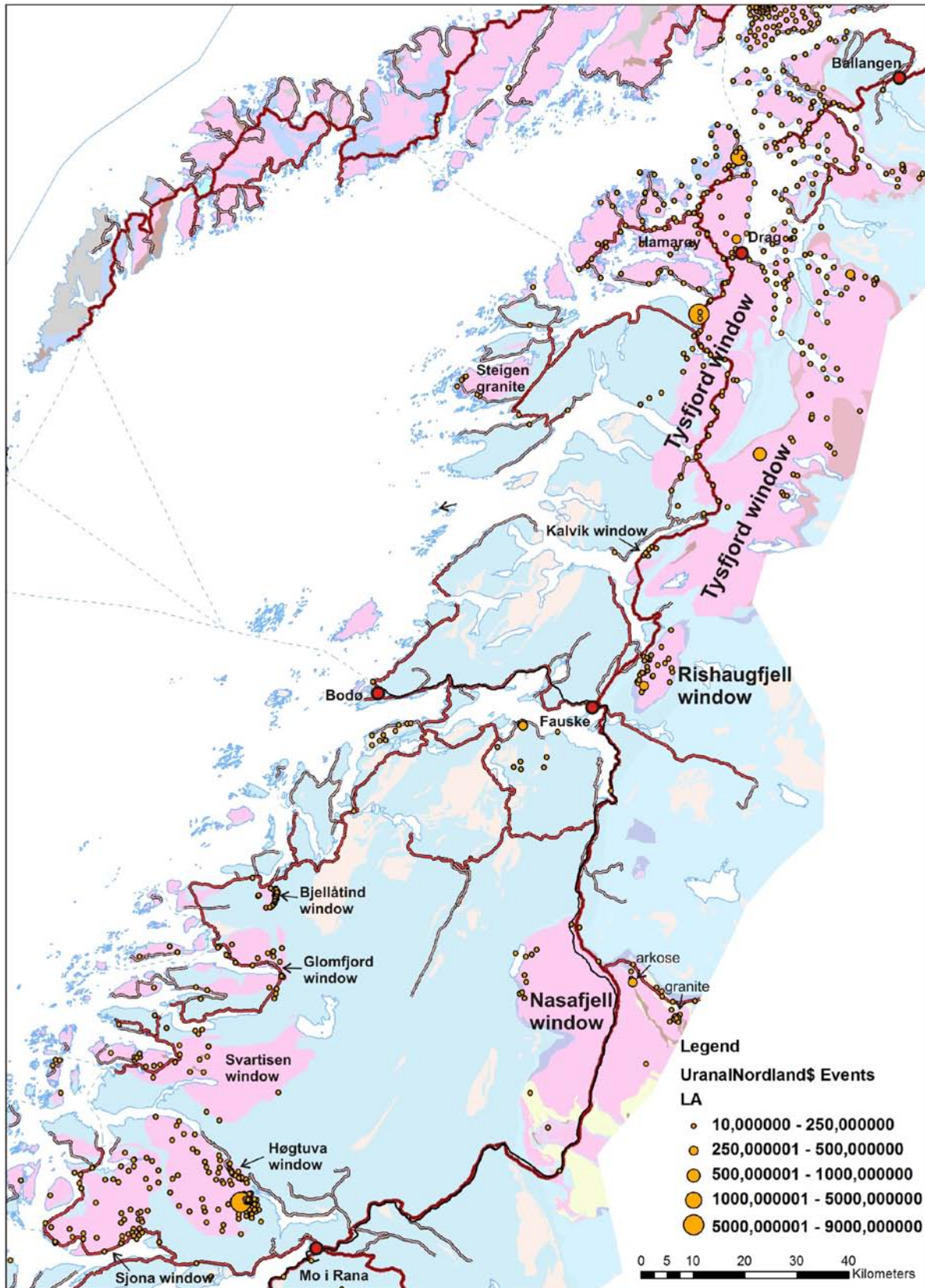


Figure 24. Simplified geological map of central and northern Nordland with La concentrations of rock samples registered at the NGU Uranium database. The pink areas are the basement windows comprising predominantly deformed and undeformed TIB-granites.

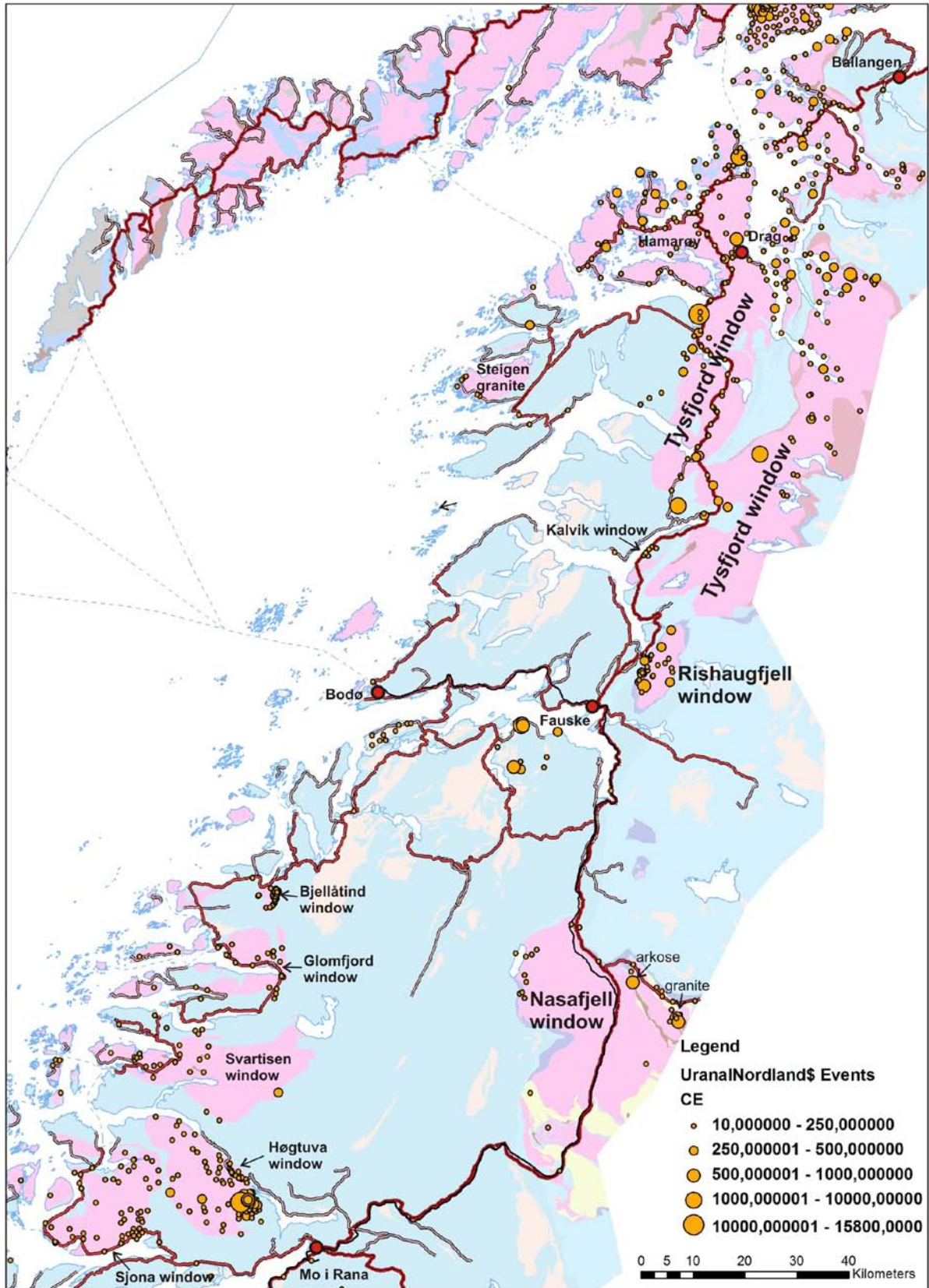


Figure 25. Simplified geological map of central and northern Nordland with Ce concentrations of rock samples registered at the NGU Uranal database. The pink areas are the basement windows comprising predominantly deformed and undeformed TIB-granites.

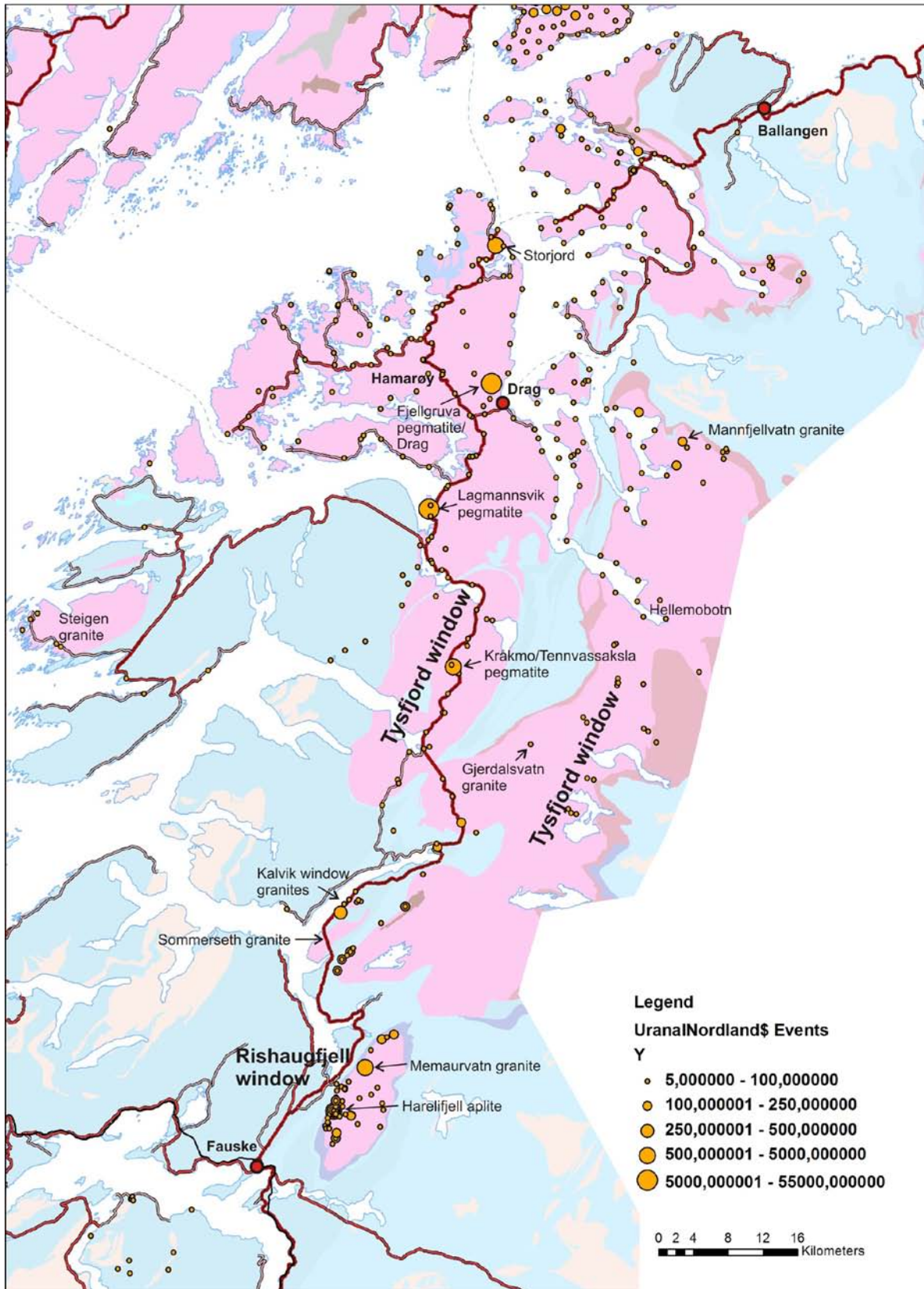


Figure 26. Simplified geological map of northern Nordland with Y concentrations of rock samples registered at the NGU Uranal database. The pink areas are the basement windows comprising predominantly deformed and undeformed TIB-granites.

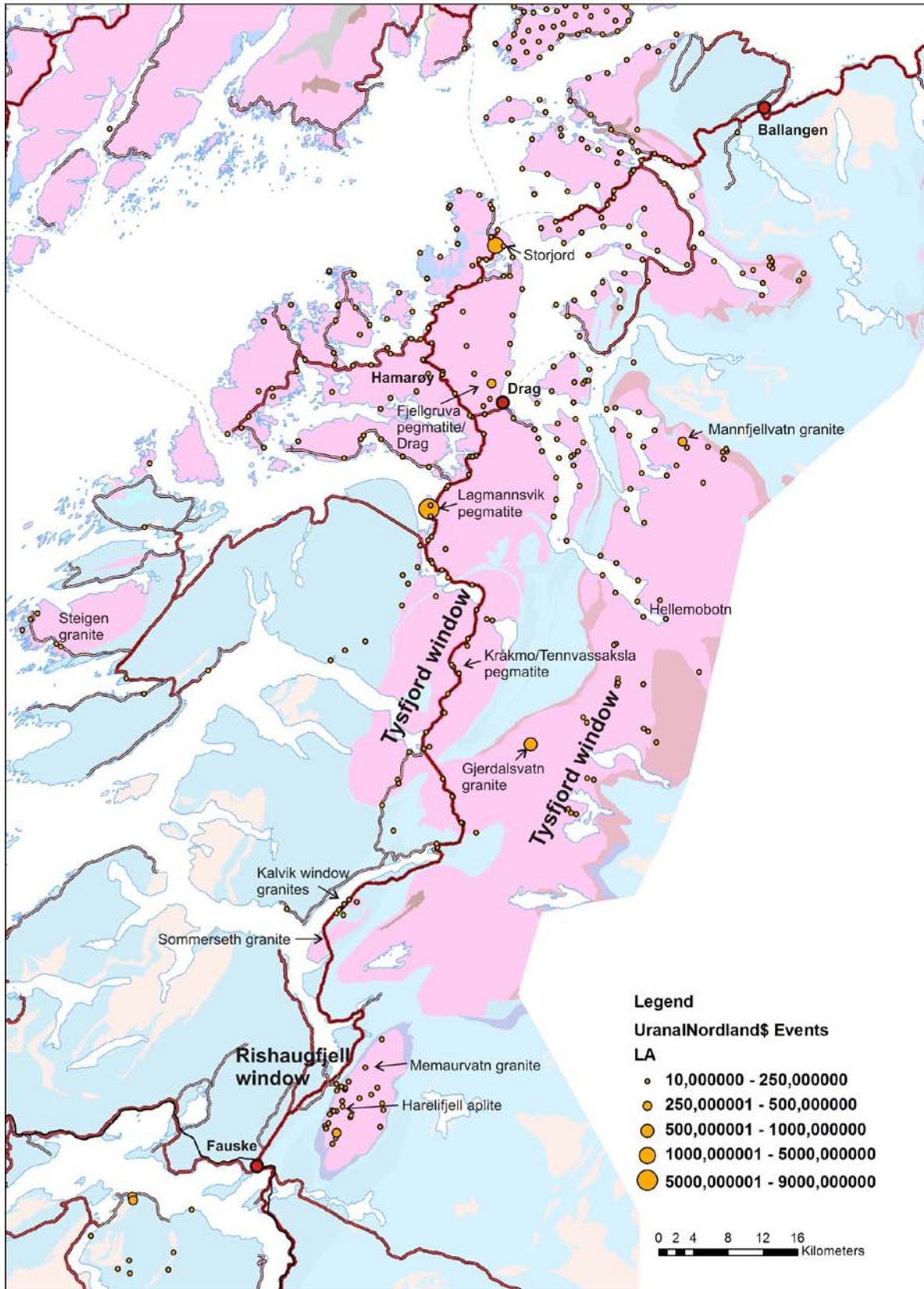


Figure 27. Simplified geological map of northern Nordland with La concentrations of rock samples registered at the NGU Uranal database. The pink areas are the basement windows comprising predominantly deformed and undeformed TIB-granites.

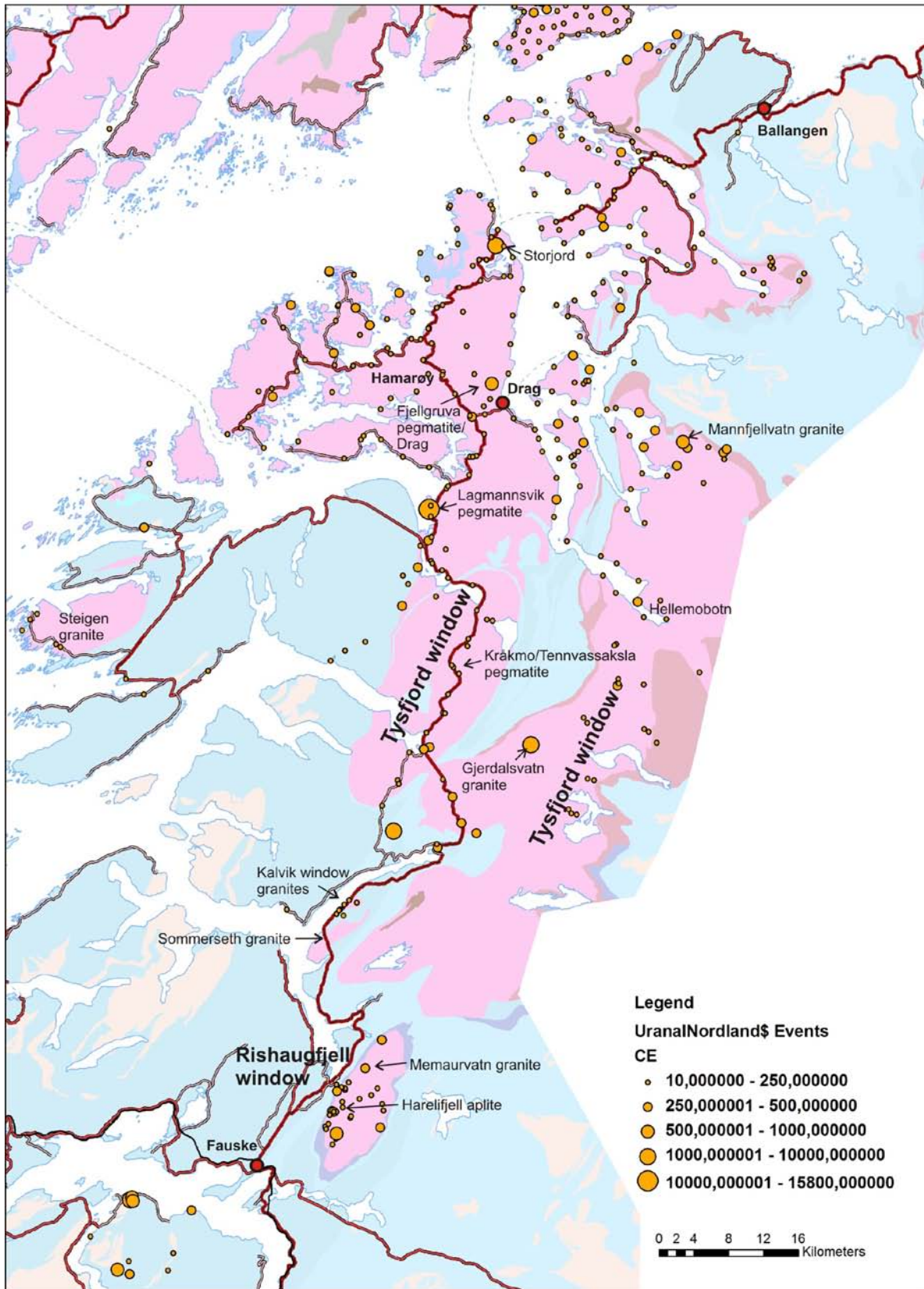


Figure 28. Simplified geological map of northern Nordland with Ce concentrations of rock samples registered at the NGU Uranal database. The pink areas are the basement windows comprising predominantly deformed and undeformed TIB-granites.

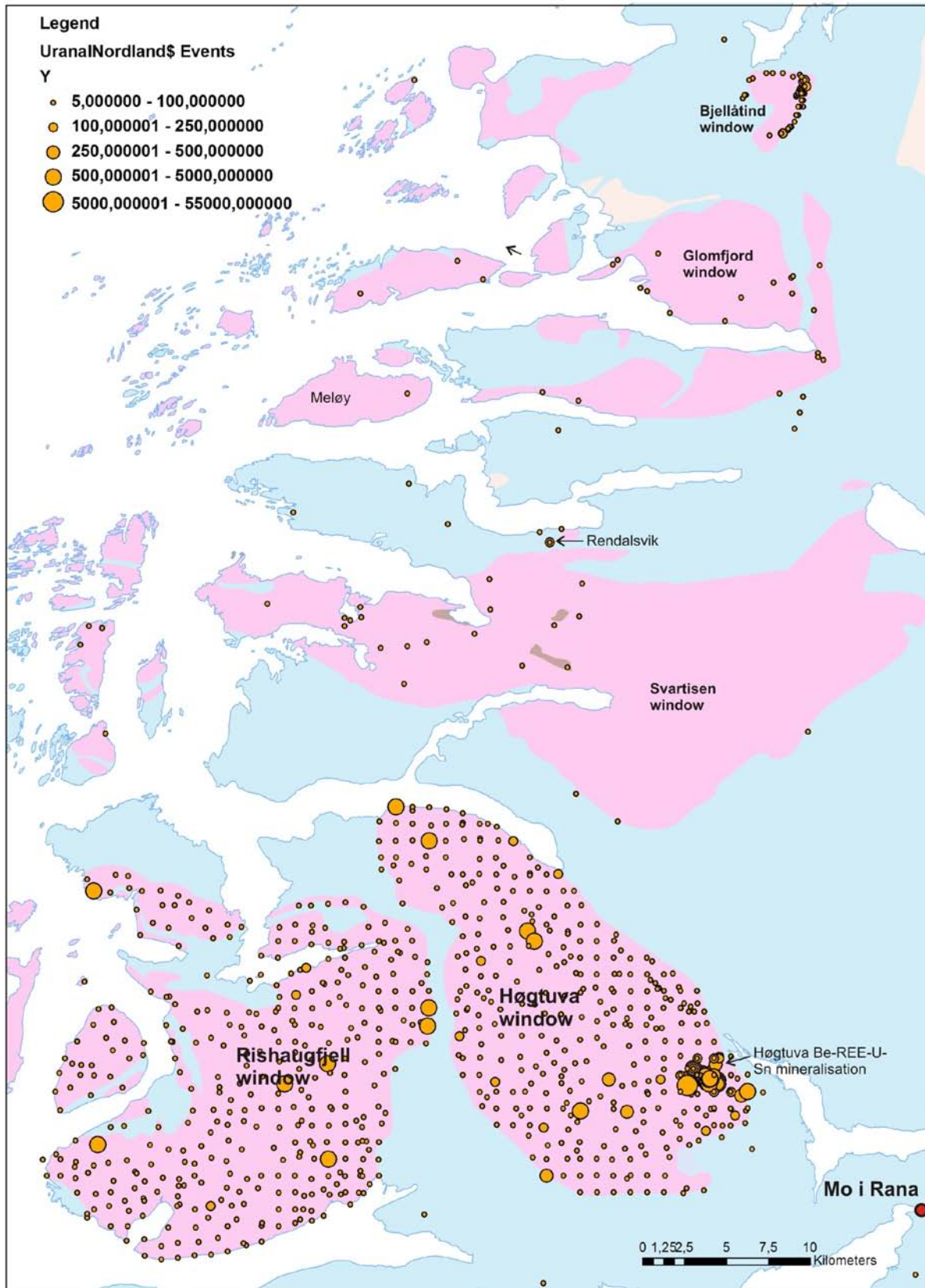


Figure 29. Simplified geological map of central Nordland with Y concentrations of rock samples registered at the NGU Uranyl database. The pink areas are the basement windows comprising predominantly deformed and undeformed TIB-granites.

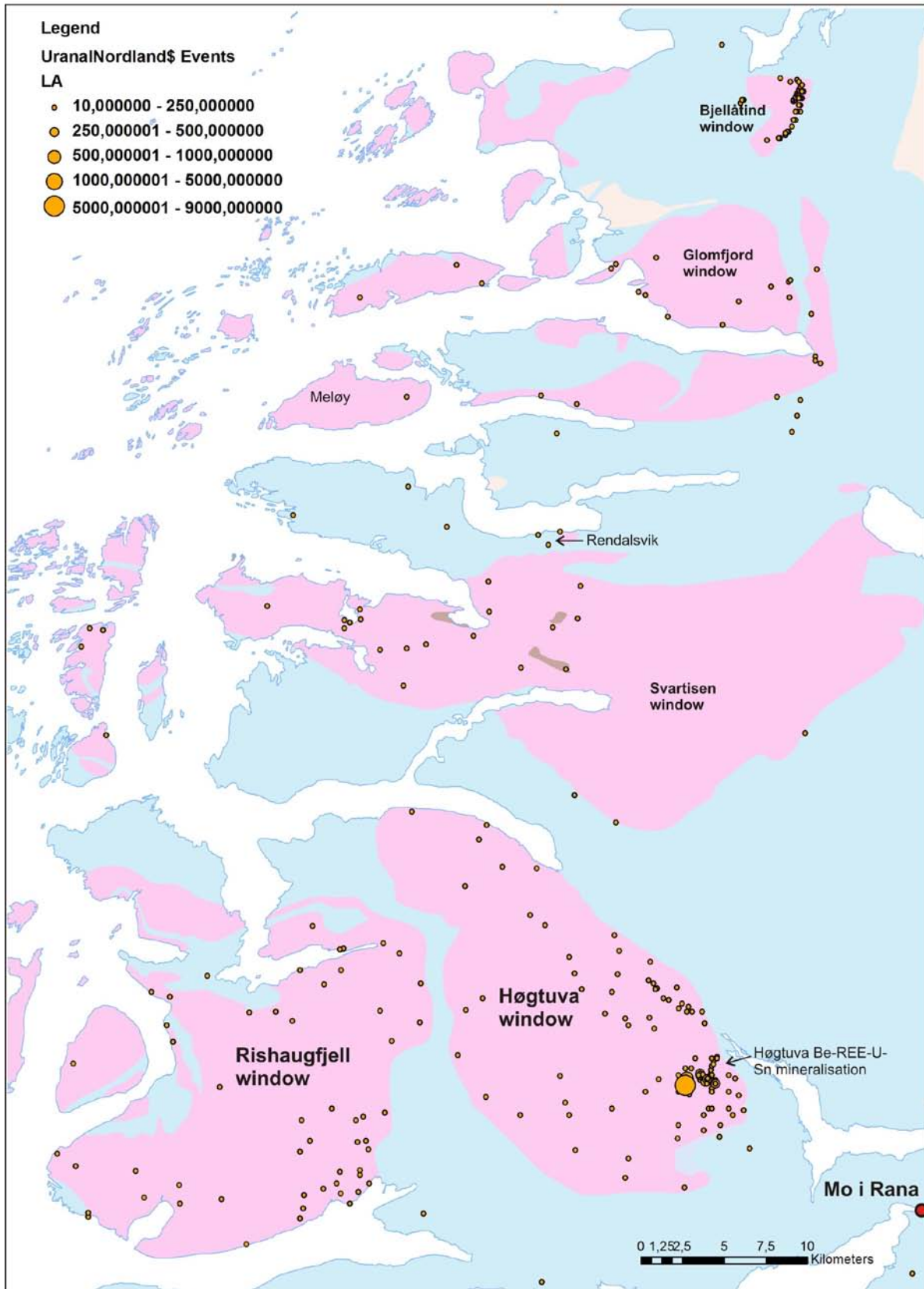


Figure 30. Simplified geological map of central Nordland with La concentrations of rock samples registered at the NGU Uranal database. The pink areas are the basement windows comprising predominantly deformed and undeformed TIB-granites.

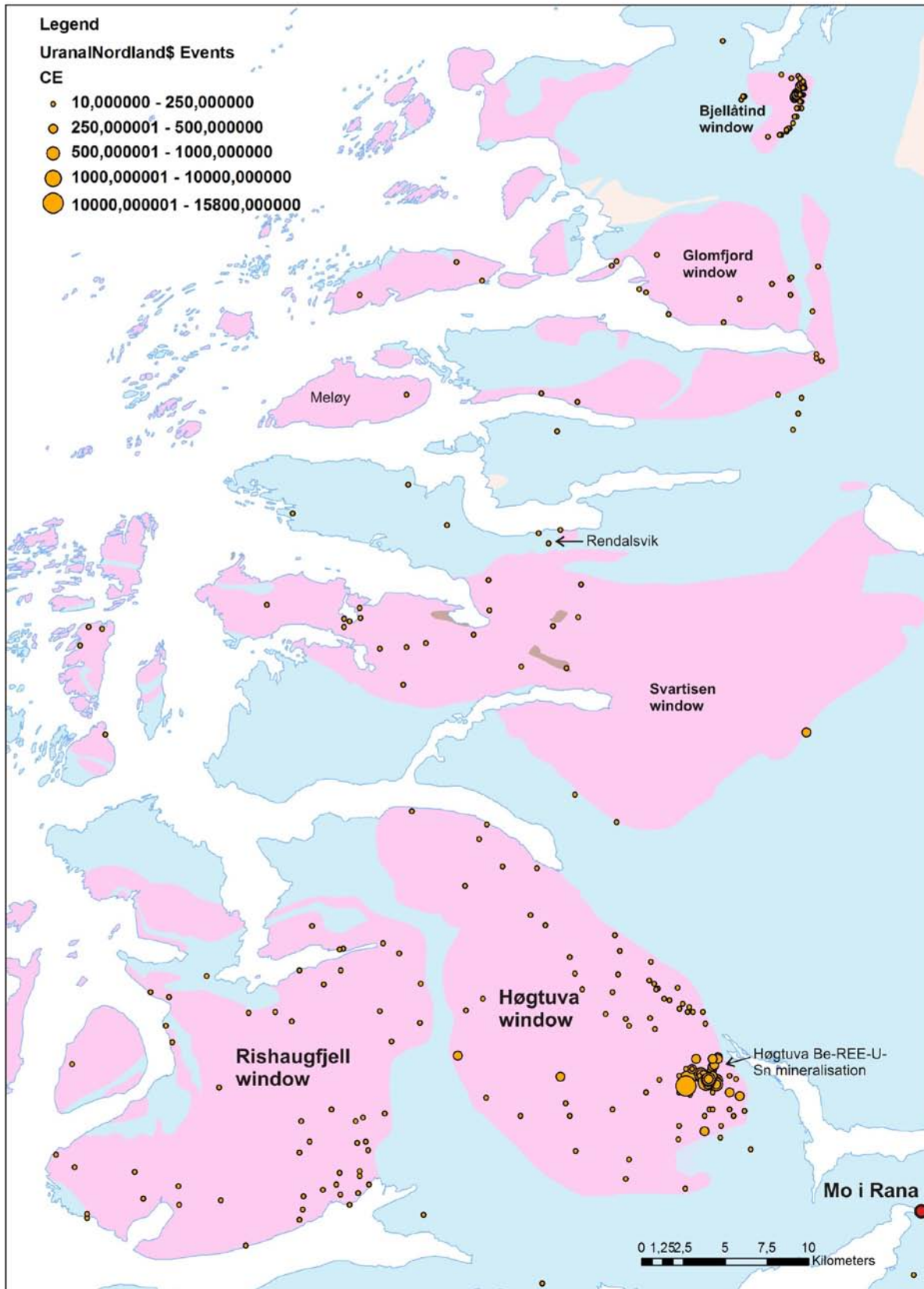


Figure 31. Simplified geological map of central Nordland with Ce concentrations of rock samples registered at the NGU Uranal database. The pink areas are the basement windows comprising predominantly deformed and undeformed TIB-granites.

6. NGU geochemical database of stream sediments

The NGU stream sediments geochemical database was checked for additional indications of REE mineralisation in the study area. Figures 32 to 34 illustrate that REE-rich stream sediment samples cluster in the Tysfjord basement window, supporting the statements made in the previous chapters that the most fractionated TIB-granites occur in this area. There are two sample locations outside the Tysfjord basement window which show elevated REE concentrations: inner Værangsfjord (western Svartisen window) and inner Misvær fjord (SW of Fauske). However, in the framework of this project it is suggested that these are given a lower priority, because there are no other indications for a significant REE-mineralisation in these areas. Stream sediments originating from rocks in the Upper and Uppermost Allochthons show no particular REE-anomalies (Figs. 35 and 36).

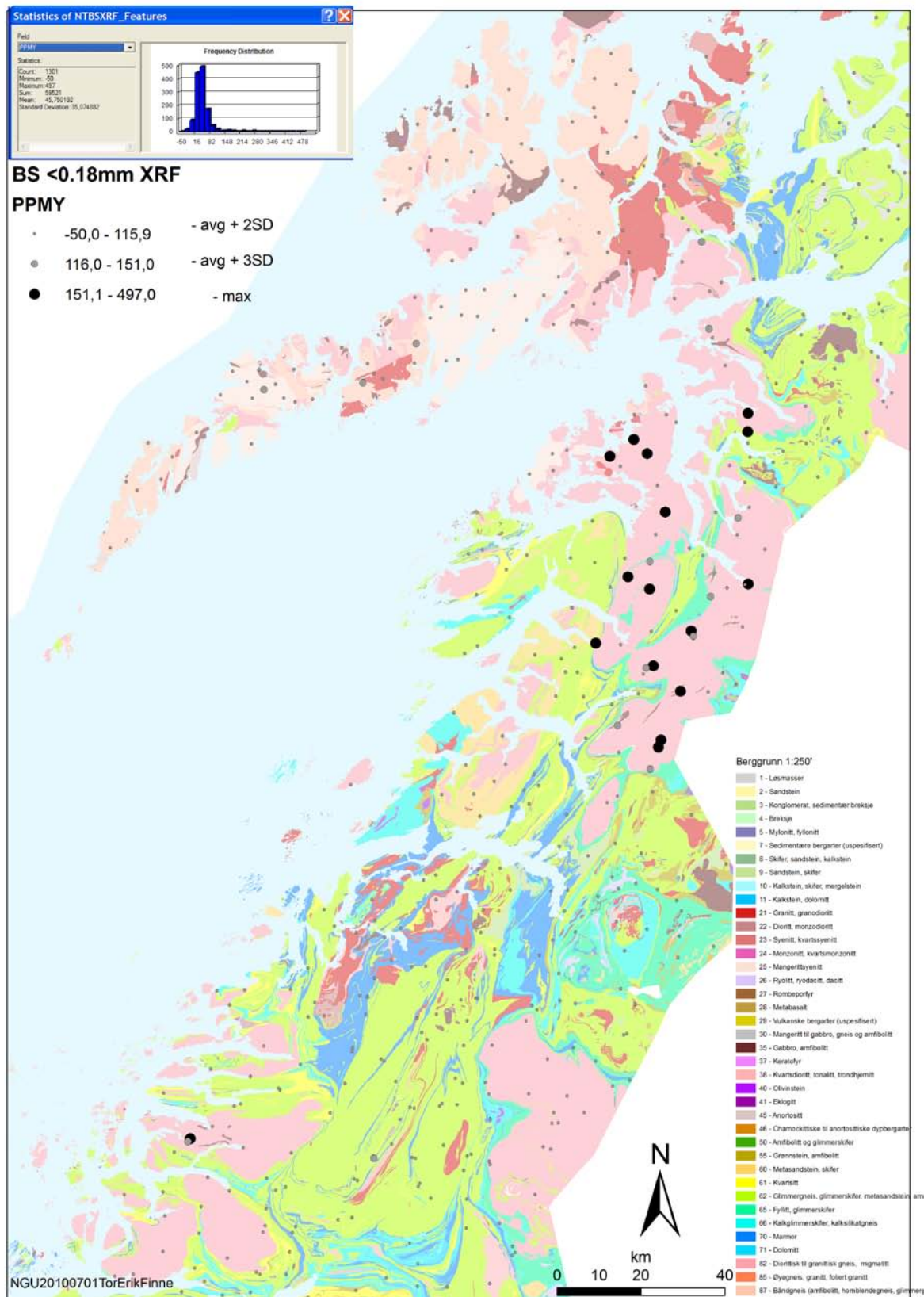


Figure 32. Simplified geological map of central and northern Nordland with Y concentrations of stream sediments registered at the NGU geochemical database. The distinct cluster of elevated Y concentrations in the Tysfjord basement window supports the conclusion that the most fractionated TIB-granites occur in this area. Another Y-rich sample originates from inner Værangsfjord, Glomfjord window.

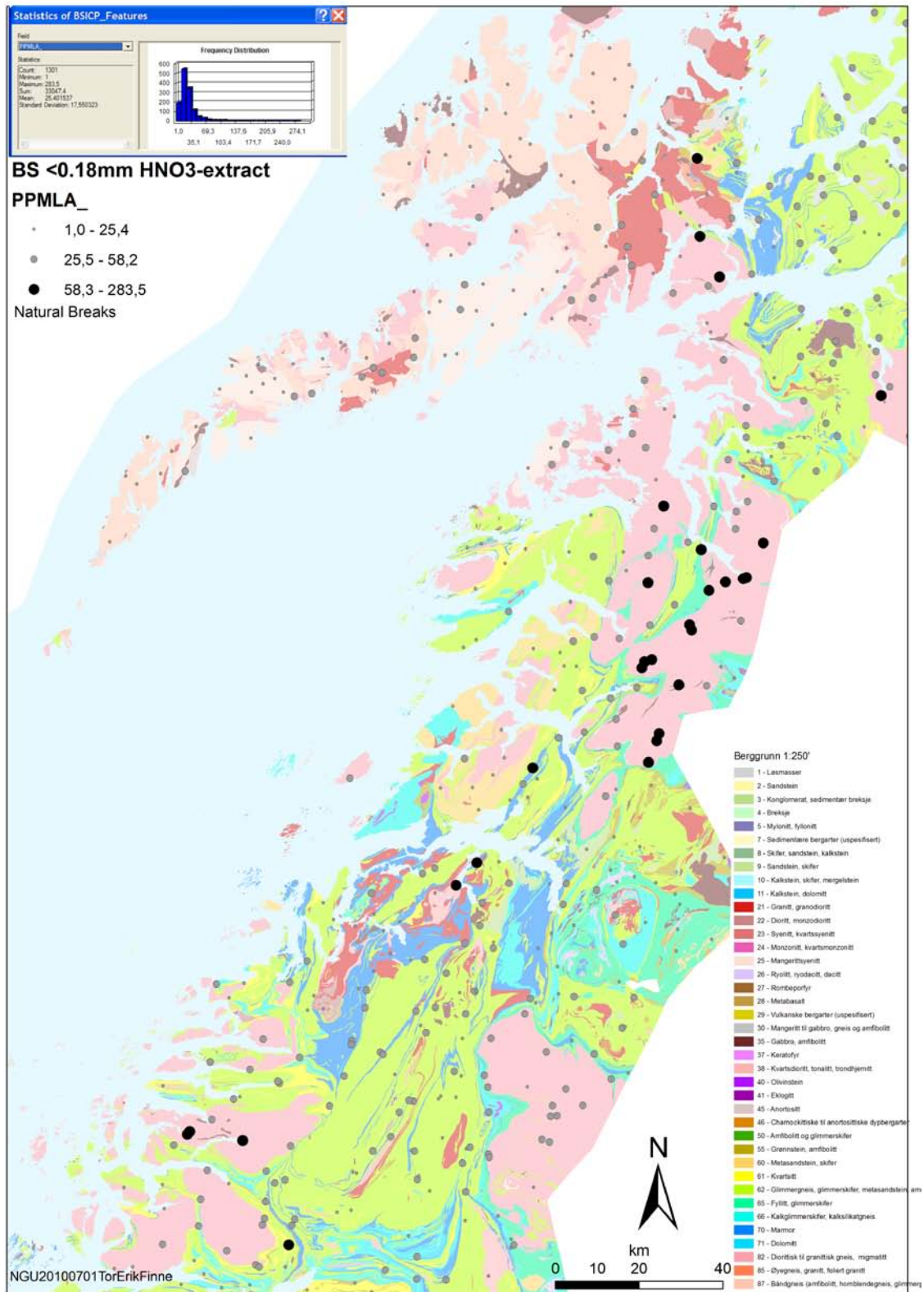


Figure 33. Simplified geological map of central and northern Nordland with La concentrations of stream sediments registered at the NGU geochemical database. The distinct cluster of elevated La concentrations in the Tysfjord basement window supports the conclusion that the most fractionated TIB-granites occur in this area. Other La-rich samples originate from the Glomfjord window, the eastern margin of the Høgtuva window, the Valnesfjord W-skarn and inner Misværffjord.

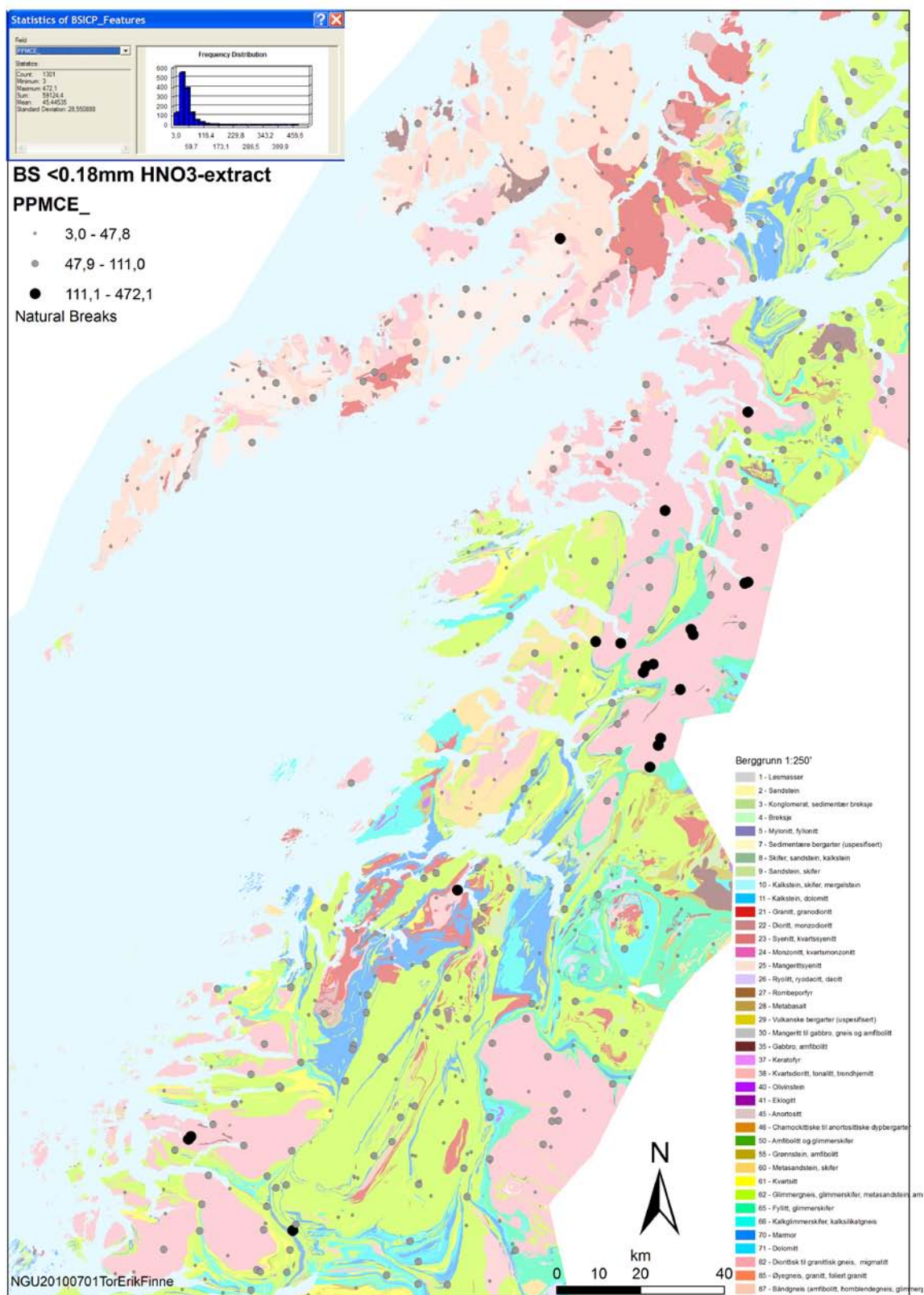


Figure 34. Simplified geological map of central and northern Nordland with Ce concentrations of stream sediments registered at the NGU geochemical database. The distinct cluster of elevated Ce concentrations in the Tysfjord basement window supports the conclusion that the most fractionated TIB-granites occur in this area. Other Ce-rich samples originate from the inner Værangsfjord (Glomfjord window), the eastern margin of the Høgtuva window and the inner Misværffjord.

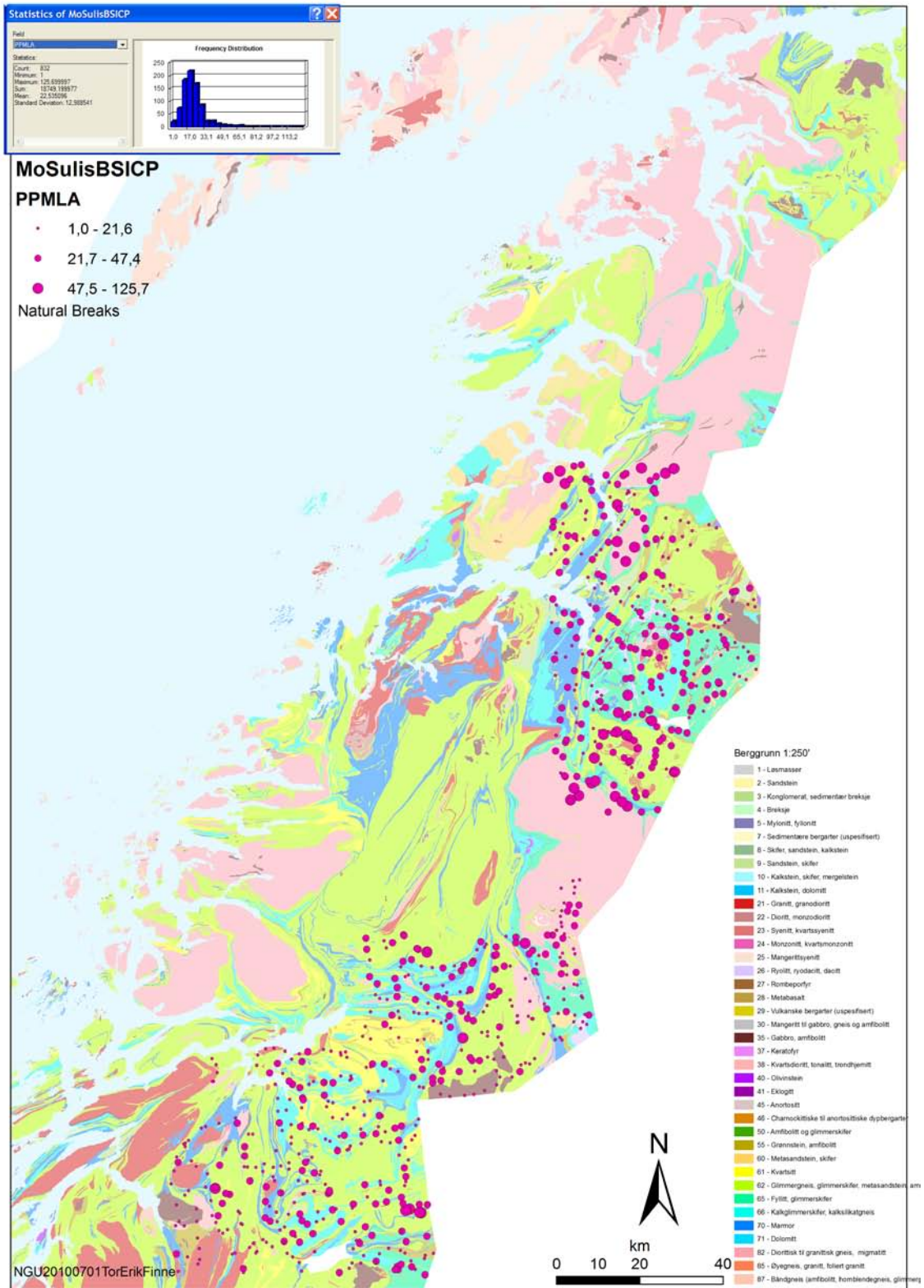


Figure 35. Simplified geological map of central and northern Nordland with La concentrations of stream sediments in areas covered by Caledonian nappes. Source NGU geochemical database. The concentration distribution illustrates that there are no particular REE-anomalies in these areas.

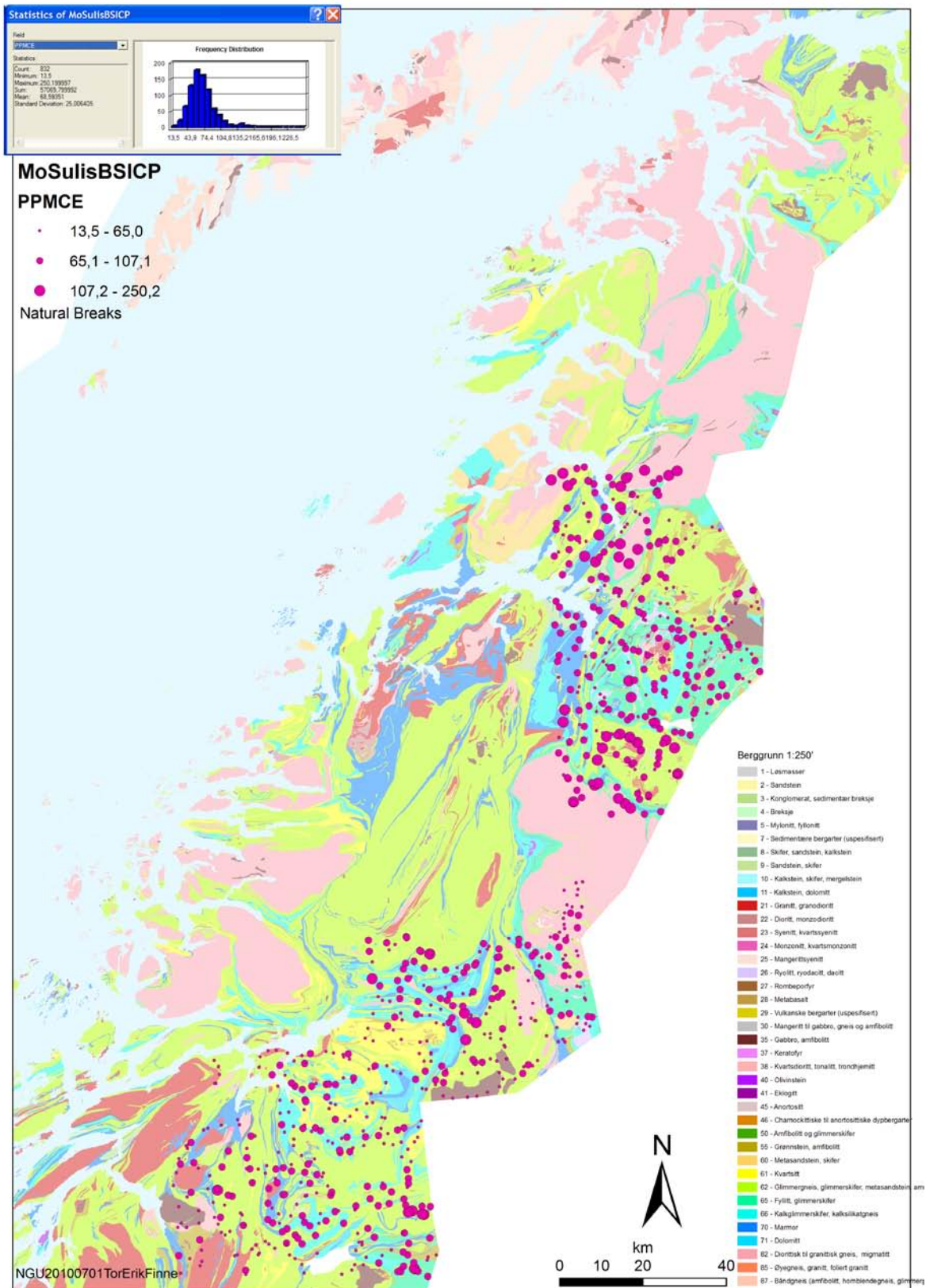


Figure 36. Simplified geological map of central and northern Nordland with Ce concentrations of stream sediments in areas covered by Caledonian nappes. Source NGU geochemical database. The concentration distribution illustrates that there are no particular REE-anomalies in these areas.

7. Summary, discussion and outlook

Accessible literature and mineralogical, geochemical and geophysical data on REE-mineralisations and Zr-, Be-, U-, Th-, (W-) mineralisations, which might be associated with REE-mineralisations, were studied in order to indicate potential target areas for future exploration activity. The primary focus was to evaluate the potential of:

- (1) the Høgtuva Be-REE-U-Sn mineralisation
- (2) strongly fractionated granite intrusions
- (3) REE-fluorite mineralisations
- (4) regional REE anomalies in stream sediments and tills
- (5) REE-silicates (allanite) in granites
- (6) NYF pegmatites
- (7) hydrothermal Fe-deposits with associated REE enrichments
- (8) Th- and allanite-bearing rocks by checking regional radiometric measurements
- (9) basement granites which possibly contain 2-3% REE-oxides by checking NGU databases

As discussed in the above chapters, mineralisations and types of mineralisations named under points (3), (6) and (7) are currently not of economic interest. The Høgtuva Be-REE-U-Sn mineralisation may be not an economic mineralisation at present: However, it is considered as Europe's largest Be mineralisation. A final conclusion should await a more comprehensive presentation and analysis of the available data, possible supplemented for gaps on topics which were not of great interest in the 1980s.

The major outcome of the study is, that some of the more evolved Proterozoic TIB- type granites of the Tysfjord basement window have a potential for sub-economic to economic Zr-REE-mineralisations. Previously published data by Romer et al. (1992) on the TIB-2 (younger) Hellemobotn granites revealed concentrations of up to 1200 ppm Zr, 232 ppm Y, 722 ppm La, 1150 ppm Ce, 249 ppm Th, and 53 ppm U. These concentrations are sub-economic but the resources are presumably large (>1 Mt), representing most probably a granitic intrusive. The samples were collected by A. Korneliussen from NGU in the late 1980s. Because the TIB-granites of the basement window are poorly sampled, there is the potential to identify more TIB-granites with similar or higher-grade Zr-REE mineralisations. This conclusion is supported by anomalies in stream sediment data for REE and in regional radiometric measurements carried out in some parts of the Tysfjord basement window. The possible carriers of the mineralisation are zircon and allanite, based on mineralogical studies by Foslie (1941). The identified Zr-REE-enriched TIB-2 granites are SiO₂-rich, subalkaline, metaluminous A-type (anorogenic) granites with low (Na₂O+K₂O)/CaO ratio (<6; Figs. 37-40). They represent a specific final fractionation trend of the TIB-2 granites (Fig. 37). This mineralisation type is relatively unknown. Possible examples are Zr-REE-mineralised alkaline granites in Saudi Arabia described by (Dysdall et al. 1984). These granites comprise LREE- and HREE-rich types with an estimated range from 6 to 440 Mt with Y concentrations from 0.13 to 0.52 %.

The suggested exploration target areas of Zr-REE-mineralised TIB-(2?) granites are (Fig. 41):

- 1) Northern Tysfjord window:
 - 1a) Tilthorn (Ulsvåg)
 - 1b) Kjerrfjellet-Kjerrvatnet (Drag)
 - 1c) Hundholmen
- 2) Central Tysfjord window:
 - 2a) Hellemobotn
 - 2b) Reinoksfjellet

- 2c) Gjerdalsvatnet
- 3) Southern Tysfjord window:
 - 3a) Sommerseth
 - 3b) Faulevatnet
- 4) Northern Rishaugfjell window

The TIB-granites of the basement windows in central Nordland (Høgtuva, Sjona, Svartisen, Glomfjord, Bjellåtind) are generally less fractionated than the TIB-granites of the Tysfjord window as indicated by geochemical data covering the area with high density. The only exception is the well-investigated Høgtuva mineralisation, which is interpreted as an intrusion-related and subsequently metamorphosed Be-REE-U-Sn mineralisation.

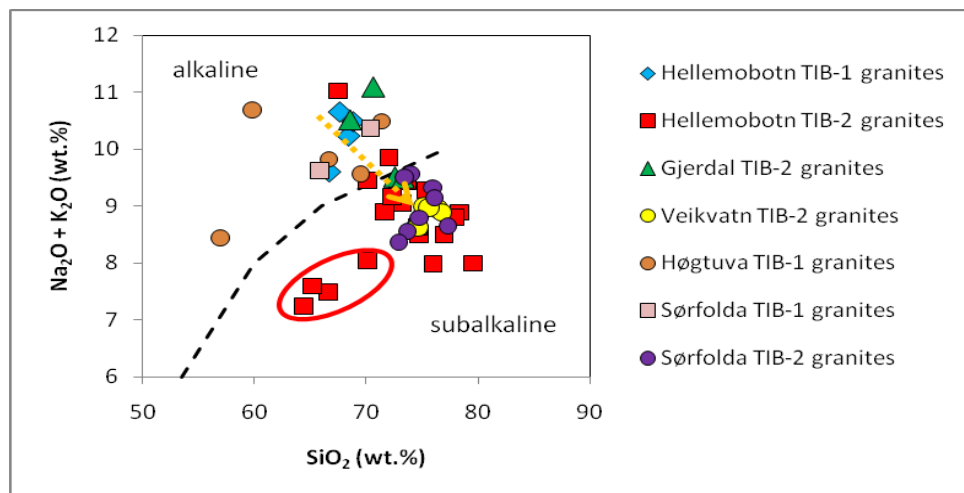


Figure 37. Subalkaline-alkaline classification diagram showing that the older TIB-1 granites have alkaline character which develop to subalkaline TIB-2 granites (orange arrow). The REE-enriched TIB-2 granites from Hellembotn (red ellipse) show a specific fractionation with decreasing SiO_2 during further evolution. Data from Romer et al. (1992).

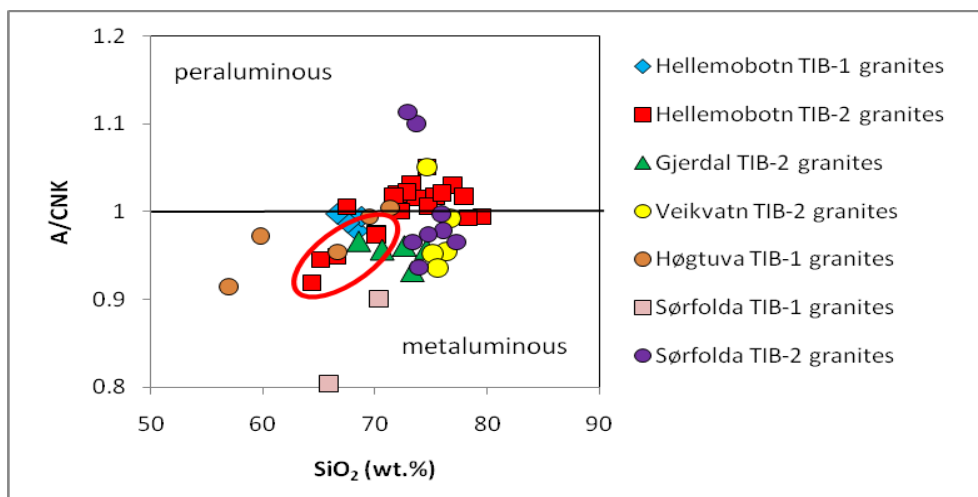


Figure 38. Peraluminous-metaluminous classification diagram showing that the TIB-1 and TIB-2 granites plot in the peraluminous as well in the metaluminous field. The mineralised TIB-2 granites plot in the metaluminous field (red ellipse). $A/CNK = \text{Al}_2\text{O}_3 / (\text{CaO} + \text{Na}_2\text{O} + \text{K}_2\text{O})$ in molecular weight. Data from Romer et al. (1992).

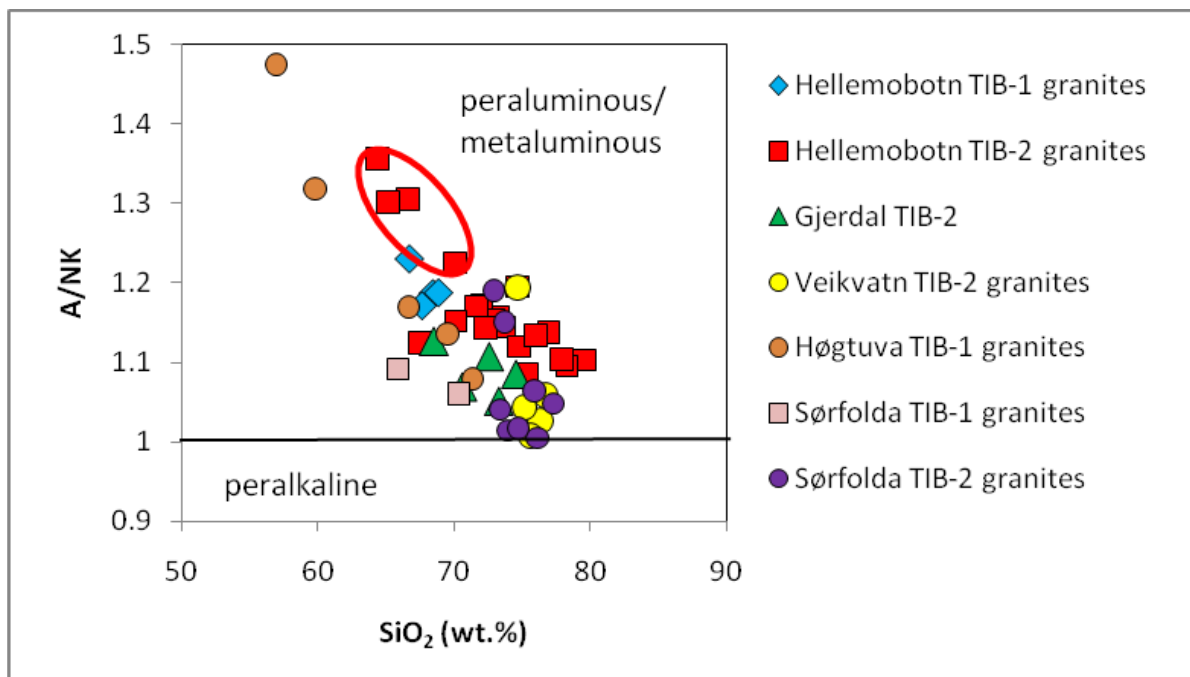


Figure 39. Metaluminous-peralkaline classification diagram showing that none of the TIB-1 and TIB-2 granites plot in the peralkaline field. The mineralised TIB-2 granites are indicated by the red ellipse. $A/NK = Al_2O_3/(Na_2O+K_2O)$ in molecular weight. Data from Romer et al. (1992).

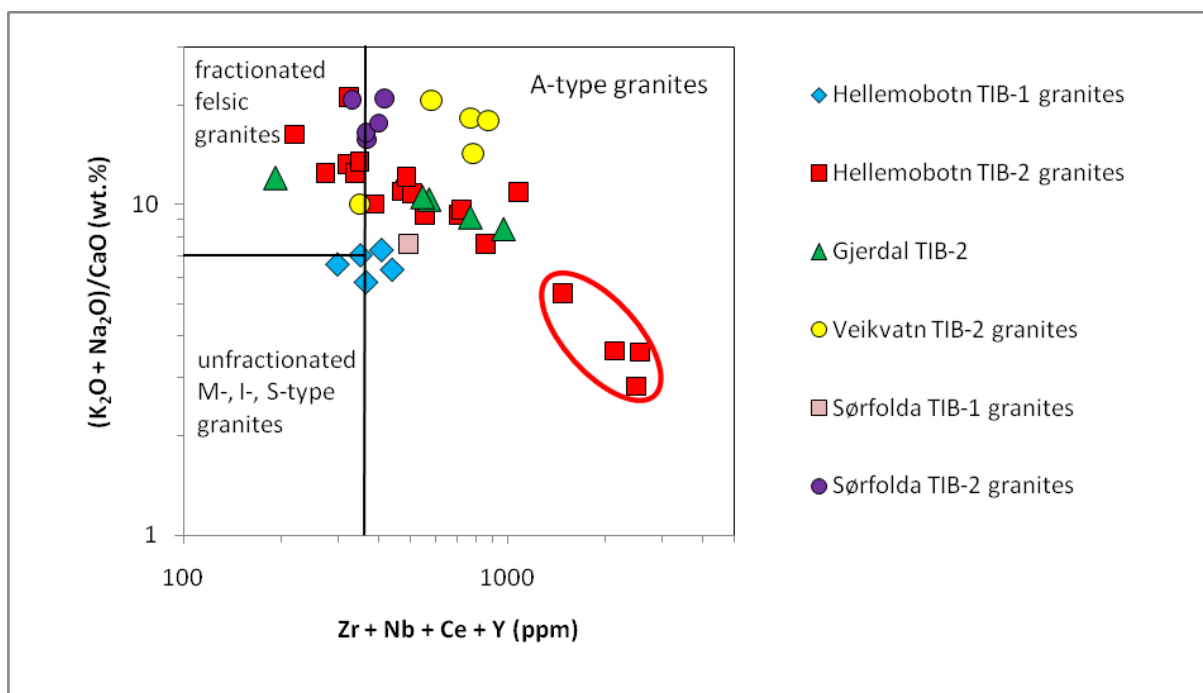


Figure 40. A-type granite classification diagram showing that most of the TIB-granites have A-type affinity in particular the REE-enriched granites from Hellembotn (red ellipse). Data from Romer et al. (1992).

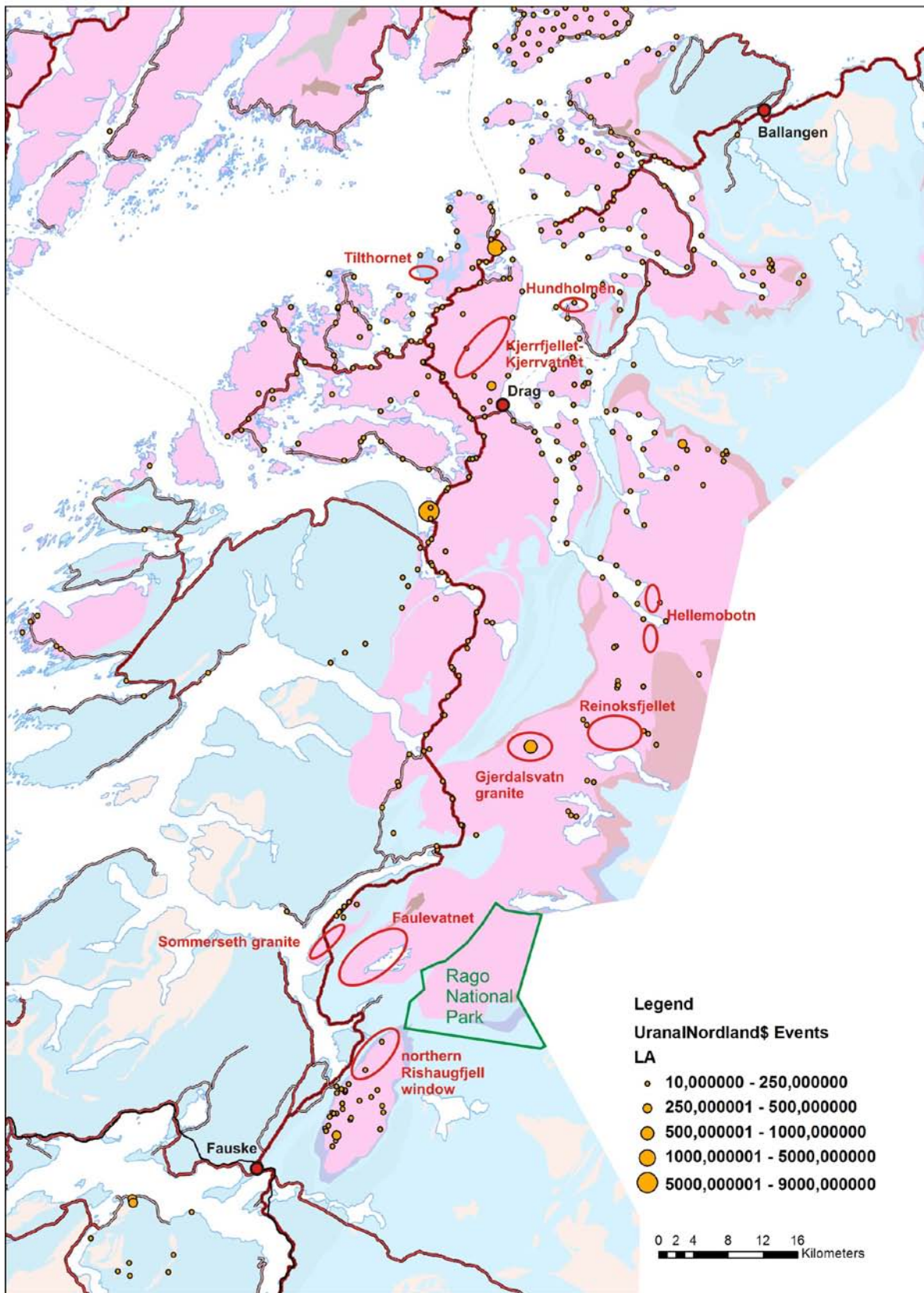


Figure 41. Simplified geological map of northern Nordland with suggested target areas for sampling of REE-Zr-enriched TIB-2 granites.

8. References

- Andersson U.B. (1997) Petrogenesis of some Proterozoic granitoid suites and associated basic rocks in Sweden (geochemistry and isotope geology). Sveriges Geologiska Undersökning, Rapporter och meddelanden 91. 216 p.
- Andréasson P.G. (1994) The Baltoscandian margin in Neoproterozoic–early Palaeozoic time. Some constraints on terrane derivation and accretion in the Arctic Scandinavian Caledonides: *Tectonophysics* 231:1–32, doi: 10.1016/0040-1951(94)90118-X.
- Barnes C.G., Frost C.D., Yoshinobu A.S., McArthur K., Barnes M.A., Allen C.M., Nordgulen Ø., Prestvik T. (2007) Timing of sedimentation, metamorphism, and plutonism in the Helgeland Nappe Complex, north-central Norwegian Caledonides. *Geosphere* 3:683–703, doi: 10.1130/GES00138.1.
- Bingen B., Andersson J., Söderlund U., Möller C. (2008) The Mesoproterozoic in the Nordic countries. *Episodes* 31:29-34.
- Bjørlykke A., Sangster D.F., Feyn U. (1991) Relationships between high heat-production (HHP) granites and stratabound lead-zinc deposits. In: Pagel M., Leroy J.L. (eds.) *Source, transport and deposition of metals. SGA 25 Years Anniversary Meeting, Nancy, France, 257-260.*
- Bonin B. (2007) A-type granites and related rocks: Evolution of a concept, problems and prospects. *Lithos* 97:1-29.
- Bruton D.L., Harper D.A.T. (1985) Early Ordovician (Arenig-Llanvirn) faunas from oceanic islands in the Appalachians-Caledonide orogen. In: Gee, D. G., Sturt, B. A. (eds.) *The Caledonide Orogen — Scandinavia and Related Areas.* John Wiley & Sons, Chichester, pp. 359-368.
- Bugge A. (1963) Norges Molybden-forekomster. NGU 217.
- Busch K. (1989) Tungsten deposits related to solution-remobilization during regional metamorphism in the Bjellåtind area, Nordland, Norway (Danish). M.Sc. thesis University of Copenhagen.
- Černý P., Trueman D.L. (1985) Polythionite from the rare-metal deposit of the Blackford Lake alkaline complex, N.W.T., Canada. *Am. Mineral.* 70:1127-1134.
- Chappell B.W., White A.J.R. (2001) Two contrasting granite types: 25 years later. *Australian J. Earth Sci.* 48:489-499.
- Cribb S.J. (1981) Rb-Sr geochronological evidence suggesting a reinterpretation of part of the north Norwegian Caledonides. *Norsk Geologisk Tidsskrift* 61:97-110.
- Drivenes K. (2010) Wolframmineralisert diopsidskarn ved Bjellåtinden: Petrologi og væsleinnslutningsstudiar. Master thesis, Norges Teknisk-Naturvitenskapelige Universitet, 100 p.
- Drysdall A.R., Jackson N.J., Ramsay C.R., Douch C.J., Hackett D. (1984) Rare element mineralization related to Precambrian alkali granites in the Arabian Shield. *Economic Geology* 79:1366-1377.
- Essex R., Gromet L.P. (1996) Constraints on the timing of Caledonide thrust stack emplacement from U-Pb metamorphic ages of basement gneiss, Nasafjellet Window (66.5N 15.5E), Scandinavian Caledonides. *Geol. Soc. Amer. Abst. Prog.* 28, A501.
- Flood E. (1944) Angående molybdenforekomst i Kalvik i Sørfold. NGU report, Bergarkivet BA 3600, 1 p.

- Foslie S. (1941) Tysfjords geologi. Beskrivelse til det geologiske gradteigskart Tysfjord. NGU. 149, 298 p.
- Foslie S. (1942) Hellemobotn og Linnajavrre. Geologisk beskrivelse til kartbladene. NGU 150, 119 p.
- Furuhaug L. (1984) Prøvetaking og radiometriske målinger ved Bordvedåga, Høgtuva-vinduet. NGU report 84.014, 11 p.
- Furuhaug L. (1990) Prøvetaking, særlig med tanke på Be. Veikvatn – Linajav'ri – området, Nordland. NGU report 90.135, 19 p.
- Gee D.G., Sturt B.A. (eds.) (1985) The Caledonide Orogen—Scandinavia and related areas: New York, Wiley, 1266 p.
- Gee D.G., Fossen H., Henriksen N., Higgins A.K. (2008) From the early Paleozoic Platforms of Baltica and Laurentia to the Caledonide Orogen of Scandinavia and Greenland. *Epsisodes* 31:44-51.
- Gemmel J.B., Zantop H., Meinert L.D. (1992) Genesis of the Aguilar zinc-lead silver deposit, Argentina: Contact metasomatic versus sedimentary exhalative. *Econ. Geol.* 87:2085-2112.
- Gorbatshev, R. (1985) Precambrian basement of the Caledonides. In: Gee, D. G., Sturt, B. A. (eds.) *The Caledonide Orogen — Scandinavia and Related Areas*. John Wiley & Sons, Chichester, pp. 197-212.
- Gower C.F. (1992) The relevance of Baltic shield metallogeny to mineral exploration in Labrador. In: *Current Research*. Newfoundland Department of Mines and Energy, Geol. Surv. Report 92-1, p. 331-366.
- Grauch R.I., Lindahl I., Evans H.T., Jr., Burt D.M., Fitzpatrick J.J., Foord E.E., Graff P.-R., Hysingjord J. (1994) Høgtuvaite, a new beryllian member of the aenigmatite group from Norway, with new X-ray data on aenigmatite. *Can. Mineral.* 32:439-448.
- Grenne T., Ihlen P., Vokes F. (1999) Scandinavian Caledonide metallogeny in a plate tectonic perspective: *Mineralium Deposita* 34:422–471, doi: 10.1007/s001260050215.
- Gust J., Thoresen H (1981) Radiometriske malinger og prøvetaking I Rendalsvik grafittfelt, Meløy, Nordland. NGU report 1650/59A, 16 p.
- Gustavson M., Gjelle S.T. (1991) Geological Map of Norway (1:250 000) Mo i Rana. Geological Survey of Norway.
- Hansen A.K. (1983) Undersøkelse af Mo-U-W mineraliseringer i Kalvikvinduet ved Sommerset, Sørfold, Nordland. NGU rapport nr 1900/30F
- Högdahl K., Andersson U.B., Eklund O. (2004) The Transscandinavian Igneous Belt (TIB) in Sweden: a review of its character and evolution. Geological Survey of Finland, Special Paper 37, 125 pp.
- Husdal T. (2008): The minerals of the pegmatites within the Tysfjord granite, northern Norway. *Norsk Bergverksmuseum Skrift* 38:5-28.
- Karlsen T.A. (2000) Economic potential of potassic feldspar-rich gneisses in Tysfjord/Hamarøy, northern Norway. *NGU Bull.* 436:129-135.
- Karlstrøm H.J. (1990) Underøkelse av noen Cu, Fe og kisforekomster i Tysfjordområde. NGU rapport 90.092, 21 p.
- Kjeldsen S. (1987) Geokjemisk kartlegging i Nordland og Troms. ICAP-analyse av løsmassenes fin fraksjon. NGU report 87.142.
- Korneliussen A., Krog R., Furuhaug L., Mathiesen C.O. (1989) Sjeldne jordartselementer I Hellemobotn-Linnajavrre-regionen, Tysfjord, Hamarøy and Sørfold kommuner, Nordland. NGU report 89.099, 26 p.

- Krog R. (1988) Litogeokjemisk undersøkelse av Høgtuva og Sjona grunnfjellsvinduer. Flussyreløselige Be og saltpetersyreløselige konsentrasjoner av 21 andre elementer. NGU report 88.107.
- Kwak T.A.P., Abeysinghe P.B. (1987) Rare earth and uranium minerals present as daughter crystals in fluid inclusions, Mary Kathleen U-REE skarn, Queensland, Australia: *Mineral. Mag.* 51:665-670.
- Lahtinen R., Garde A.A., Melezhik V.A. (2008) Paleoproterozoic evolution of Fennoscandia and Greenland. *Episodes* 31:20-28.
- Larsen R. (2007) Re-Os dating of orogenic W-Mo deposits in the Mid-Norwegian Caledonides. GSA Denver Annual Meeting 28th-31st October 2007, Paper No. 100-10.
- Lentz D. (1991) Radioelement distribution in U, Th Mo, and rare-earth-element pegmatites, skarns and veins in a portion of the Grenville province, Ontario and Quebec. *Can. J. Earth Sc.* 28:1-12.
- Lentz D. (1998) Late-tectonic U-Th-Mo-REE skarn and carbonatitic vein-dyke systems in the southwestern Grenville province: A pegmatite-related pneumatolytic model linked to marble melting (limestone syntexis). *Mineral. Ass. Can. Short Course Series* 26:519-658.
- Lindah I. (1977) Radiometriske bilmålinger og radiometriske målinger i Gildeskål - Meløyområdet. NGU report 1389/4, 18 p.
- Lindah I. (1983) Classification of uranium mineralization in Norway. *Nor. Geol. Unders.* 380:125-142.
- Lindah I. (1984) Rishaugfjellvinduet og Harelifjell uranmineralisering, Sørfold, Nordland. NGU report 84.057, 131p.
- Lindah I. (1990) Berylliumundersøkelse på Tjeldøya, Nordland. NGU report 90.006, 55 p.
- Lindah I., Furuhaug L. (1987a) Malmprospektering Oterstrand-Laksådal, Gildeskål, Nordland, NGU report 1430/20A, 14 p.
- Lindah I., Furuhaug L. (1987b) Geologisk, geokjemisk og radiometrisk kartlegging av mineralisert gneiss ved Bordvedåga, Høgtuva-vinduet, Rana, Nordland. NGU report 87.029, 33 p.
- Lindah I., Grauch R.I. (1988) Be-REE-U-Sn-mineralization in Precambrian granitic gneisses, Nordland County, Norway. In: Zachrisson E. (ed.) *Proceedings of the Seventh Quadrennial IAGOD Symposium, Luleå, Sweden*, p. 583-594. E. Schweizerbart'sche Verlagsbuchhandlung, Stuttgart.
- Lindqvist J.-E. (1983) A diamictite in the Nasafjäll window, central Scandinavian Caledonides. *GGF* 105:223-227.
- Lindqvist J.-E. (1988) Tectonic implications of U-, Mo- and V-enriched graphitic phyllites in the Høgtuva and Nasafjäll windows, Scandinavian Caledonides. *Norsk Geologisk Tidsskrift* 68:187-199.
- Lindsey D.A. (1982) Tertiary volcanic rocks and uranium in the Thomas Range and northern Drum mountains, Juab County, Utah. *U.S. Geol. Surv. Prof. Papers* 1221, 71 p.
- Linnen R.L., Cuney M. (2005) Granite-related rare-element deposits and experimental constraints on Ta-Nb-W-Sn-Zr-Hf mineralization. In: Linnen R.L., Samson I.M. (eds.) *Rare-element geochemistry and ore deposits*. Geol. Assoc. of Canada, Short Course Notes, Ottawa, 17:406-452.
- Möller P. (1989a) REE(Y), Nb, and Ta enrichment in pegmatites and carbonatite-alkalic rock complexes. In: Möller P., Černý P., Saupé F. (eds.) *Lanthanides, Tantalum and Niobium*. Springer, Berlin, Heidelberg, p. 103-144.

- Möller P. (1989b) Rare earth mineral deposits and their industrial importance. In: Möller P., Černý P., Saupé F. (eds.) *Lanthanides, Tantalum and Niobium*. Springer, Berlin, Heidelberg, p. 103-144.
- Müller A., Furuhaug L., Korneliussen A. (2008) Resource evaluation of the Målvika tungsten deposit, Nordland. Norges Geologiske Undersøkelse Rapport 2008.008
- Neumann H. (1952) Rendalsvik glimmer -og grafittforekomsters Interessetentselskap. NGU report Bergarkivet; No.BA 6035. 1 p.
- Neumann H. (1985) Norges mineraler. NGU 68, 278 p.
- Nilsson L.P. (2004) Befaring av flusspat-lokalitet ved Lille Mannfjellvatn i Tysfjord. NGU notat, 14th December 2004.
- Oftedal I. (1950) En litiumførende granittpegmatitt i Nordland. Norsk Geologisk Tidsskrift 28:234-237.
- Often M. (1979) Orienterende undersøkelser og diamantboring av grensesonen Prekambrium/Kaledon i Saltdal - Sørfold - regionen. NGU report 1650/30A, 26 p.
- Often M. (1980) Gruvegeologiske undersøkelser i Laksådal og Oterstrand gruver. NGU report 1575/20E, 15 p.
- Öhlander B. (1986) Proterozoic mineralizations associated with granitoids in northern Sweden, Sveriges Geologiska Undersökning. Ser. Ca, Avhandlingar Och Uppsatser vol. 65, 39 pp.
- Petersen L.R., Stendal H. (1987) Tungsten exploration in the Valnesfjord region, Nordland, Northern Norway. *Journal of Geochemical Exploration* 29:151-163.
- Ramberg I.B., Bryhni I., Nøttvedt A. (2006) Landet blir til – Norges geologi. Norsk Geologisk Forening.
- Rekstad J. (1919) Geologiske iakttagelser på strekningen Folla-Tysfjord. Årbok for 1918 og 19. NGU 83:1-60.
- Roberts D. (2003) The Scandinavian Caledonides: Event chronology, palaeogeographic settings and likely modern analogues: *Tectonophysics* 365:283–299, doi: 10.1016/S0040-1951(03)00026-X.
- Roberts D., Gee D.G. (1985) An introduction to the structure of the Scandinavian Caledonides. In: Gee D.G., Sturt B.A. (eds.) *The Caledonide Orogen—Scandinavia and related areas*: New York, Wiley, p. 55–68.
- Roberts D., Nordgulen Ø., Melezhik V. (2007) The Uppermost Allochthon in the Scandinavian Caledonides: From a Laurentian ancestry through Taconian orogeny to Scandian crustal growth on Baltica. In: Hatcher R.D., Jr., et al. (eds.) *4-D framework of continental crust*. Geological Society of America Memoir 200:357–377, doi: 10.1130/2007.1200(18).
- Romer R.L., Smeds S.-A. (1996) U-Pb columbite ages of pegmatites from Sveconorwegian terranes in southwestern Sweden. *Precambrian Res.* 76:15-30.
- Romer R.L., Kjøsnes B., Korneliussen A., Lindahl I., Skyseth T., Stendal M., Sundvoll B., (1992) The Archaean-Proterozoic boundary beneath the Caledonides of northern Norway and Sweden: U-Pb, Rb-Sr and Nd isotope data from the Rombak-Tysfjord area. NGU report 91.225, 67 p.
- Rutland R.W.R., Holmes M., Jones M.A. (1960) Granites in the Glomfjord area, Northern Norway. In: *International Geological Congress 21:1960 København, Part XiX*, pp.43-53.
- Rutland R.W.R., Sutherland D.S. (1967) The chemical composition of granitic gneisses and sparagmitic metasediments in the Glomfjord region, Northern Norway. NGU 47:359-374.

- Rønning J.S. (1986) Geofysiske og petrofysiske undersøkelser ved Storjord I 1984 og 1985. NGU report 86.053, 46 p.
- Samson I.M., Wood S.A. (2005) The rare earth elements: behavior in hydrothermal fluids and concentration in hydrothermal mineral deposits, exclusive alkaline settings. In: Linnen R.L., Samson I.M. (eds.) Rare-element geochemistry and ore deposits. Geol. Assoc. of Canada, Short Course Notes, Ottawa, 17:406-452.
- Skjeseth S., Sørensen H (1953) An example of granitization in the central zone of the Caledonides of northern Norway. *Nor. Geol. Unders.* 184:154-187.
- Skår Ø. (2002) U-Pb geochronology and geochemistry of the early Proterozoic rocks of the tectonic basement windows in central Nordland, Caledonides of north-central Norway. *Precambrian Res.* 116:265-283.
- Solli A., Nordgulen Ø. (2006) Bedrock map of Norway and the Caledonides in Sweden and Finland scale 1 : 2 000 000. Geological Survey of Norway.
- Stendal H. (1990) Mineraliseringspotensial af granitiske bjergarter I den sydlige del af Tysfjordvinduet, Nordland, Norge. *Geolognytt* 1/90:106-107.
- Stendal H. (1992) Wolfram og molybden i Nordlandsregionen. Geologisk Institut, Københavns Universitet. Rapport.
- Stephens M. B. (1988) The Scandinavian Caledonides: a complexity of collisions. *Geology Today* 4:20-26.
- Stephens M.B., Furnes H., Robins B., Sturt B.A. (1985) Igneous activity within the Scandinavian Caledonides. In: Gee D.G., Sturt B.A. (eds.) *The Caledonide Orogen - Scandinavia and related areas Part 2*, New York, Wiley, pp. 623-656.
- Sverdrup T.L., Thorkildsen C.D., Bjørlykke H. (1967) Uran and thorium I Norge. *Norges Geol. Unders.* 250A, 31 p.
- Taylor S.R., McClennan J.C. (1985) *The continental crust: Its composition and evolution*. Oxford, UK, Blackwell Scientific Publications.
- Vogt T. (1922) Über Thalenit von Hundholmen. *Vid.-Selsk. Skrifter I.M.-N. Kl.* 1:19-47.
- Vogt T. (1923) Über die seltenen Erden im Yttrifluorit von Hundholmen. *Centralblatt für Mineralogie, Geologie und Paläontologie* 1923:673-676.
- Whalen J.B., Currie K.L., Chapell B.W. (1987) A-type granites: geochemical characteristics, discrimination and petrogenesis. *Contrib. Mineral. Petrol.* 95:407-419.
- Wilberg R. (1987a) Granitophile elements in granitoid rocks in Precambrian basement windows in Nordland, Northern Norway, with special reference to the rare-element enriched gneiss at Bordvedåga, Høgtuva window. NGU report 87.043, 79 p.
- Wilberg R. (1987b) Resultater fra oppboring av Bordvåga berylliumforekomst I 1987. NGU report 87.172.
- Wilberg R. (1987c) Bilagsrapport til NGU rapport 87.043: Bergartsanalyser fra Høgtuva, Sjøna og andre prekambriske grunnfjellvinduer i Nordland. NGU report 87.158.
- Wilberg R. (1987d) Beryllium-mineraliseringer i Bordvedåga-området, Høgtuva-vinduet. NGU report 87.171.
- Wilberg R. (1988) Sporelementinnhold og -variasjoner i beryllium-forekomstene ved Bordvedåga, Høgtuva-vinduet. NGU report 88.177.
- Wilberg R. (1989a) Snøfjellet beryllium-mineralisering, Høgtuva-vinduet. NGU report 89.070, 34 p.
- Wilberg R. (1989b) Økonomisk mineralogi i Bordvedåga beryllium-forekomst, Rana, Nordland. NGU report 89.083, 114 p.

- Wilberg R. (1989c) Resultater fra diamantboring i Bordvedåga-Tverrbekkfjell-området i 1988. NGU report 89.091, 40 p.
- Wilberg R. (1989d) Data for malmsonering for Bordvedåga-forekomsten, analyser fra Be-mineraliseringer og regional geologi i Høgtuva-området. NGU report 89.097, 67 p.
- Wilberg R., Furuhaug L. (1989) Nye beryllium-mineraliseringer i Bordvedåga-Tverrbekkfjell-området, Høgtuva-vinduet. NGU report 89.053, 26 p.
- Wilberg R., Lindahl I. (1991) Bordvedåga beryllium-forekomst, Rana kommune, Nordland. Samplerapport. NGU report 91.180, 38 p.
- Wilson M.R., Nicholson R. (1973) The structural setting and geochronology of basal granitic gneisses in the Caledonides of part of Nordland. *J. Geol. Soc. London* 129:365-387.
- Wilson M.R., Åkerblom G. (1980) Uranium enriched granites in Sweden. *Sveriges Geologiska Undersökning, Rapporter och meddelanden* 19. 30 p.

Appendix 1.

Mineral names and formula mentioned in this study.

mineral name	formula
allanite	$(\text{Ce,Ca,Y})_2(\text{Al,Fe}^{3+})_3(\text{SiO}_4)_3(\text{OH})$
apatite	$\text{Ca}_5(\text{PO}_4)_3(\text{F,Cl,OH})$
Be-rhönite	$\text{Ca}_2(\text{Mg,Fe}^{2+},\text{Fe}^{3+},\text{Ti})_6[\text{O}_2](\text{Si,Al})_6\text{O}_{18}$
bastnaesite	$(\text{Ce,La})[\text{CO}_3]\text{F}$
beryl	$\text{Be}_3\text{Al}_2\text{Si}_6\text{O}_{18}$
cassiterite	SnO_2
cerfluorite	$(\text{Ca,Ce})\text{F}_{2+x}$
chalcopyrite	CuFeS_2
cheralite	$(\text{Ce,Ca,Th})(\text{P,Si})\text{O}_4$
columbite	$(\text{Mn,Fe})(\text{Nb,Ta})_2\text{O}_6$
danalite	$\text{Fe}^{2+}_4\text{Be}_3[\text{Si}(\text{SiO}_4)_3]$
eudialyte	$\text{Na}_4(\text{Ca,Ce})_2(\text{Fe}^{2+},\text{Mn,Y})\text{ZrSi}_8\text{O}_{22}(\text{OH,Cl})_2$
fluocerite	$(\text{La,Ce})\text{F}_3$
fluorite	CaF_2
gadolinite	$\text{Y}_2\text{Fe}^{2+}\text{Be}_2\text{Si}_2\text{O}_{10}$
genthelvite	$\text{Zn}_4\text{Be}_3[\text{Si}(\text{SiO}_4)_3]$
helvite	$\text{Mn}^{2+}_4\text{Be}_3[\text{Si}(\text{SiO}_4)_3]$
høgtuvaite	$(\text{Ca,Na})_2(\text{Fe}^{2+},\text{Fe}^{3+},\text{Ti})_6[\text{O}_2]\text{Be}(\text{Si,Al})_5\text{O}_{18}$
loparite	$(\text{Ce,Na,Ca})_2(\text{Ti,Nb})_2\text{O}_6$
magnetite	$\text{Fe}^{2+}\text{Fe}^{3+}_2\text{O}$
microlite	$(\text{Na,Ca})(\text{Ta,Nb})_2\text{O}_6(\text{OH,F})$
molybdenite	MoS_2
monazite	$\text{Ce,La,Nd,Th})\text{PO}_4$
phenacite,	(BeSiO_4)
phosphorite	Ca-phosphate-rich rock
scheelite	$\text{Ca}[\text{WO}_4]$
spodumen	$\text{LiAlSi}_2\text{O}_6$
thorite	$(\text{Th,U})\text{SiO}_4$
titanite	CaTiSiO_5
tourmaline	$\text{AD}_3\text{G}_6(\text{BO}_3)_3[\text{T}_6\text{O}_{18}]\text{Y}_3\text{Z}$ where A = Ca, Na, K; D = Al, Fe ²⁺ , Fe ³⁺ , Li ⁺ , Mg ²⁺ , Mn ²⁺ ; G = Al ³⁺ , Cr ³⁺ , Fe ³⁺ , V ³⁺ ; T = Si (and sometimes minor Al ³⁺ , B ³⁺); Y = O and/or OH; Z = F, O and/or OH
uraninite	UO_2
xenotime	YPO_4
yttrifluorite	$(\text{Ca}_{1-x}\text{Y}_x)\text{F}_{2+x}$ where $0.05 < x < 0.3$
zircon	ZrSiO_4

Appendix 2.

Analyses of rocks associated with the Storjord magnetite mineralisation according to Rønning (1986).

rock type	sample	SiO ₂	Al ₂ O ₃	Fe ₂ O ₃	TiO ₂	MgO	CaO	Na ₂ O	K ₂ O	MnO	P ₂ O ₅	Gl tap	total	Nb	Zr	Y	Sr	Rb	Ba	U	Th	Ce	La
pegmatite	K61.84													0	0	0	148	337	2600	0	0	38	19
pegmatite	K9A.84													18	127	104	99	148	1200	0	10	78	25
pegmatite	K9B.84													9	104	64	123	250	1500	0	0	65	24
skarn	K4A.84													0	247	50	612	0	38	11	40	173	86
skarn	K4B.84													0	316	35	661	0	76	0	51	199	95
skarn	K52.84													19	166	32	514	60	875	20	11	123	56
skarn	K64.84													6	206	65	89	10	30	92	0	44	23
skarn	K56.84													46	284	45	291	274	8600	11	21	124	44
granitic gneiss	F2.84													28	477	64	85	249	498	0	33	154	56
granitic gneiss	F3.84													22	383	58	120	232	660	0	20	150	50
gneiss	K35.84	59.92	14.55	5.28	0.67	0.82	6.1	4.8	4.67	0.39	0.18	0.56	97.94	33	431	126	230	114	1500	0	0	186	70
gneiss	K44.84	52.23	15.89	9.77	0.74	5.76	4.49	4.4	3.47	0.18	0.34	0.94	98.21	0	123	15	617	120	1200	0	0	53	18
granite	K45.84	77.14	12.24	0.85	0.03	0.01	0.4	4.5	3.8	0.02	0.01	0.38	99.36	17	177	51	30	231	60	0	18	43	13
intermediate granite	K47.84													8	160	23	314	60	768	0	0	67	29
mafic gneiss	K34.84	49.02	8.96	24.82	0.34	3.67	6.53	2.5	2.03	0.45	0.1	-0.05	98.37	35	239	360	124	31	287	0	38	568	206
mafic gneiss	K31.84	52.85	8.46	21.41	0.36	2.34	6.8	3.8	0.77	0.37	0.4	-0.08	97.48	0	261	1400	124	9	161	44	321	2600	947
mafic gneiss	K32.84	60.74	12.03	6.73	0.23	3.01	7.97	5.9	1.74	0.44	0.08	0.14	99.01	11	313	94	111	42	427	0	0	174	70
ultramafic mangerite	K5.84	37.26	7.16	27.27	5.29	5.83	9.4	1.9	1.28	0.54	3.41	-1.71	97.63	10	127	89	321	13	1300	0	10	238	99
mafic mangerite	K7.84	54.36	13.24	12.43	2.12	1.96	4.3	4	4.26	0.26	1.13	-0.06	98	23	404	83	235	70	2000	0	0	281	128
K-rich volcanite	K2A.84	68.56	14.9	2.61	0.18	0.17	1.51	2.4	7.84	0.05	0.03	0.19	98.44	17	251	23	106	279	926	0	23	119	56
K-rich volcanite	K2B.84	67.76	15.51	3.01	0.24	0.34	1.49	2.4	7.9	0.06	0.06	0.23	99	15	304	23	123	280	1000	0	20	141	60
K-rich volcanite	K40.84													0	0	10	8	809	29	0	0	0	0
volcanite	K53.84													22	334	40	98	200	513	0	23	127	54
volcanite	K58.84													23	136	0	181	163	2700	0	13	0	0

Appendix 2. Continued.

rock type	sample	SiO ₂	Al ₂ O ₃	Fe ₂ O ₃	TiO ₂	MgO	CaO	Na ₂ O	K ₂ O	MnO	P ₂ O ₅	Gl tap	total	Nb	Zr	Y	Sr	Rb	Ba	U	Th	Ce	La
volcanite	K65.84	62.79	16.73	2.95	0.93	2.14	2.92	8.3	0.72	0.09	0.3	0.29	98.16	10	279	27	207	38	166	0	13	119	65
intermediate volcanite	K48.84	53.96	13.98	8.99	0.8	3.29	9.08	3.9	2.78	0.24	0.45	0.43	97.9	8	164	29	483	77	1100	0	0	79	39
amphibolite	K14A.84	20.86	0.94	51.58	0.55	1.57	17.32	0.2	0.01	0.61	0.25	5	98.88	99	136	2100	100	6	34	58	214	1900	691
amphibolite	K14B.84													76	88	902	19	17	32	714	140	1400	531
amphibolite	K15.84													11	98	28	116	120	634	0	0	41	16
amphibolite	K16A.84	17.56	1.27	71.03	0.73	1.24	5.96	0.3	0.03	0.5	0.59	-1.28	97.93	109	39	1800	31	7	48	81	445	5100	1900
amphibolite	K16B.84													97	18	1400	31	6	40	111	385	4100	1500
amphibolite	K17.84	34.55	0.49	56.05	0.54	0.57	8.02	0.1	0.01	0.39	0.08	-0.07	100.62	100	187	792	25	0	38	69	130	1300	407
amphibolite	K18A.84	23.42	0.82	67.19	0.52	1.52	4.95	0.1	0.07	0.27	0.44	-1.39	97.81	21	18	1500	15	0	28	31	290	3300	1200
amphibolite	K18B.84													0	9	1600	20	0	29	37	333	3300	1200
amphibolite	K19.84													171	182	598	7	0	26	21	69	718	208
amphibolite	K20.84													194	96	999	54	9	1300	96	208	2000	719
amphibolite	K21.84													164	120	1600	11	7	34	176	245	2700	1000
amphibolite	K22.84													72	95	1900	37	8	42	71	289	2900	1100
amphibolite	K23.84													66	37	1500	8	0	43	39	280	3400	1300
amphibolite	K24A.84													73	166	582	24	8	76	0	29	637	252
amphibolite	K24B.84													118	103	515	15	9	43	27	76	974	367
amphibolite	K26.84													26	38	1400	35	8	47	38	290	3400	1300
amphibolite	K27.84	19.04	1.83	65.41	0.37	1.58	9.41	0.3	0.01	0.54	0.65	-1.25	97.81	63	38	1300	78	6	35	99	509	5500	2200
amphibolite	K28.84													137	143	302	0	7	75	0	37	375	87
amphibolite	K33.84	30.78	5.8	46.75	0.54	3.08	7.17	1	0.91	0.7	0.88	-0.59	97.02	0	101	2300	62	15	69	73	476	5300	2100

Appendix 3.

Analyses of TIB-granites of the Tysfjord basement window according to Romer et al. (1992).

Sample	SiO ₂	Al ₂ O ₃	Fe ₂ O ₃	MnO	TiO ₂	MgO	CaO	K ₂ O	Na ₂ O	P ₂ O ₅	total	LOI	Ba	La	Sr	Y	Zr	Nb	Rb	Ce	Sm	Hf	Ta	Th	U	
Tysfjord (Hellemobotn): older granites																										
MH1-42	68.41	16.3	2.48	0.04	0.34	0.32	1.61	5.51	4.72	0.11	100.2	0.35	788	98	197	34	209	18	194	180	10	7	1	31	7	
MH2-43	68.82	16.55	2.26	0.04	0.28	0.31	1.49	5.89	4.59	0.09	100.68	0.37	854	73	203	24	185	13	201	130	5	7	1	24	3	
MH3-44	67.61	16.69	2.15	0.04	0.3	0.26	1.46	5.83	4.82	0.09	99.73	0.5	884	90	200	25	213	11	190	160	6	7	1	28	3	
MH4-45	66.67	15.82	3.26	0.05	0.42	0.49	1.65	5.23	4.37	0.12	98.96	0.87	751	80	192	31	157	18	206	160	7	8	1	26	4	
MH5-46		16.43	2.25	0.04	0.28	0.29	1.56	5.54	4.75	0.08	100.7	0.51	751	56	192	31	157	13	206	98	6	6	1	23	5	
Tysfjord (Hellemobotn): younger granites																										
KH50A-1	73.25	14.09	2.6	0.04	0.26	0.21	0.81	4.8	4.25	0.04	100.56	0.2	294	35	87	46	332	23	317	86	5.6	16	4	82	17	
KH51-3**	72.02	15.06	3.01	0.05	0.32	0.25	1.06	5.98	3.87	0.06	101.89	0.22	443	150	64	59	329	30	214	290	17	14	3	58	9	
KH52-4	73.66	14.12	2.02	0.03	0.19	0.08	0.86	5.62	3.8	0.03	100.58	0.18	288	120	61	44	202	18	244	210	12	7		60	12	
KH55-7	72.86	14.22	2.11	0.03	0.28	0.46	0.87	5.64	3.78	0.06	100.62	0.31	706	97	172	15	252	12	173	230	8	8		29	3	
KH56C-10	71.67	13.6	2.48	0.03	0.31	0.31	0.96	5.38	3.52	0.07	98.53	0.2	348	130	76	60	260	27	265	210	12	10	3	53	10	
KH57A-11	75.37	13.11	1.73	0.03	0.15	0.09	0.44	5.66	3.62	0.02	100.41	0.19	107	53	27	40	177	22	370	85	6	9	2	52	10	
KH58-13	79.55	11.76	1.12	0.02	0.07	0.00	0.64	4.41	3.58	0.005	101.36	0.24	5	28	6	64	123	16	266	72	4	7		56	22	
KH59-14	76.95	12.61	1.65	0.03	0.16	0.08	0.64	5.16	3.34	0.02	100.81	0.17	85	53	38	27	165	18	281	110	5	6	1	46	11	
KH60-15**	74.74	12.6	1.81	0.03	0.18	0.15	0.7	4.86	3.64	0.03	98.9	0.17	79	130	38	60	180	18	262	230	13	8	2	70	20	
KH61-16	75.97	11.88	1.88	0.03	0.18	0.12	0.64	4.72	3.26	0.02	98.94	0.23	71	52	34	29	190	22	262	99	5	9	2	67	10	
KH62-17	70.14	14.36	3.1	0.05	0.36	0.73	1.24	5.47	3.98	0.06	99.76	0.26	244	210	67	66	391	28	258	370	18	16	2	69	11	
KH63-18	66.61	13.09	8.17	0.14	0.99	0.77	2.07	4.08	3.41	0.15	99.87	0.38	191	585	60	191	939	69	323	940	47	34	6	206	42	
GH1-33	74.63	13.63	2.03	0.03	0.23	0.24	0.86	4.96	3.67	0.04	100.52	0.21	295	39	75	40	211	27	299	110	4	11	5	59	15	
GH2A-34	72.29	13.85	2.5	0.04	0.27	0.1	0.95	5.28	3.89	0.05	99.58	0.35	140	140	49	128	296	26	340	270	16	13	5	68	24	
GH2B-35	78.3	12.73	0.28	0.00	0.03	0.00	0.66	5.34	3.55	0.005	101.03	0.19	94	20	44	64	172	55	269	59	5	14	5	27	29	
GH3-36	77.9	12.82	1.09	0.02	0.08	0.00	0.54	5.09	3.71	0.02	101.37	0.18	13	17	18	34	114	22	280	50		7	3	58	13	
GH4-37	67.49	17.44	2.03	0.03	0.5	0.95	1.01	4.66	6.36	0.11	101.04	0.47	237	210	40	105	514	54	184	410	21	19	6	67	10	

Appendix 3. Continued.

Sample	SiO ₂	Al ₂ O ₃	Fe ₂ O ₃	MnO	TiO ₂	MgO	CaO	K ₂ O	Na ₂ O	P ₂ O ₅	total	LOI	Ba	La	Sr	Y	Zr	Nb	Rb	Ce	Sm	Hf	Ta	Th	U	
Tysfjord (Hellemobotn): younger granites																										
GH5-39	64.39	13.25	8.84	0.13	1.14	1.08	2.56	3.81	3.43	0.19	99.18	0.38	235	677	91	211	1200	78	213	1000	60	45	6	218	45	
GH6-40	70.09	12.84	5.22	0.1	0.63	0.51	1.49	4.88	3.16	0.12	99.33	0.3	208	410	60	130	655	48	257	650	33	26	4	110	26	
GH6B-41	65.15	13.31	8.82	0.15	1.11	0.76	2.12	4.02	3.57	0.17	99.65	0.46	193	722	57	232	1100	79	332	1150	57	43	8	249	53	
Tysfjord (Gjerdal): younger granites																										
KG65B-20	74.54	12.55	2.02	0.04	0.17	0.00	0.85	5.21	3.6	0.01	99.21	0.22	187	88	41	93	279	32	310	170	17	14	3	26	11	
KG66B-23	72.57	13.75	2.77	0.06	0.23	0.00	1.04	5.74	3.77	0.02	100.04	0.16	220	130	48	90	396	44	302	240	20	17	3			
KG67-24	70.61	15.17	1.22	0.02	0.09	0.00	0.92	7.25	3.85	0.005	99.42	0.34	232	44	55	39	53	18	325	82	3	3	2	141	35	
KG68-25	73.29	13.39	2.29	0.04	0.28	0.17	0.9	5.12	4.37	0.07	100.33	0.41	370	110	83	50	271	27	237	200	11	9	2	45	11	
KG69-26**	68.53	15.43	3.1	0.07	0.32	0.00	1.25	6.42	4.1	0.02	99.38	0.13	455	190	86	76	513	37	189	350	24	21	2	24	4	
Tysfjord (Veikvatn): younger granites																										
KV71A-28	76.35	12.1	1.99	0.03	0.13	0.00	0.49	5.23	3.72	0.005	100.21	0.23	26	130	13	157	357	23	410	230	21	19	2	25	8	
KV72A-29	75.16	12.33	2.06	0.03	0.15	0.00	0.63	5.3	3.69	0.01	99.63	0.28	50	150	23	173	308	42	400	260	21	16	4	48	17	
KV73-30**	76.73	12.43	1.44	0.02	0.1	0.03	0.43	5.12	3.77	0.005	100.32	0.23	43	120	23	107	221	43	390	210	14	14	4	50	15	
KV74-31	75.61	11.85	2.26	0.04	0.15	0.00	0.5	5.34	3.63	0.005	99.6	0.26	42	150	13	158	412	34	425	270	20	22	3	53	14	
KV75-32	74.63	13.63	2.03	0.03	0.23	0.24	0.86	4.96	3.67	0.04	100.52	0.21		210						350	26	19	4	51	13	

Appendix 4.

Analyses of rocks associated the Halerifjell U-mineralisation. Source NGU Uranal database.

sample	rock type	Nb	Zr	Y	Sr	Rb	Zn	Cu	Ba	Mo	U	Th	Pb	Ce	La
730038	granite	35	580	101	115	265	131	9	432	7	14	44	70	304	129
2825	granite	32	11700	515	57	215	88	9	273	36	560	43	95	340	29
730517	granite	31	468	100	61	283	47	5	432	5	13	32	37	244	115
1806	granite	22	356	100	120	233	58	10	365	10	10	10	36	141	73
1022	granite	34	536	68	111	261		10	582	10	20	30	47	221	116
607	granite	21	323	54	63	258		10	466	10	20	20	38	137	69
2424	granite	32	657	70	69	317		5	859	5	35	26	37	145	58
730034	granite	25	481	58	80	242	78	5	470	5	13	26	34	194	90
730035	granite	28	482	75	68	257	83	5	436	5	10	21	46	247	116
730033	granite	24	463	59	108	245	68	5	635	5	10	34	43	139	69
730031	granite	30	457	69	91	238	69	5	536	5	10	25	44	189	88
795155	granite	30	445	46	71	243	103	5	437	5	13	38	44	215	41
795156	granite	47	407	71	67	317	129	5	413	5	10	21	55	154	43
795165	granite	30	398	61	56	215	71	5	370	5	10	25	35	311	176
795166	granite	35	445	86	72	254	79	5	354	5	10	51	40	285	179
795167	granite	34	424	62	66	285	118	5	420	5	10	27	52	235	126
795168	granite	38	411	74	64	313	117	5	354	5	10	38	46	325	164
1813	granite	39	538	119	40	287	22	10	406	10	11	16	12	114	59
2427	granite	34	462	98	62	288		5	373	5	16	28	38	285	153
2425	granite	62	1100	140	49	643		5	563	5	69	144	33	855	293
1809	granite	40	474	138	70	438	49	10	340	10	22	99	17	129	66
1810	granite	37	370	92	52	385	33	10	348	14	17	69	15	82	35
1015	pegmatite	13	143	25	52	453		10	844	26	20	20	20	54	20
796119	pegmatite	13	134	12	73	237	93	44	634	5	10	10	45	73	33
796123	pegmatite	23	280	12	93	311	72	70	715	892	10	10	76	60	24
1808	pegmatite	17	10	10	679	50	49	22	158	5600	10	16	84	23	10

Appendix 4. Continued.

sample	rock type	Nb	Zr	Y	Sr	Rb	Zn	Cu	Ba	Mo	U	Th	Pb	Ce	La
1814	aplite	30	157	57	18	362	34	10	78	10	52	34	127	85	47
1396	aplite	100	152	100	100	313	24	10	63	100	21	29	64	60	32
1397	aplite	100	155	100	100	299	20	10	204	100	28	35	75	96	46
1398	aplite	100	133	100	100	325	61	10	91	100	275	52	82	137	78
1399	aplite	100	160	100	100	262	61	10	56	100	58	31	57	178	89
1400	aplite	100	155	100	100	281	109	14	63	100	198	39	97	140	69
1401	aplite	100	184	114	100	311	58	10	78	100	98	44	88	177	87
1402	aplite	100	160	112	100	334	43	28	72	100	2100	42	226	123	59
1403	aplite	100	190	159	100	308	776	10	74	100	3900	56	294	193	84
1404	aplite	100	220	200	100	339	981	10	93	142	5300	70	335	133	61
1405	aplite	100	164	100	100	320	62	10	87	100	103	20	104	128	65
1406	aplite	100	146	100	100	333	338	10	86	100	508	36	128	123	57
1407	aplite	100	570	700	100	600	3000	52	63	400	49000	138	2300	204	95
1408	aplite	100	190	100	100	290	171	10	57	111	5200	31	274	174	90
1409	aplite	100	163	100	100	375	188	10	75	127	4900	36	407	176	86
1410	aplite	100	160	120	100	312	306	11	75	100	3800	46	278	171	82
1411	aplite	100	410	200	100	500	190	31	49	300	27000	78	1700	79	27
1412	aplite	100	390	400	100	500	140	31	51	300	30000	83	1600	101	35
1413	aplite	100	148	100	100	338	139	10	77	100	300	40	238	10	10
1414	aplite	100	580	1300	100	800	507	50	63	400	53000	780	3800	257	82
1415	aplite	100	160	100	100	291	60	10	53	100	431	58	226	59	28
1416	aplite	100	188	100	100	333	29	10	91	100	1200	60	299	10	10
1417	aplite	100	189	100	100	334	30	10	91	100	1200	62	303	10	10
1418	aplite	100	171	100	100	306	94	10	76	100	1300	46	152	115	56
1419	aplite	100	220	270	100	360	364	10	76	130	7700	67	420	137	57
1420	aplite	100	170	100	100	260	688	10	89	100	3000	18	150	127	64
1421	aplite	100	470	700	100	600	584	29	50	300	33000	168	2000	105	23

Appendix 4. Continued.

sample	rock type	Nb	Zr	Y	Sr	Rb	Zn	Cu	Ba	Mo	U	Th	Pb	Ce	La
1422	aplite	100	320	540	100	500	2500	20	61	300	21000	129	993	155	71
1423	aplite	100	220	120	100	510	146	10	59	148	8700	137	684	147	68
1424	aplite	100	210	200	100	280	62	10	59	100	4300	99	380	132	59
1425	aplite	100	220	130	100	310	992	10	61	151	8500	40	452	219	108
1426	aplite	100	190	140	100	390	290	10	81	107	5200	51	390	92	42
1427	aplite	100	179	100	100	262	102	10	76	100	204	40	98	13	10
1428	aplite	100	190	120	100	400	1500	12	80	139	7500	64	864	44	10
1429	aplite	100	189	134	100	350	881	10	79	100	3100	51	272	135	64
1430	aplite	100	320	650	100	500	1900	22	47	300	23000	148	1100	172	75
1431	aplite	100	194	100	100	300	551	10	93	100	3400	33	291	98	46
1432	aplite	100	350	600	100	500	214	30	24	300	25000	186	1200	135	56
1433	aplite	100	250	140	100	370	1100	12	87	152	8600	59	521	117	51
1434	aplite	100	290	400	100	500	265	12	62	300	20000	114	979	222	94
1435	aplite	100	152	100	100	313	105	10	84	100	523	54	190	113	53
1436	aplite	100	250	150	100	420	661	10	91	161	10500	78	708	186	98
1437	aplite	100	150	100	100	236	27	10	66	100	269	53	85	10	10
1811	aplite	11	222	11	10	255	195	10	73	24	423	118	197	42	22
1818	aplite	29	141	69	14	297	70	13	69	14	245	27	86	125	69
1819	aplite	27	155	64	20	272	59	21	68	6	76	28	84	121	71
1820	aplite	29	149	61	23	260	106	6	68	5	54	31	84	137	78
1821	aplite	26	159	71	17	285	120	9	69	7	79	29	82	137	67
1822	aplite	23	165	66	16	277	64	6	62	5	73	33	90	130	72
1823	aplite	41	110	72	5	302	77	5	65	51	1400	30	171	118	66
1824	aplite	34	139	67	12	297	114	5	67	19	461	31	143	153	86
1825	aplite	40	100	62	5	299	93	5	66	54	1600	28	267	110	62
1826	aplite	26	156	56	17	285	57	5	67	5	42	31	83	150	84
1827	aplite	27	141	68	13	272	114	5	60	7	101	26	75	131	64

Appendix 4. Continued.

sample	rock type	Nb	Zr	Y	Sr	Rb	Zn	Cu	Ba	Mo	U	Th	Pb	Ce	La
1828	aplite	27	140	60	11	306	200	8	78	20	407	27	123	128	72
1829	aplite	27	143	67	14	287	43	5	76	8	225	27	84	121	69
1830	aplite	22	165	51	11	301	297	5	86	18	524	24	103	127	73
1831	aplite	25	143	62	18	274	48	6	63	12	170	31	95	132	75
1832	aplite	25	138	65	19	287	45	5	71	5	73	28	88	133	74
1833	aplite	30	146	63	10	283	135	5	70	18	415	31	115	108	59
1834	aplite	28	157	65	14	274	274	6	73	12	273	30	114	130	69
1835	aplite	30	151	65	26	298	136	6	78	11	220	30	120	108	62
1836	aplite	22	154	53	19	298	59	5	69	6	89	26	99	117	66
1837	aplite	25	157	60	17	302	56	12	68	5	86	30	122	115	61
1838	aplite	27	164	58	16	285	96	9	60	12	57	27	115	112	57
1839	aplite	26	144	53	14	275	44	7	58	5	58	25	83	95	51
1840	aplite	32	167	84	17	297	53	9	68	5	102	30	87	101	56
1841	aplite	28	155	129	11	249	541	9	60	39	297	27	82	97	56
2022	aplite	23	153	59	17	283	106	6	79	22	126	25	110	112	62
2023	aplite	20	152	68	15	266	154	5	66	13	84	27	79	133	69
2024	aplite	25	164	49	13	278	82	5	74	5	87	27	107	117	65
2025	aplite	26	167	50	12	308	394	6	101	29	547	27	177	111	68
2026	aplite	23	163	45	14	278	156	5	81	12	224	22	163	113	57
2027	aplite	26	159	61	15	265	93	5	65	18	86	31	115	123	73
2028	aplite	19	153	47	9	175	208	5	54	35	285	27	88	106	61
830901	aplite	33	136	85	11	272	31	12	56	5	19	40	51	169	76
830902	aplite	24	153	76	23	292	47	12	69	21	17	29	54	124	64
830903	aplite	31	156	66	13	289	37	8	64	5	34	26	47	133	65
830904	aplite	24	168	38	25	277	52	5	92	6	13	10	69	73	38
830905	aplite	26	301	60	30	288	74	5	110	5	11	25	42	147	73
830906	aplite	23	150	60	19	308	25	5	63	5	32	34	68	109	54

Appendix 4. Continued.

sample	rock type	Nb	Zr	Y	Sr	Rb	Zn	Cu	Ba	Mo	U	Th	Pb	Ce	La
830907	aplite	33	150	86	11	285	32	5	61	5	29	31	50	146	67
830908	aplite	20	162	47	14	279	22	5	68	5	19	15	61	110	53
830909	aplite	31	140	66	13	256	73	5	57	5	37	28	73	122	53
830910	aplite	21	154	47	13	259	38	5	57	6	28	27	88	108	50
830911	aplite	22	157	60	18	290	49	7	76	5	106	20	87	105	50
830912	aplite	25	139	54	15	297	56	10	68	5	40	26	74	108	52
830913	aplite	36	279	216	34	621	435	5	313	5	22	49	168	84	39
830914	aplite	28	153	62	22	290	97	5	84	8	37	31	66	107	48
830915	aplite	19	159	50	12	241	161	21	71	15	104	19	77	101	46
830916	aplite	22	161	61	17	306	33	5	66	5	91	34	64	122	56
830917	aplite	21	131	51	13	222	105	5	60	5	24	24	95	98	43
830918	aplite	23	133	57	12	287	45	15	65	5	51	25	84	112	50
830919	aplite	27	141	58	12	296	41	5	68	5	24	30	84	108	47
830920	aplite	32	150	68	17	335	33	5	61	17	32	23	72	104	49
830921	aplite	20	146	49	19	286	46	5	94	5	10	23	62	107	54
830922	aplite	10	146	100	10	304	182	9	67	20	819	29	129	122	57
830923	aplite	12	149	44	14	279	109	8	74	7	136	28	104	98	50
830924	aplite	16	150	43	15	300	74	5	72	5	146	15	73	85	40
830925	aplite	25	145	68	8	324	128	5	61	7	160	31	89	118	53
830926	aplite	25	150	58	18	302	55	9	54	5	36	17	70	85	34
830927	aplite	28	162	78	21	278	35	5	58	12	174	30	59	109	54
830928	aplite	24	143	63	21	294	183	5	89	5	89	24	70	116	61
830929	aplite	26	144	62	22	293	189	5	91	5	93	18	67	124	60
830930	aplite	19	146	56	17	314	46	5	71	17	161	29	85	120	55
830931	aplite	20	151	61	14	289	237	5	66	17	139	176	77	109	55
1807	aplite	23	172	12	13	296	20	10	89	10	10	12	84	10	10
1812	aplite	31	179	34	31	305	108	10	104	10	10	14	44	85	24

Appendix 4. Continued.

sample	rock type	Nb	Zr	Y	Sr	Rb	Zn	Cu	Ba	Mo	U	Th	Pb	Ce	La
2426	aplite	21	95	19	40	348		5	162	5	17	30	35	109	21
2423	aplite	26	248	77	9	238		5	10	5	39	68	47	114	32
796124	arkose	20	270	42	87	226	43	20	531	5	10	19	27	129	63
796125	arkose	20	158	49	80	216	35	47	319	5	10	26	38	120	55
796126	arkose	14	270	36	77	292	39	6	752	5	10	16	17	87	35
796127	arkose	30	481	77	53	387	25	5	652	5	10	32	10	372	160
1815	arkose	10	104	10	17	195	12	10	428	10	10	10	12	10	10
796118	arkose	17	216	27	103	132	52	12	495	5	10	17	66	151	82
1011	mica schist	85	416	35	344	25		13	223	10	20	20	20	130	59
795157	mica schist	17	248	18	246	158	85	5	697	5	10	10	30	78	23
795158	mica schist	12	257	11	24	81	27	5	213	5	10	14	10	47	10
795159	mica schist	11	255	17	33	39	20	5	185	5	10	12	10	91	10
795160	mica schist	18	223	13	78	131	56	5	487	8	10	14	23	16	10
795161	mica schist	18	239	18	147	136	71	5	500	5	10	13	25	23	10
795162	mica schist	14	184	12	173	130	91	5	519	5	10	10	23	85	13
795163	mica schist	11	164	5	111	72	66	5	208	5	10	10	22	10	10
795164	mica schist	17	224	20	272	125	87	18	815	5	10	12	21	87	38
796120	mica schist	18	200	22	53	272	84	50	375	5	10	15	22	84	42
796121	mica schist	16	181	21	41	220	54	19	369	5	10	13	14	85	43
796122	mica schist	25	132	14	68	496	123	75	553	13	10	14	41	105	72
2824	graphite schist	21	309	7	52	188	21	5	1100	29	10	18	18	10	10
1021	amphibolite	10	51	27	114	10		57	32	10	20	20	20	20	20

Appendix 5.

Analyses of graphite schists of the Rendalsvik U-mineralisation according to Gust and Thoresen (1981).

sample	U	Th	Nb	Zr	Y	Sr	Rb	Pb	Cu	Ba	Mo	V	Ce	La	Co	Zn
892	10	5	17	271	19	60	155	15	13	490	0	20	61	20	6	55
893	10	19	18	347	24	67	176	20	11	762	0	20	184	102	6	95
894	12	4	13	108	19	102	269	15	35	1700	20	191	22	20	6	42
895	25	4	17	164	34	143	137	45	116	651	32	298	52	20	30	88
896	103	18	25	191	69	171	10	55	145	26	210	325	122	62	60	60
897	41	3	15	130	39	115	201	35	103	955	45	212	49	20	30	55
898	64	0	14	130	30	135	170	25	117	809	80	247	49	20	30	290
899	136	21	19	203	76	203	62	55	148	408	300	605	79	37	30	114
900	89	13	16	155	47	182	133	60	146	569	115	497	65	29	30	61
901	62	10	14	142	30	135	167	50	111	817	100	259	45	20	30	65
902	118	18	14	153	58	194	64	50	108	643	180	978	67	32	60	110
903	58	12	13	125	42	104	118	35	132	1200	138	3400	20	20	30	555
904	2	0	10	19	13	424	10	85	21	561	20	21	20	20	6	27
905	80	0	12	89	29	159	10	40	68	20	80	2300	40	20	10	110
906	111	33	10	68	61	134	10	45	146	20	450	1100	70	35	60	108
907	183	10	13	103	93	204	10	40	111	82	530	984	94	46	60	435
908	148	19	10	155	142	155	20	50	124	33	210	342	92	49	60	60
909	36	0	23	172	36	116	181	30	96	907	72	220	43	20	10	60
910	102	19	21	182	51	267	103	60	145	1500	190	274	82	44	60	76
911	54	24	18	147	36	138	169	35	135	808	80	231	57	26	30	150
912	12	9	22	234	40	159	112	40	64	456	18	243	91	48	30	95
913	19	25	29	256	28	143	291	25	103	1300	35	511	54	24	30	115
914	52	11	15	282	76	162	161	30	95	1000	85	612	113	44	30	170
915	15	5	10	39	18	502	11	95	27	1900	70	94	20	20	6	100
916	157	11	16	212	72	372	10	30	111	136	110	3000	161	90	30	380
917	27	15	19	213	48	234	225	35	100	648	20	444	95	38	30	110

Appendix 5. Continued.

sample	U	Th	Nb	Zr	Y	Sr	Rb	Pb	Cu	Ba	Mo	V	Ce	La	Co	Zn
918	50	16	20	224	54	310	86	35	137	477	100	875	107	56	60	87
919	12	22	22	294	50	120	105	35	64	134	25	199	72	24	30	110
920	11	11	21	260	42	217	78	40	63	364	18	164	110	54	30	77
921	7	12	24	252	48	218	93	50	44	370	15	190	115	61	30	105
922	14	0	18	218	45	195	36	45	51	39	20	148	83	35	30	55
923	15	20	20	240	51	160	62	50	56	100	28	182	74	26	30	75
924	0	0	10	198	10	16	16	10	10	44	8	20	20	20	6	10
925	8	9	15	317	18	164	141	10	7	707	10	60	33	20	6	30
926	6	16	17	320	28	65	62	35	43	113	15	101	84	33	30	55
927	14	17	21	255	42	136	149	40	68	451	20	236	67	31	30	110
928	9	25	21	237	47	167	50	35	87	218	18	226	103	49	60	85
929	17	4	18	212	45	97	159	30	73	519	32	335	79	33	30	80
930	16	12	21	254	41	129	65	40	71	138	38	267	96	47	30	78
931	8	6	15	250	30	181	161	45	49	1100	18	178	75	28	30	85
932	32	21	17	167	36	30	118	30	68	164	130	507	115	53	30	105
933	30	0	11	136	38	115	110	40	96	208	95	423	52	20	60	95
934	35	13	22	223	43	223	97	55	105	870	100	267	79	35	30	90
935	50	0	16	125	46	169	159	40	100	757	75	234	62	22	30	150
936	12	23	22	238	37	126	197	30	67	839	18	165	68	27	20	115
937	77	0	15	134	37	207	10	40	122	22	155	861	60	23	60	108
938	38	0	14	108	30	84	177	30	125	906	52	165	42	20	30	100
939	76	0	19	167	36	264	201	55	116	2000	130	319	54	20	30	75
940	25	18	19	202	36	189	145	50	100	1600	45	322	81	36	30	90
941	14	8	22	257	45	201	84	55	78	678	15	157	96	42	30	112
942	19	2	19	199	40	84	171	35	83	605	25	326	60	22	30	360
943	5	12	15	315	27	86	113	25	35	305	8	69	54	20	10	60
944	8	16	23	300	25	58	240	30	20	550	0	114	44	20	10	85

Appendix 5. Continued.

sample	U	Th	Nb	Zr	Y	Sr	Rb	Pb	Cu	Ba	Mo	V	Ce	La	Co	Zn
945	22	0	17	174	24	37	247	10	35	1000	85	872	54	21	6	55
946	45	12	21	188	28	151	219	45	80	2100	170	538	51	22	10	50
947	11	0	21	158	22	39	242	0	32	1000	55	857	24	20	6	24
948	75	19	18	162	62	82	71	45	71	301	165	3944	103	42	10	23
949	40	10	23	178	46	97	258	40	66	1300	75	371	74	29	6	28
950	27	3	20	139	36	81	162	40	48	826	58	222	62	23	10	225
951	52	6	17	133	34	118	174	45	127	1100	70	278	50	20	30	115
952	50	0	17	145	42	114	144	50	175	210	60	186	67	28	30	135
953	6	0	10	64	18	10	421	25	76	159	35	255	20	20	6	40
954	89	7	17	158	46	109	59	50	150	34	190	432	70	28	30	210
955	72	12	19	177	47	145	127	60	138	649	185	453	70	26	60	75
956	46	27	18	153	39	131	186	55	124	1100	55	217	66	25	10	118
957	91	9	18	177	49	213	190	65	99	2200	155	505	90	35	30	46
958	52	16	12	120	39	86	97	50	116	297	105	695	42	20	100	102
959	6	21	24	307	33	90	171	35	49	360	10	283	62	22	30	35
960	9	19	26	238	40	57	176	20	48	332	8	196	65	23	30	42
961	8	12	19	170	24	120	251	15	73	749	40	370	30	20	6	68
962	44	7	20	146	37	97	219	50	77	960	50	221	61	25	30	75
963	38	16	21	158	47	72	186	45	62	985	35	300	73	28	6	20
964	14	0	11	95	12	96	222	20	51	1600	30	167	22	20	6	17
965	18	0	13	118	19	80	277	15	17	1800	45	205	46	20	6	12
966	32	6	19	154	37	110	242	45	42	1300	50	358	58	20	6	50

Appendix 6.

Analyses of rocks associated with the Høgtuva Be-REE-U-Sn mineralisation. Only analyses with >1000 ppm Zr and >1000 ppm Y+La+Ce are listed. Source NGU Uranal database.

sample	Nb	Zr	Y	Sr	Rb	Zn	Ba	Sn	Mo	U	Th	Pb	Co	Ce	La
1628	580	13000	1100	14	1600	567	25	202	81	230	550	105	54	199	54
1630	350	16800	925	17	1200	622	15	70	10	189	310	355	40	437	108
1631	470	23200	2100	16	1500	358	44	150	10	247	400	234	104	500	144
1632	290	20800	920	10	1300	542	21	52	10	214	97	512	43	240	57
1633	640	23000	2400	16	1500	620	43	82	10	366	570	1900	113	735	236
1634	360	17300	820	10	1300	399	21	126	10	234	560	254	46	275	51
1642	560	4100	1400	14	847	232	18	321	15	176	440	166	84	498	171
1655	440	10000	543	15	813	123	15	51	72	161	230	82	35	636	180
1656	1300	35800	2200	16	2900	1400	74	798	10	1100	720	324	146	678	217
2176	500	38000	800	23	1300	500	16	156	5	330	700	111	112	370	57
2177	911	2900	1800	11	947	314	12	289	5	368	565	112	135	473	105
2178	200	17000	553	13	910	220	16	110	5	168	65	91	38	377	94
2180	150	2500	462	9	856	129	13	64	5	79	111	54	34	520	157
2184	300	8200	816	15	980	98	18	175	5	140	159	77	55	208	52
2194	358	4100	1000	20	951	199	36	91	5	139	235	110	71	835	270
2196	234	6200	739	15	1300	208	10	131	5	119	125	246	46	212	50
2198	447	3400	1000	20	1400	304	13	146	5	208	440	122	64	214	49
2200	367	6400	910	37	1300	189	46	131	5	113	663	153	53	427	145
2201	400	8500	1100	17	1200	227	15	306	5	149	282	92	66	299	71
2202	505	3300	1000	13	1300	269	11	186	5	247	738	123	68	345	88
2203	440	6600	1300	8	1200	160	19	99	8	298	717	138	76	448	124
2204	429	965	787	15	1300	322	15	109	5	189	464	326	53	503	150
2205	396	6700	833	11	1100	154	15	102	5	164	229	110	55	317	92
2207	500	8100	736	26	1000	183	36	99	5	171	231	172	52	220	54
2208	300	10900	760	14	790	126	18	35	5	223	356	131	51	346	82

Appendix 6. Continued.

sample	Nb	Zr	Y	Sr	Rb	Zn	Ba	Sn	Mo	U	Th	Pb	Co	Ce	La
2210	400	20400	800	30	1300	178	52	68	100	200	410	166	90	576	174
2225	155	4400	617	14	936	61	10	45	5	88	73	92	41	340	123
2228	244	4400	600	10	1100	99	10	54	5	138	175	196	43	524	134
2237	192	1100	530	14	881	262	11	62	5	106	182	68	31	475	165
2238	200	7800	799	16	1000	387	13	67	5	138	227	94	52	1000	346
2831	5600	88000	4800	5	2500	3700	55	144	135	1700	4200	635	640	375	69
2832	2800	8000	3400	5	410	535	11	23	5	940	2400	880	190	420	117
2833	1400	15900	2100	5	135	410	10	85	25	555	1500	595	130	599	176
2834	1800	14000	1800	5	1400	2300	16	84	18	675	2400	150	130	608	209
2835	6200	48700	6600	5	1300	1300	10	345	40	1500	3200	415	335	1200	203
2836	935	15200	4600	5	3400	1100	46	230	14	2700	42300	1600	366	1100	430
2917	12300	20400	3100	5	604	1300	39	569	5	20500	39700	1200	19	1900	624
832004	191	5900	740	12	724	160	22	52	15	111	256	78	58	977	351
832007	314	8700	560	13	832	413	21	75	37	158	295	536	50	483	179
832008	278	10500	832	13	1300	354	18	76	34	162	266	141	57	581	208
832009	281	7900	663	14	1000	181	17	80	31	129	205	472	48	466	146
832010	320	8200	702	15	1000	263	17	75	26	115	157	119	44	483	188
832011	444	4000	940	25	965	216	30	194	5	160	356	93	66	614	220
832012	670	8100	1100	23	785	200	47	160	20	198	318	114	81	648	228
832013	467	5900	1200	33	594	135	42	66	5	144	323	102	85	681	238
832014	670	13600	1600	14	881	195	29	80	31	267	414	166	93	532	204
832015	723	19000	1100	20	1400	129	25	155	91	304	538	130	76	380	139
832016	520	11000	796	9	565	157	17	246	44	266	764	80	64	433	181
832017	550	11200	1400	18	1000	192	22	138	22	269	378	196	80	558	179
832018	650	17100	1900	28	1100	203	45	95	67	347	611	155	118	806	268
832019	276	4200	774	35	913	184	16	57	6	100	162	69	45	529	197
832020	223	6300	845	20	1000	161	18	37	20	152	224	77	47	370	150
832026	53	1800	364	13	622	56	19	25	5	26	43	37	16	470	203

Appendix 6. Continued.

sample	Nb	Zr	Y	Sr	Rb	Zn	Ba	Sn	Mo	U	Th	Pb	Co	Ce	La
832028	124	4100	659	32	495	75	44	44	8	118	195	79	36	709	260
832029	161	2400	775	18	798	91	11	60	5	80	403	63	49	644	223
832030	175	7300	612	15	695	103	28	71	31	96	107	143	11	680	260
832035	259	3200	667	69	758	171	127	54	5	74	86	173	34	391	121
832036	70	1900	477	18	814	109	18	35	5	43	74	125	29	489	189
832052	640	139300	1900	51	2100	2000	22	168	786	890	2300	1200	116	1500	473
832053	18000	85300	23000	76	1100	1300	140	338	5	7400	7200	889	2100	15800	5500
840001	323	8100	857	19	1200	213	17	77	12	177	295	248	52	454	147
840002	358	9100	936	17	1200	282	16	101	11	168	220	343	58	452	138
840003	380	9100	885	18	1200	266	20	107	11	175	216	303	56	395	125
840004	414	6300	850	19	1000	280	13	119	8	183	261	114	50	441	132
840005	363	7500	738	16	886	349	15	92	6	173	341	200	46	380	117
840006	479	8000	924	21	877	346	19	133	9	184	272	858	60	394	117
840007	368	6800	930	48	631	222	60	121	6	171	347	366	58	385	122
840008	333	4900	656	13	834	241	20	108	5	153	452	352	36	369	125
840009	255	6500	869	29	737	194	108	103	9	135	319	174	55	406	143
840010	181	3800	1000	76	607	221	134	74	5	95	226	96	54	904	346
840011	180	3700	851	62	534	120	91	48	5	89	201	273	33	585	216
840012	560	8300	1200	26	1100	284	26	85	5	235	370	142	69	574	175
840013	522	8900	1200	18	1300	202	19	140	5	217	368	92	65	478	150
840014	467	9400	1200	19	1200	201	24	91	9	201	283	97	61	403	119
840015	302	5000	775	29	961	265	39	75	8	152	343	265	41	427	136
840016	405	15600	1100	36	1100	410	32	94	22	232	338	108	62	462	139
840017	454	9200	1200	24	1100	362	27	123	6	208	346	633	72	441	139
840018	303	6200	703	28	1200	226	47	122	5	129	230	1600	37	317	93
840019	382	7600	872	18	931	374	25	97	5	163	330	575	52	429	130
840020	404	9500	850	38	847	400	32	88	13	196	313	671	55	438	134

Appendix 6. Continued.

sample	Nb	Zr	Y	Sr	Rb	Zn	Ba	Sn	Mo	U	Th	Pb	Co	Ce	La
840022	498	10300	1100	44	797	437	41	88	13	240	313	1200	63	414	132
840023	361	4100	695	23	763	286	17	142	5	145	335	292	39	330	101
840024	528	13100	1500	13	1400	352	25	134	11	273	583	315	86	424	126
840025	510	7800	1300	17	1400	213	23	128	5	229	346	119	71	499	153
840026	500	10400	1200	14	1400	208	19	100	8	230	323	94	68	481	143
840027	479	9900	1100	25	1300	240	25	84	10	221	364	101	63	491	152
840028	554	8600	1300	16	1300	270	24	142	5	241	546	451	67	485	152
840029	412	12400	1400	19	1300	693	22	110	10	230	391	747	79	475	149
840030	636	14200	1800	23	1000	774	21	164	14	336	437	970	113	590	176
840031	498	14200	1100	25	1100	432	23	137	11	259	224	1400	74	389	116
840032	303	17400	1100	15	1400	690	16	49	13	229	242	259	60	387	114
840033	421	12200	1000	16	1300	523	13	92	7	226	326	690	62	418	120
840034	457	9400	1100	15	1300	514	16	70	8	238	408	1300	65	459	140
840035	424	7600	1000	23	1400	669	19	110	5	189	325	2100	53	502	154
840036	396	10600	1100	17	1200	627	15	118	6	197	255	1600	65	410	116
840037	641	12300	1200	17	1200	306	29	105	18	349	834	362	92	624	240
840038	590	12200	1000	14	1300	192	18	226	16	280	641	80	68	286	83
840039	550	12200	1400	16	1500	205	28	169	9	282	465	191	87	410	122
840040	484	12000	1700	13	1700	402	20	203	5	265	490	124	118	604	202
840041	536	12100	1500	14	1100	300	23	213	5	291	707	175	91	570	193
840042	460	12800	2000	20	1300	284	25	113	5	280	462	189	96	537	163
840043	499	12400	1800	23	1700	349	24	265	8	278	564	1100	90	509	158
840044	588	13100	1600	21	1600	554	19	168	8	286	431	862	94	517	156
840045	492	11300	1400	19	1400	727	16	120	7	260	368	694	74	410	124
840046	521	12500	1300	20	1300	697	15	139	11	269	314	802	80	431	130
840047	381	14300	1300	18	1400	964	22	117	17	225	328	634	76	406	124
840048	561	11700	1500	19	1100	180	24	123	8	262	455	132	82	528	163

Appendix 6. Continued.

sample	Nb	Zr	Y	Sr	Rb	Zn	Ba	Sn	Mo	U	Th	Pb	Co	Ce	La
840049	382	11000	1300	18	1200	137	22	95	8	230	318	101	74	463	150
840050	592	12800	1200	17	1100	127	28	151	13	340	663	122	81	445	140
840051	560	9900	1500	25	1400	350	24	148	5	251	440	141	85	535	159
840052	588	10300	1500	19	1500	294	23	154	5	280	492	179	85	512	166
840053	489	11100	1400	29	1600	357	24	154	8	245	374	131	84	511	164
840054	617	10600	870	34	1800	314	35	175	17	300	429	275	71	388	121
840055	905	15300	798	8	900	204	19	295	29	603	1700	166	74	343	99
840056	507	11600	1200	20	1600	466	31	177	10	253	492	657	71	448	149
840057	519	10100	1400	20	1700	573	21	129	11	264	445	742	80	531	168
840058	498	11800	1600	17	1800	806	21	172	6	256	387	697	90	500	154